

Evaluating TRAM-34 as an anti-Glioma Agent

Dissertation

der Mathematisch-Naturwissenschaftlichen Fakultät
der Eberhard Karls Universität Tübingen
zur Erlangung des Grades eines
Doktors der Naturwissenschaften
(Dr. rer. nat.)

vorgelegt von
Nicolai Stransky
aus Göppingen (Fils)

Tübingen
2024

Gedruckt mit Genehmigung der Mathematisch-Naturwissenschaftlichen Fakultät der Eberhard Karls Universität Tübingen.

Tag der mündlichen Qualifikation:	03.09.2024
Dekan:	Prof. Dr. Thilo Stehle
1. Berichterstatter/-in:	Prof. Dr. Peter Ruth
2. Berichterstatter/-in:	Prof. Dr. Stephan M. Huber
3. Berichterstatter/-in:	Prof. Dr. Albrecht Schwab
4. Berichterstatter/-in:	Prof. Dr. Luis Pardo

“Nature was not designed to make life easy for biologists.”

[Colin Tudge, 2007](#)

Contents

Contents	iv
Summary	v
Zusammenfassung	vi
Introduction	1
Aim of this work	9
Results and Discussion	10
List of references	28
Acknowledgments	39
Appendix	40

Summary

Despite multimodal treatment, consisting of surgery, radio-, chemo- and electrotherapy, the prognosis of glioblastoma patients remains poor. In this work, we evaluated TRAM-34 as a new potential drug candidate against glioblastoma. TRAM-34 inhibits the intermediate-conductance calcium-activated potassium channel $K_{Ca3.1}$ and was previously shown to inhibit glioma cell migration or invasion. In addition, it increased the efficacy of radiation and temozolomide treatment. More recent findings indicate that $K_{Ca3.1}$ may act as a rhythm generator within communication networks of glioma cells, ultimately boosting tumor growth.

In our attempts to generalize these findings to more glioma cell lines, we found varying effects of TRAM-34 treatment *in vitro*. Our findings indicate that TRAM-34 exerts little radiosensitizing effects in the glioma cell lines used in our studies. Similarly, among the cell lines tested, only one was sensitized to temozolomide treatment by TRAM-34. Last, direct proliferation-inhibiting effects of TRAM-34 were detected for two out of five glioma cell lines. Interestingly, findings indicating efficacy of TRAM-34, were only present when stem-cell-enriching cell culture conditions were used, hence, in a cell population most commonly associated with therapy resistance. Nevertheless, our *in vitro* findings point towards modest effects of TRAM-34 treatment on glioma cell viability, both on its own or as an add-on therapy.

On the contrary, the results of our *in vivo* experiments suggest a synergistic effect of radiation and TRAM-34 in the syngeneic glioma model SMA-560/VM/Dk. As such, we found a prolonged survival of mice co-treated with radiation and TRAM-34. We hypothesize that TRAM-34 inhibits the radiation-induced hypermigration of glioma cells, as shown by our histological analyses. Mechanistically, irradiation led to an increased secretion of TGF- β and expression of *MMP-9*, which was blunted by TRAM-34. We found no detrimental effects of the treatment on the infiltration of reactive macrophages, cytotoxic, or regulatory T cells into the tumor tissue. Last, weight changes or blood counts of the mice indicated few treatment-specific adverse events, pointing towards a well-tolerated treatment strategy.

In conclusion, we found modest effects of TRAM-34 *in vitro*, and synergistic effects of TRAM-34 to radiation treatment in a glioma mouse model. Further research is necessary to expand these findings to other animal models and gain more confidence in the veracity of our results.

Zusammenfassung

Trotz multimodaler Behandlung, die aus Operation, Radio-, Chemo- und Elektrotherapie besteht, ist die Prognose von Glioblastom-Patienten noch immer schlecht. In dieser Arbeit untersuchten wir TRAM-34 als neuen potenziellen Arzneimittelkandidaten gegen verschiedene Gliomzelllinien. TRAM-34, ein Inhibitor des Kalzium-aktivierten Kaliumkanals $K_{Ca}3.1$, konnte in vorherigen Studien bereits zeigen, dass er die Migration und Invasion von Gliomzellen hemmt. Darüber hinaus erhöhte es die Wirksamkeit einer Strahlen- oder Temozolomid-Therapie. Neue Erkenntnisse deuten darauf hin, dass $K_{Ca}3.1$ als Taktgeber innerhalb von Kommunikationsnetzwerken von Gliomzellen fungiert, was letztlich das Tumorwachstum fördert.

In unseren Versuchen, diese Ergebnisse auf weitere Gliomzelllinien zu generalisieren, stellten wir zelllinienabhängige Effekte der TRAM-34-Behandlung *in vitro* fest. Unsere Ergebnisse zeigen, dass TRAM-34 nur geringe radiosensibilisierende Wirkungen auf die von uns getesteten Gliomzelllinien entfaltete. Ebenso wurde von den verwendeten Zelllinien nur eine durch TRAM-34 für die Behandlung mit Temozolomid sensibilisiert. Schließlich stellten wir bei zwei von fünf Gliomzelllinien eine direkte proliferationshemmende Wirkung von TRAM-34 fest. Interessanterweise waren die Ergebnisse, die eine Wirksamkeit von TRAM-34 andeuteten, nur dann vorhanden, wenn stammzellanreichernde Zellkulturbedingungen verwendet wurden, also gegen eine Zellpopulation, die am häufigsten mit Therapieresistenz in Verbindung gebracht wird. Insgesamt weisen unsere *in vitro* Ergebnisse jedoch nur auf eine bescheidene Wirkung von TRAM-34 auf Gliomzellen hin.

Im Gegensatz dazu fanden wir in unseren *in vivo* Experimenten eine synergistische Wirkung von Bestrahlung und TRAM-34 im syngenem Gliommodell SMA-560/VM/Dk. So stellten wir bei Mäusen, die mit Bestrahlung und TRAM-34 behandelt wurden, eine verlängerte Überlebenszeit fest. Dies führen wir am ehesten auf die Hemmung der strahleninduzierte Hypermigration von Gliomzellen durch TRAM-34 zurück. Mechanistisch gesehen führte die Bestrahlung zu einer erhöhten Sekretion von TGF- β und Expression von *MMP-9*, die durch TRAM-34 reduziert wurde. Wir fanden keine nachteiligen Auswirkungen der Behandlung auf die Infiltration von reaktiven Makrophagen, zytotoxischen oder regulatorischen T-Zellen in das

Tumorgewebe. Analysen der Gewichtsveränderungen und Blutbilder der Mäuse deuteten auf wenige behandlungsspezifische Nebenwirkungen hin, was eine gut verträgliche Behandlungsstrategie erwarten lässt.

Zusammenfassend fanden wir *in vitro* lediglich bescheidene Wirkungen von TRAM-34, sowie eine synergistische Wirkung von TRAM-34 auf die Strahlentherapie in einem Gliommausmodell. Weitere Untersuchungen sind notwendig, um diese Ergebnisse auf andere Tiermodelle auszuweiten und mehr Vertrauen in die Aussagekraft unserer Ergebnisse zu gewinnen.

Introduction

The prognosis of glioblastoma patients remains dire, with median overall survival times of only slightly above 1.5 years in selected trial populations¹. The current standard of care comprises the gross total resection, radiotherapy with concomitant temozolomide chemotherapy, temozolomide maintenance therapy, and Tumor Treating Fields (TTFields) maintenance therapy¹ in the newly diagnosed disease setting. The main pillars of therapy remained more or less the same since the pivotal trial by Stupp *et al.* in 2005², except for the optional addition of tumor-treating fields¹.

New treatment options for glioblastoma patients are lacking

An overview of phase III trial results of new treatment approaches in glioblastoma patients since 2012 is given in Table 1. There exists some evidence for prolonged survival times by lomustine, an alkylating agent, to temozolomide chemotherapy³. However, its implementation is mainly restricted to Germany owing to the trial's small sample size (n = 141), increasing its likelihood of a false-positive result⁴. An additional concern is that it potentially deprives patients of lomustine treatment in the relapsed setting⁵. Multiple other phase III studies failed to exert survival benefits for the newly diagnosed patient cohort, for example, the EGFRvIII-targeting tumor vaccine rindopepimut⁶, the antibody-drug conjugate depatuxizumab mafodotin⁷ or tumor checkpoint blockade with nivolumab⁸.

After disease relapse, treatment options become even scarcer. These may include re-surgery, especially for symptomatic patients, re-irradiation, anti-VEGF therapy (bevacizumab), and aforementioned alkylating chemotherapy with lomustine. In general, all interventions in the relapsed setting lack evidence of, or even failed to achieve prolonged survival times in placebo-controlled randomized clinical trials (e.g., lomustine⁹, bevacizumab¹⁰ or re-irradiation¹¹). Furthermore, most other translational attempts, such as immune-checkpoint blockade with nivolumab¹², electrotherapy with TTFields¹³, or viral therapy¹⁴ failed to achieve a survival benefit after relapse.

Two apparently 'contradicting' and often discussed examples suffer from methodological weaknesses: First, regorafenib, a multikinase inhibitor, showed a prolonged survival as compared with lomustine chemotherapy in a recent phase II study¹⁵.

Table 1: Overview of phase III studies evaluating new treatments for glioblastoma treatment since 2012[#]

Intervention	Mechanism of action	Date	Disease setting	N	Efficacy	Comment	Ref.
TTFields	multifactorial	2012	recurrence	237	OS (n.s.)		Stupp <i>et al.</i> ¹³
sitimagene ceradenovec + ganciclovir	gene therapy sensitizing to ganciclovir	2013	newly diagnosed	250	TTD/TTR (*) OS (n.s.)		Westphal <i>et al.</i> ¹⁶
cediranib	anti-VEGFR	2013	recurrence	325	PFS (n.s.)		Batchelor <i>et al.</i> ¹⁷
bevacizumab	anti-VEGF	2014	newly diagnosed	921	PFS (*) OS (n.s.)	Pseudoresponse?	Chinot <i>et al.</i> ¹⁸
bevacizumab	anti-VEGF	2014	newly diagnosed	637	PFS (*) OS (n.s.)	See above	Gilbert <i>et al.</i> ¹⁹
cilengitide	integrin inhibitor	2014	newly diagnosed	545	OS (n.s.)		Stupp <i>et al.</i> ²⁰
O(6)-benzylguanine	MGMT inhibition	2015	newly diagnosed	183	OS (n.s.)		Blumenthal <i>et al.</i> ²¹
nimotuzumab	anti-EGFR	2015	newly diagnosed	142	PFS (n.s.) OS (n.s.)		Westphal <i>et al.</i> ²²
adoptive cell immunotherapy		2017	newly diagnosed	180	PFS (*) OS (n.s.)		Kong <i>et al.</i> ²³
rindopepimut	EGFRvIII vaccination	2017	newly diagnosed	745	OS (n.s.)		Weller <i>et al.</i> ⁶
TTFields	multifactorial	2017	newly diagnosed	695	PFS (*) OS (*)		Stupp <i>et al.</i> ¹
personalized peptide vaccine	HLA-A24	2019	recurrence	88	OS (n.s.)		Narita <i>et al.</i> ²⁴
lomustine	alkylating agent	2019	newly diagnosed	141	OS (*)	Crossover? Small sample size?	Herrlinger <i>et al.</i> ³
VB-111 virotherapy	anti-angiogenesis, immune adjuvant	2020	recurrence	256	OS (n.s.)		Cloughesy <i>et al.</i> ¹⁴
nivolumab	anti-PD-1	2020	recurrence	439	OS (n.s.)		Reardon <i>et al.</i> ¹²
Vocimagene Amiretrorepvec + Flucytosin	gene therapy sensitizing to flucytosin	2020	recurrence	403	OS (n.s.)		Cloughesy <i>et al.</i> ²⁵
nivolumab	anti-PD-1	2023	newly diagnosed	560	OS (*)	Worse OS	Omuro <i>et al.</i> ⁸
nivolumab	anti-PD-1	2023	newly diagnosed	716	OS (n.s.) PFS (n.s.)		Lim <i>et al.</i> ²⁶
DCVax-L	dendritic cell vaccination	2023	newly diagnosed/ recurrence	331	OS (*)	Crossover. Non-randomized.	Liau <i>et al.</i> ²⁷
depatuxizumab mafodotin	antibody-drug conjugate	2023	newly diagnosed	639	OS (n.s.) PFS (*)		Lassman <i>et al.</i> ⁷

[#] all articles, identified by a PubMed search, were analyzed (as of 10/2023). Note that only new treatment interventions are depicted, while TMZ or irradiation dose modifications are omitted from this table. Endpoints depicted in bold were the primary endpoint of the study. Abbreviations: N = sample size; Ref. = reference; TTFields = Tumor-treating fields; OS = overall survival; n.s. = not significantly different; TTD/TTR = time to death/re-intervention; * = statistically significant difference; VEGFR = vascular endothelial growth factor receptor; PFS = progression-free survival; MGMT = methylguanine methyltransferase; EGFR = epidermal growth factor receptor.

However, this finding comes with a large uncertainty: in REGOMA, 119 patients with relapsed glioblastoma were randomized. While its primary endpoint was overall survival, the study was only powered to detect a difference assuming a one-sided significance level $\alpha = 0.20$. Hence, these data should be replicated in a larger phase III study before the widespread implementation of this new treatment option. Second, a phase III study of DCVax-L, a dendritic cell vaccination, recently claimed survival benefits in both newly diagnosed and relapsed glioblastoma patients²⁷. The study protocol allowed crossover of patients in the control arm to DCVax-L, ultimately leading the study authors to use an 'external control arm' (also known as historical control). This renders the trial unable to analyze effects on survival in an unbiased way, due to comparing nonrandomized groups.

Combined, these observations underline the importance of identifying new drug targets and new drug candidates. To achieve this, efforts to repurpose drugs, as well as to identify *de novo* drug candidates are currently ongoing.

Repurposing efforts in glioblastoma research

Drug repurposing refers to identifying new therapeutic uses for drugs, already approved for other indications. This comes with the benefits of well-known pharmacokinetic and pharmacodynamic properties, as well as lower development times and costs²⁸. Multiple already approved drugs show preclinical efficacy against glioblastoma, such as atorvastatin²⁹, losartan³⁰, or disulfiram^{31,32}. This led to the implementation of multi-drug regimens, some of which use up to nine different repurposed drugs in addition to standard temozolomide therapy (CUSP-9)³³, which show preclinical efficacy against a range of glioma cells³⁴.

Among the successful examples of drug repurposing in oncology, thalidomide for the treatment of multiple myeloma stands out. After its discovery, thalidomide was prescribed as a sleeping pill and for morning sickness in pregnant women in the 1960s. Early on, reports of birth defects in children, whose mothers were exposed to thalidomide, were noted and it is estimated that up to 15.000 children have been harmed³⁵. Hence, thalidomide was withdrawn from the market until its potential inhibitory effects on angiogenesis were reported. After subsequent positive clinical trials in the late 1990s³⁶, it was finally approved by the FDA for the treatment of multiple myeloma in 2006.

In recent years, another drug became famous for its supposed repurposing potential: methadone. Reports of its anti-cancer effects against leukemia^{37,38} or glioblastoma cells³⁹ *in vitro* and case reports of long-term cancer survivors, ostensibly caused by taking methadone, in the public media ultimately led to cancer patients demanding methadone prescriptions from their treating physicians⁴⁰. However, there exists reasonable doubt of methadone's translational potential, mainly regarding its ambiguous effects on cancer cells, the usage of clinically irrelevant very high concentrations in the *in vitro* studies, challenging pharmacokinetic properties of the molecule itself, and missing clinical data^{41,42}.

Whether repurposing strategies will benefit glioblastoma patients in the end remains to be seen, with clinical studies ongoing for, e.g., metformin (NCT03243851), disulfiram (NCT02678975) or multi-drug regimens, such as the previously mentioned CUSP-9 regimen. Nevertheless, the paucity of successfully repurposed drugs in oncology in general, may dampen the early optimism for drug repurposing efforts.

TRAM-34, a *de novo* drug candidate, targets the K_{Ca}3.1 potassium channel

There exist multiple *de novo* drug candidates for the treatment of glioblastoma^{43,44}, one of which is TRAM-34. TRAM-34 was initially developed as an inhibitor of the intermediate-conductance calcium-activated potassium channel K_{Ca}3.1 (IK, IK_{Ca}, SK4, Gardos channel; encoded by the *KCNN4* gene) in 2000 by Heike Wulff and colleagues. The authors aimed at synthesizing clotrimazole derivatives with preserved anti-K_{Ca}3.1 activity but reduced cytochrome P450 inhibiting properties^{45,46}. This was accomplished by replacing the imidazole moiety of clotrimazole with a pyrazole (see Figure 1), which also led to slightly more potent IC₅₀ values in electrophysiological experiments (TRAM-34: 20 nM; Clotrimazole: 70 nM) and retained selectivity over a multitude of other tested ion channels⁴⁵. Nevertheless, other authors found off-target effects of TRAM-34 on non-selective cation channels⁴⁷.

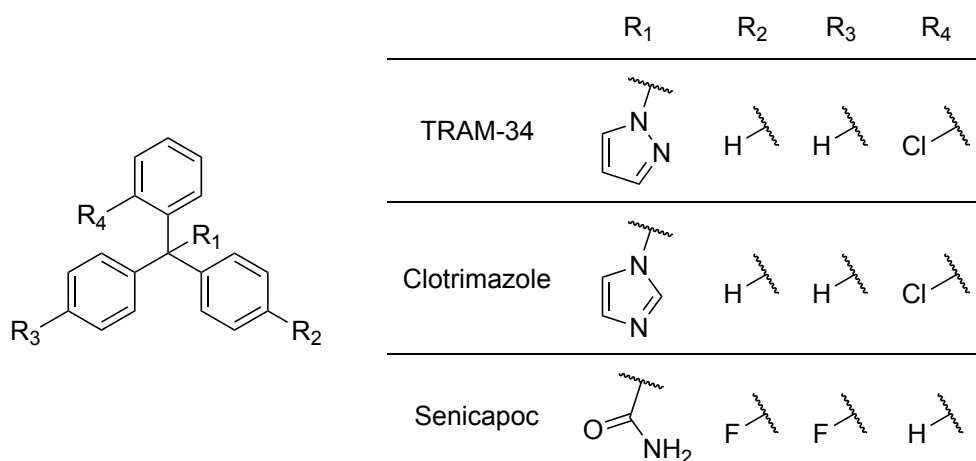


Figure 1: Chemical structure of $K_{Ca3.1}$ inhibitors TRAM-34, Clotrimazole, and Senicapoc.

TRAM-34 exerts anti-migratory effects in glioma

Early work reported on clotrimazole's anti-glioblastoma activity *in vitro*⁴⁸ and *in vivo*⁴⁹ and explained these effects by affecting intracellular K^+ and Ca^{2+} concentrations. The first report of the expression of the $K_{Ca3.1}$ channel in one glioma cell line dates back to 2004⁵⁰. In 2010, reports indicated a functional role of $K_{Ca3.1}$ in the invasiveness of glioblastoma, as blocking $K_{Ca3.1}$ with TRAM-34 inhibited glioma cell migration⁵¹. As a consequence, this finding led one of the initiators of the aforementioned CUSP-9 repurposing project to propose clotrimazole as of "adjunctive benefit during standard current cytoablative treatment of glioblastoma" due to its $K_{Ca3.1}$ blocking properties⁵². One may speculate why clotrimazole was not part of the initial set of drugs subsequently tested in clinical trials⁵³, however it appears likely that its cytochrome P450 inhibiting properties and, hence, large risk of drug-drug-interactions were at least part of the reason.

Inspired by the first signs of TRAM-34's anti-migratory effects in the glioblastoma cell line GL-15⁵¹, more studies verified $K_{Ca3.1}$'s role in glioma migration and invasion in U-87MG cells⁵⁴, the primary glioma line FCN9⁵⁵, in a xenograft mouse model with GL-15 cells⁵⁶, in brain slices with D54 cells⁵⁷ as well as in another xenograft study with primary glioblastoma cells⁵⁸. All but the latter of these studies applied TRAM-34 and it consistently decreased migration or invasion of glioma cells. Mechanistically, $K_{Ca3.1}$ has been proposed to shape Ca^{2+} signals involved in programming cell migration/brain infiltration⁵⁹. Moreover, $K_{Ca3.1}$ probably participates in the execution of glioblastoma cell migration by mediating K^+ efflux at the rear of the migrating cell. Co-

fluxes of Cl⁻ counterions and iso-osmotically obliged H₂O and the consequent local loss of cell volume results in the retraction of the cell rear⁵⁷.

Additional anti-glioma effects of TRAM-34

Early reports assessing TRAM-34's effect on cancer cell proliferation found a reduced proliferation rate in U-251 glioma cells with very high IC₅₀ values of around 14 μM. However, the authors attributed this to targets other than K_{Ca}3.1⁶⁰. Moreover, other work delineated the importance of K_{Ca}3.1 for the intrinsic apoptotic pathway, as TRAM-34 potentially inhibited or at least slowed this process⁶¹. Nevertheless, two manuscripts reported reduced tumor growth after TRAM-34 treatment in different *in vivo* models^{62,63} and sensitization of glioma cells to temozolomide⁶² and irradiation⁶⁴ by concurrent TRAM-34 treatment. These findings hint towards TRAM-34's synergistic potential to two of the main pillars of current glioblastoma therapy. Last, new findings associate K_{Ca}3.1's activity with communication among networks of glioma cells governed by rhythmic intercellular Ca²⁺ waves within the network. Autonomous activity within these networks, driven by K_{Ca}3.1, may ultimately boost glioma growth and invasiveness and explain TRAM-34's anti-glioma effects⁶⁵.

TRAM-34 as an immunomodulating agent

While up to this day few articles report on TRAM-34's effect on the immune system in cancer models, this is and will be an important topic for further research. This is partly due to the expression of K_{Ca}3.1 in many immune cells, such as T helper cells, memory B cells, mast cells, or macrophages⁶⁶. Among others, K_{Ca}3.1 is important for T cell activation and proliferation, cytokine production, or chemotaxis of macrophages. Interestingly, blockade of K_{Ca}3.1 is beneficial in several inflammatory disease models, such as colitis^{67,68}, asthma⁶⁹ or allograft vasculopathy⁷⁰. This might hint at an immunomodulating (if not immunosuppressing) mode of action of TRAM-34, which could be detrimental as an anti-glioblastoma agent. More recent findings are hence important first steps to dispel these concerns: Grimaldi *et al.* found a decreased expression of genes associated with 'pro-tumor' activity and an increased expression of genes associated with an 'anti-tumor' activity in microglia/macrophages after TRAM-34 treatment in both a syngeneic glioma mouse model and in *ex vivo* treated human brain slices⁶³. Moreover, *KCNN4* expression was increased in 'pro-tumor' microglia of tumor-bearing mice, which was reversed by TRAM-34 treatment⁶³. The same group used two-photon time-lapsed imaging to follow up their initial findings, which again

found TRAM-34-induced changes towards an anti-tumor branching phenotype of microglia. This was accompanied by a reduced growth rate of both cancer cells but also tumor-associated microglia/macrophages⁷¹.

Combined, the largest body of evidence for TRAM-34's anti-glioblastoma effects are its anti-migratory and anti-invasive properties (Table 2 gives an overview of all preclinical studies evaluating TRAM-34 against glioma cells). While the exact molecular basis for its anti-proliferative effects on glioma remains unclear, there appears to be a direct tumoricidal or at least proliferation-slowing property of TRAM-34 in selected glioblastoma cell lines. Moreover, TRAM-34 was shown to sensitize glioblastoma cell lines towards irradiation and temozolomide, which are currently the main treatment options for glioblastoma patients after surgery. Last, while theoretical considerations let us assume a potential immunosuppressing effect of TRAM-34 treatment, the hitherto results rather point to an immunomodulating mode of action, potentially even reversing the 'pro-tumor' nature of the tumor microenvironment. These findings, combined with the low levels of reported adverse events in *KCNN4*^{-/-} animal models (except for impairments in the volume control of erythrocytes and lymphocytes)^{72,73}, but also of the structurally related K_{Ca}3.1 blocker senicapoc in a phase III study of sickle cell patients⁷⁴, make TRAM-34 an attractive new drug candidate for glioblastoma patients.

Table 2: Overview of preclinical anti-glioma effects of TRAM-34#.

Effect	Cell Line / animal model	Notes	Concentration/ Drug dose	Ref.
Inhibition of migration	GL-15	Induced by CXCL12	2.5-10 μ M for 4 hours	51
Inhibition of proliferation	U-251	Not due to KCa3.1 blockage	IC 50 > 10 μ M	60
Inhibition of migration	U-87MG		1-3 μ M for 6-21 hours	54
Inhibition of migration	FCN9	Greater reductions in stem-cell enriched subpopulation	1-3 μ M for 48 hours	55
Inhibition of intrinsic apoptosis pathway	D54-MG	Mechanistically	1 μ M	61
Inhibition of migration	D54	Migration induced by Bradykinin	1 μ M for 5.5 hours	57
Inhibition of invasion	D54 in SCID brain slices		10 μ M for up to 7 days	
Inhibition of invasion	GL-15 in SCID mice	Same effect by silencing KCa3.1 in GL-15 cells	120 mg/kg b.w. i.p. for four weeks	56
Inhibition of migration	Jx12 Jx15	Cell lines with low KCa3.1 (e.g., Jx22) not affected	1 μ M for 5 hours	58
Inhibition of invasion	U-251			
Radiosensitization	T98G U-87MG	Effect diminished after shRNA knockdown of KCa3.1	10 μ M for 24 hours	64
Delay of tumor growth after irradiation	U-87MG in nude mice		120 mg/kg b.w. i.p., for 5 consecutive days	
Reductions in tumor volume and microglia phenotype switches toward anti-tumor phenotype	GL-261 cells in C57BL/6 mice Human biopsies	Tumor volume reductions only in murine glioma model	120 mg/kg i.p. for 10 days	63
Sensitization to temozolomide in vitro (migration, invasion, clonogenicity, apoptosis) and in vivo (apoptosis, survival)	GL-261 cells in C57BL/6 mice U-87MG Primary GBM cells	TRAM-34 with additional neuroprotective roles (microglia mediated)	2.5 μ M 120 mg/kg b.w. i.p. for up to 14 days	62
Radiosensitization	Primary GBM cells	Only in ALDH1A3 high cell line; only γ H2AX foci	1 μ M for 24 hours	75
Inhibition of migration and invasion after irradiation	GL-15 Primary GBM	Irradiation increases KCa3.1 mRNA and migration	5 μ M for 24 hours	76
Reduced proliferation of glioma cells and induction of an anti-tumor phenotype of TAMs	GL-261 cells in Cx3cr1GFP/WT mice		120 mg/kg b.w. i.p. for 10 days	71
Inhibition of autonomous rhythms between cancer cells leading to the inhibition of proliferation and migration.	Primary GBM cells		120 mg/kg b.w. i.p. twice daily for 14 days 1 μ M	65

all articles identified by the PubMed search ("TRAM-34 AND (glioma OR glioblastoma)") were analyzed. Abbreviations: Ref. = reference; b.w. = bodyweight; i.p. = intraperitoneal.

Aim of this work

There exist several studies on TRAM-34's efficacy against glioma cells, however most studies rest their findings on one or only few cell lines. Hence, this study aimed to further explore the potential of TRAM-34 as a novel therapeutic candidate for the treatment of glioblastoma. To address the generalizability of the previous findings, we analyzed the effects of $K_{Ca}3.1$ targeting with TRAM-34 in several human and murine glioma cell lines *in vitro* as well as in the syngeneic, orthotopic glioma model SMA-560/VM/Dk.

Secondly, this project aimed to identify the dependence of potential radiosensitizing or anti-invasive/anti-migratory effects of TRAM-34 on cell phenotype and the tumor microenvironment. To this end, different human and mouse glioma cell lines were either grown *in vitro* under fast proliferating and „differentiating“ culture conditions or under glioblastoma stem cell inducing/enriching cell culture conditions.

Expression of $K_{Ca}3.1$ has been demonstrated in immune cells. Consequently, $K_{Ca}3.1$ targeting in a clinical setting might exert effects beyond radiosensitizing and immobilizing glioblastoma cells, for example dampening the anti-glioblastoma immune response. Consequently, the third aim of this project was to analyze the infiltration of immune cells in the SMA-560/VM/Dk glioma model to exclude detrimental effects on the immune response.

Last, due to $K_{Ca}3.1$'s effects on the volume regulation of erythrocytes, blood counts of the mice were analyzed to assess potential adverse events of TRAM-34.

Overall, this work explored TRAM-34's potential as a glioblastoma treatment in diverse glioma cell lines and a murine, immunocompetent mouse model.

Results and Discussion

To evaluate the potential of $K_{Ca}3.1$ blockade with TRAM-34 as an anti-glioma therapy, we analyzed its effect on three murine (SMA-560, SMA-540 and GL-261) and two human (U-87MG and U-251MG) glioma cell lines. All experiments were performed with standard culture medium (DMEM + 10% fetal calf serum [FCS]) as well as FCS-free stem-cell-enriching culture medium (NSC medium) to evaluate its effects in different culture media and stem cell fractions (Figure 2). To decrease biases and avoid overestimating effect sizes⁷⁷, all experiments were conducted in a blinded fashion up until the analysis or data visualization.

First, to test TRAM-34's direct tumoricidal (proliferation-inhibiting) effects, we performed clonogenic survival assays (colony formation assay for adherent DMEM cultured cells and limited dilution assay for spheroid-forming NSC cultures). We detected no or only negligible effects of TRAM-34 on plating efficiency in all murine cell lines, regardless of culture medium.

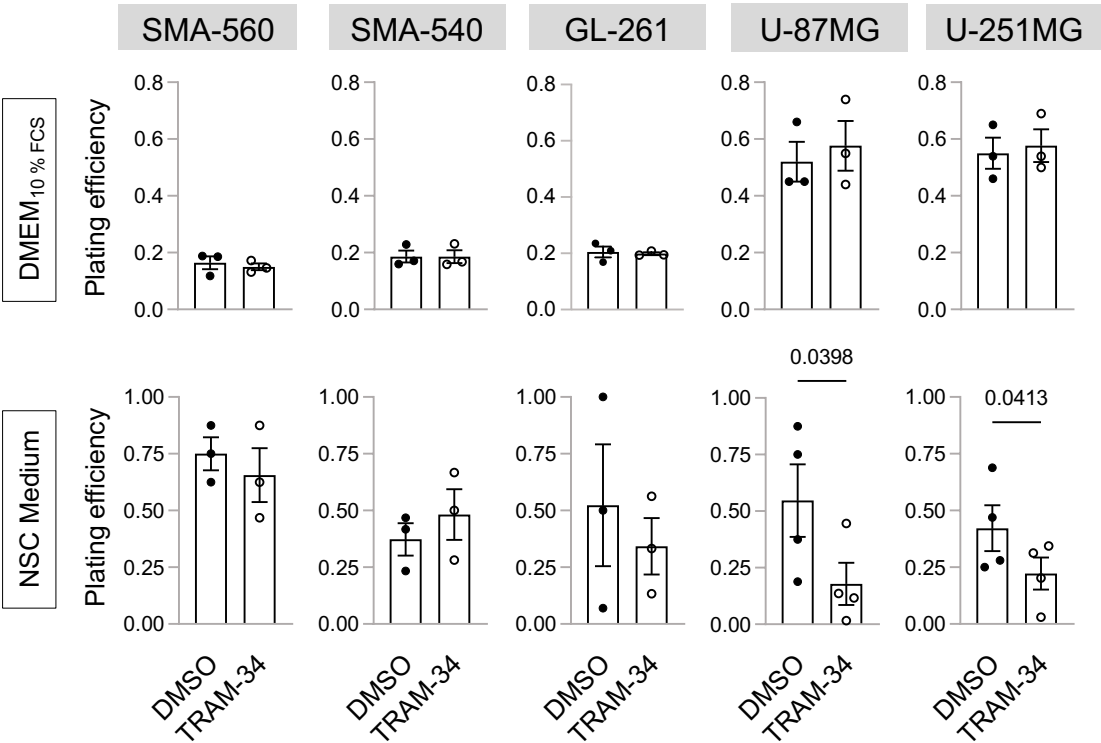


Figure 2: Tumorcidal effects of TRAM-34 in selected glioma cell lines. Figure panels show the plating efficiency as determined by colony formation assay (upper panels) or limited dilution assay (lower panels) of TRAM-34 (0 vs. 5 μ M) treatment. Shown are individual data of 3-4 independent experiments and mean values \pm sem (standard error of the mean). Numbers indicate P values as calculated by Welch-corrected two-tailed t test (from Stransky *et al.* (2022)⁷⁸, modified).

Interestingly, while TRAM-34 had no effects on plating efficiency in DMEM medium, it reduced plating efficiency of both human U-87MG and U-251MG cell lines when cultured in NSC medium. Only moderate direct tumoricidal effects were expected, as one previous study found tumoricidal effects only with an IC_{50} value of $14 \mu M^{60}$. In contrast, we used TRAM-34 concentrations of $5 \mu M$ in our experiments, which is only slightly above brain concentrations of TRAM-34 observed in murine and rat models^{56,79}.

Next, we tested $K_{Ca}3.1$'s potential role in radiosensitization. We found an increase in TRAM-34-sensitive $K_{Ca}3.1$ channel activity after irradiation in SMA-560 cells (as shown in Supplementary Figure S2 in Stransky *et al.* (2022)⁸⁰), which coincided with increased radioresistance in other glioma cell lines^{64,81}. In contrast, we found no convincing radiosensitizing effects of TRAM-34 (Figure 3), except for small radiosensitizing effects in SMA-540 cells (NSC medium).

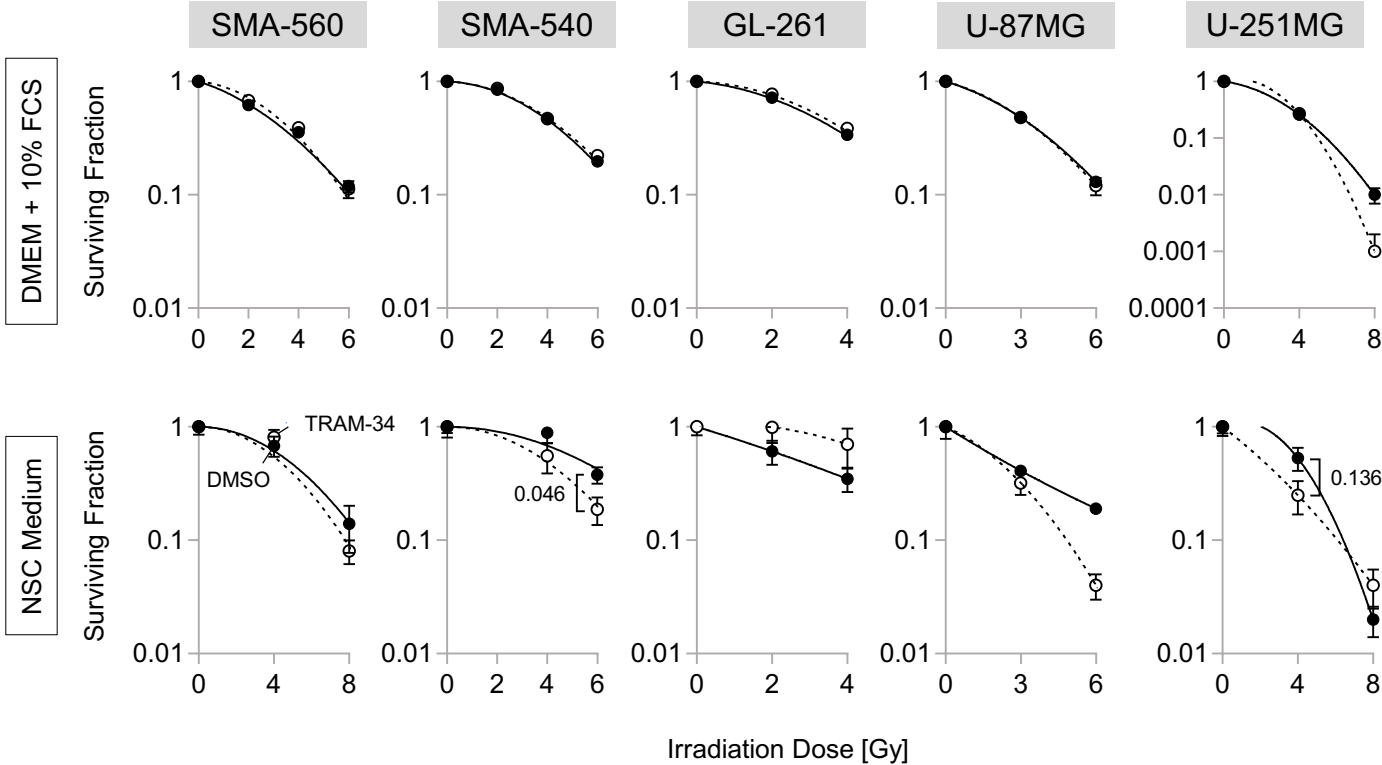


Figure 3: Radiosensitizing effects of TRAM-34 in selected glioma cell lines. Shown are the survival fraction as determined by colony formation assay (upper panels) or limited dilution assay (lower panels) after TRAM-34 (0 vs. $5 \mu M$) and radiation (0-8 Gy) treatment. Shown are mean values \pm sem of 3 independent experiments. Numbers indicate P value as calculated by Welch-corrected two-tailed t test from Stransky *et al.* (2022)⁷⁸, modified).

Conversely, a numerical increase of the surviving fraction after radiation and TRAM-34 treatment was observed for GL-261 cells (NSC medium), indicating increased radioresistance after TRAM-34 treatment.

Last, we tried to corroborate the previously described TMZ-sensitizing effects of TRAM-34. TRAM-34 had little additional effect on TMZ-sensitivity with the notable exception of U-87MG cells, when cultured in NSC medium, which showed a marked decrease of plating efficiency after the addition of TRAM-34 to TMZ (Figure 4). Furthermore, in our hands, GL-261 cells were not sensitized towards TMZ treatment in contrast to earlier findings⁶². Of note, GL-261 and U-251MG cells were very sensitive to TMZ treatment alone, making further reductions in plating efficiency after addition of TRAM-34 difficult to observe (Figure 4).

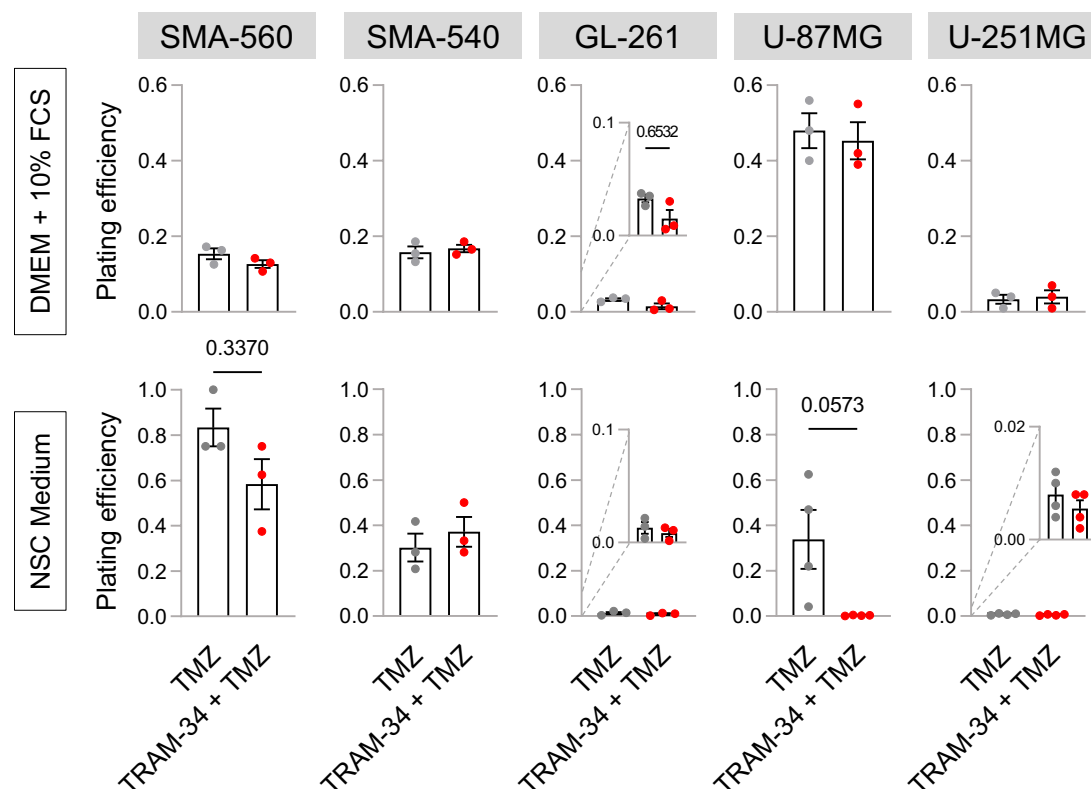


Figure 4: Temozolomide-sensitizing effects in selected glioma cell lines. Figure panels show plating efficiency as determined by colony formation assay (upper panels) or limited dilution assay (lower panels) after temozolomide (TMZ; 30 μ M) and TRAM-34 (0 vs. 5 μ M) treatment. Shown are individual data of 3-4 independent experiments and mean values \pm sem. Numbers indicate *P* values as calculated by Welch-corrected two-tailed t test from Stransky *et al.* (2022)⁷⁸, modified).

Our *in vitro* results of the $K_{Ca}3.1$ blocker TRAM-34 point towards small effects on glioma cell clonogenicity, radiosensitization and TMZ-sensitization. Interestingly, we found an increased susceptibility to TRAM-34 treatment in U-87MG and U-251MG cells

in stem-cell enriching NSC medium, which is in contrast to the generally expected higher therapy resistance of stem cells^{82,83}. While increased *KCNN4* mRNA expression in NSC as compared to DMEM culture medium may partly explain the higher susceptibility in U-251MG cells (Figure 5e), no such differences were observed for U-87MG cells (Figure 5d).

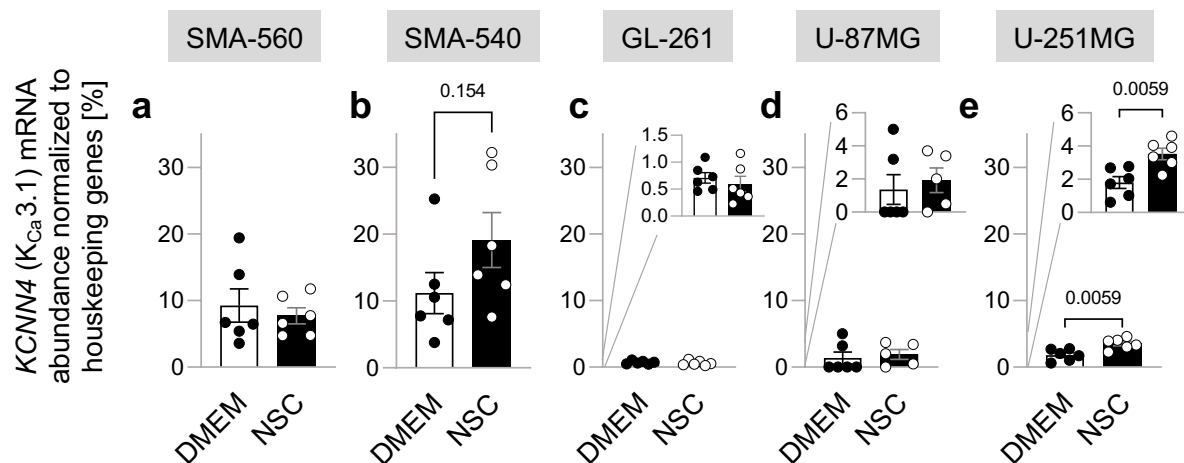


Figure 5: *KCNN4* mRNA expression of the glioma cell lines. mRNA abundances were normalized to the housekeeping genes *Pdhb1* and *GAPDH*. Shown are individual data points in addition to mean values \pm sem. Numbers (b, e) indicate *P* values as calculated by Welch-corrected two-tailed t-test (from Stransky *et al.* (2022)⁷⁸, modified).

An alternative explanation of the differential effects may be a lower free TRAM-34 concentration due to its high protein plasma binding⁷⁹ in the DMEM + 10% FCS medium. To exclude this possibility, we performed further experiments with U-87MG cells in DMEM + 1% FCS, as U-87MG cells showed the largest sensitivity towards TRAM-34's tumoricidal effects when cultured in NSC medium. Nevertheless, reductions in the amount of FCS did not lead to tumoricidal effects of TRAM-34 (as shown in Supplementary Figure S4 in Stransky *et al.* (2022)⁷⁸). This makes differences in free TRAM-34 concentrations as the explanation for differential effects in both media unlikely. Overall, these data point toward different susceptibilities to TRAM-34 treatment depending on both cell line and cultivation conditions, which was not explained by differences in the abundance of its target structure $K_{Ca}3.1$. Considering glioblastoma's high degree of inter- and intratumoral heterogeneity^{84,85}, these findings question the translatability of TRAM-34 for glioblastoma treatment.

Next, we studied TRAM-34's effects in an immune-competent, orthotopic murine glioma model. Compared to other commonly used syngeneic glioma models, SMA-560 cells expressed significantly more *KCNN4* mRNA as compared to GL-261 cells (Figure 5a, c) and, according to previous reports, show a higher transplantation success rate

compared to SMA-540 cells⁸⁶. Hence, we chose the SMA-560 VM/Dk glioma model for further testing. SMA-560 cells were originally derived from a spontaneously developed glioma in a VM/Dk mouse and serially re-transplanted into other VM/Dk mice^{87,88} to select for reliably tumor-initiating clones. In this way, several different clones (e.g., SMA-560 or SMA-540) were established and are since then commonly used as syngeneic glioma models in VM/Dk mice.

After injection of 5000 SMA-560 cells into the right striatum of VM/Dk mice (Figure 6a), tumors developed rapidly within few days and were identifiable both macro- and microscopically (Figure 6a, b). To test for functional expression of $K_{Ca}3.1$ after the transplantation of SMA-560 cells, we extracted the visible tumor 17-18 days after tumor cell injection and subsequently isolated the cells. *KCNN4* mRNA abundance was similar to or higher in two tumor lysates as compared to SMA-560 cells cultured *in vitro* (both culture media, Figure 6c). Phenotypic differences in cancer cells (as compared to non-cancer cells) made direct assessments of cancer cells via patch clamp experiments possible (Figure 6d, e; cancer cells are indicated by red arrows). In whole-cell patch clamp recordings, cancer cells showed an inward-rectifying potassium current after treatment with the $K_{Ca}3.1$ channel opener 1-EBIO, which was inhibited by additional application of TRAM-34 (Figure 6f-h, performed by Stephan M. Huber). Taken together, these data indicate a retained functional expression of $K_{Ca}3.1$ in SMA-560 cells after transplantation into VM/Dk mice.

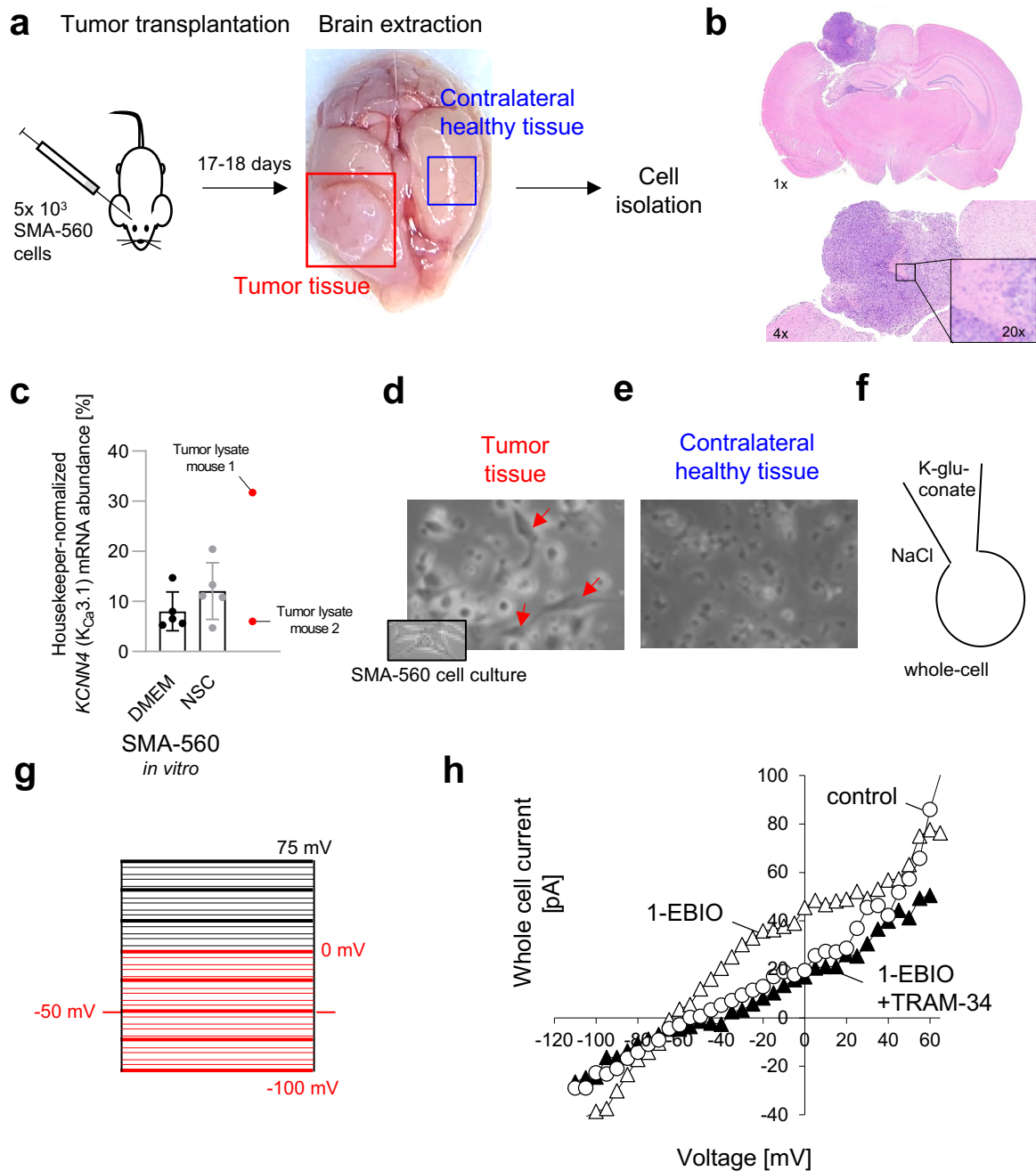


Figure 6: K_{Ca}3.1 is functionally expressed in SMA-560 cells after transplantation into VM/Dk mice. **a**, Tumor formation is accomplished by injecting 5000 SMA-560 cells into the right striatum of anaesthetized VM/Dk mice. 17-18 days after tumor cell injection, mice are sacrificed, tumor tissue (indicated by red rectangle) extracted and cells isolated (as described previously⁸⁹). **b**, Tumor presents with a very high cell density (as compared to the contralateral healthy tissue) and a partly necrotic core (as shown in 20x magnification). **c**, *KCNN4* (K_{Ca}3.1) mRNA abundance of tumor lysates is comparable to *KCNN4* mRNA abundance of SMA-560 cells cultured *in vitro*. mRNA abundance was normalized to housekeeping genes *Pdhb1* and *GAPDH*. **d**, **e**, After cell isolation of tumor tissue, some cells adhered to culture plates (indicated by red arrows) with a close phenotypical similarity to SMA-560 cells cultured *in vitro* (shown in black box). Cells retained their culture forming ability for several passages, indicating that they are cancer cells. No such cells were found when cells from the contralateral,

healthy hemisphere were plated. **f-g**, Whole-cell patch clamp experiments with adherent cells (indicated by red arrow in **d**) indicate 1-EBIO activated, TRAM-34-inhibited current. Inward-rectification and reversal potential close to K^+ equilibrium potential both indicate $K_{Ca}3.1$ expression. Patch clamp recordings were performed by Stephan M. Huber (from Stransky *et al.* (2023)⁸⁰).

Treatment of the mice was started 7 days after tumor cell injection and consisted of daily TRAM-34 application (0 vs. 120 mg/kg bodyweight via intraperitoneal injection) and additional irradiation of parts of the tumor-bearing hemispheres (0 vs. 4 Gy) on 5 consecutive days (Figure 7a). TRAM-34 was applied 6 hours before irradiation. Afterwards, animals were regularly monitored and taken off the study, as soon as they reached previously defined termination criteria (among others: weight loss $\geq 20\%$, neurologic symptoms, such as tremor or seizures, or signs of apathy).

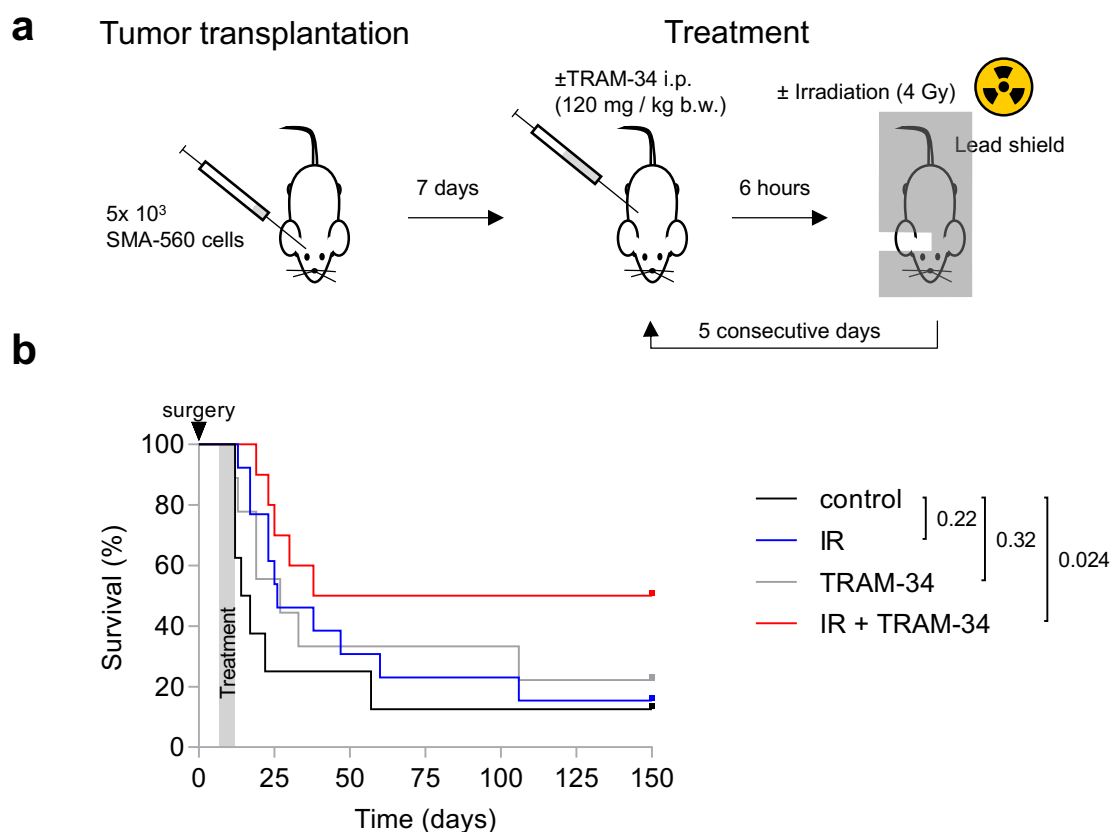


Figure 7: Combined radiation and TRAM-34 treatment prolongs survival in the syngeneic SMA-560 VM/Dk glioma model. **a**, Treatment algorithm. 7 days after tumor cell injection, the treatment is initiated. Treatment consists of TRAM-34 (0 vs. 120 mg/kg body weight) followed 6 hours afterwards by irradiation (0 vs. 4 Gy), for 5 consecutive days. **b**, Kaplan-Meier estimator from day of tumor cell injection. Shown are results of 8-13 mice per group. Grey area indicates treatment period of animals, numbers indicate P values as calculated by log-rank Mantel-Cox test (from Stransky *et al.* (2023)⁸⁰).

All animals were randomized to the respective treatment group (<https://www.randomizer.org/>). In addition, pharmacologic treatment was applied fully blinded until data analysis, whereas irradiation was applied in an un-blinded fashion due to organizational difficulties. The median overall survival of animals from the control arm was 16 days, which is comparable to previously described survival times^{90,91} (Figure 7b). Neither TRAM-34 nor irradiation alone resulted in significantly prolonged survival times of the mice. Missing efficacy of radiation treatment alone has been reported before in this glioma model^{90,92}. Although the authors used a single-dose irradiation of 12 Gy, both 5x 4 Gy and 1x 12 Gy irradiation are comparable when calculating the equivalent dose in 2 Gy fractions (EQD2, assuming an alpha/beta ratio of 10 Gy for SMA-560 cells), giving EQD2s of 22 or 23.3 Gy, respectively. In contrast, the combined radiation and TRAM-34 treatment led to an increased survival of mice in our experiments (median survival time = 38 days).

To exclude differential effects of fractionated versus single-dose irradiation on SMA-560's intrinsic radiosensitivity, we additionally performed clonogenic survival assays with SMA-560 cells after fractionated irradiation *in vitro*. Concordant to our results after single-dose irradiation (Figure 3), we found no meaningful radiosensitizing effects of TRAM-34 in SMA-560 cells after irradiation with 5x 4 Gy *in vitro* (Figure 8). This led us to explore other potential mechanisms of action.

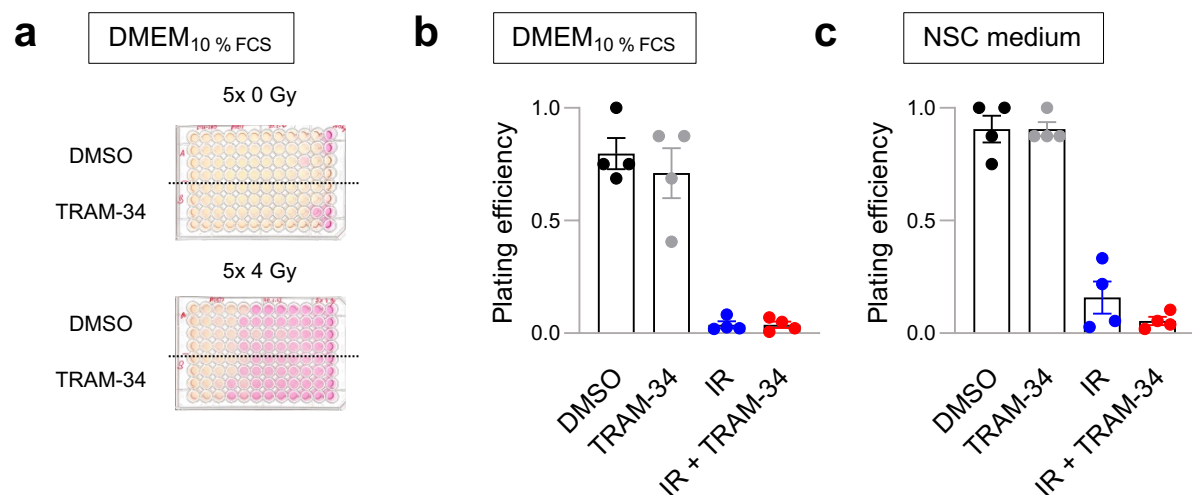


Figure 8: TRAM-34 does not lead to radiosensitization after fractionated irradiation (5x 4 Gy) in SMA-560 cells *in vitro*. **a**, Representative image of one independent experiment. **b**, **c**, Plating efficiencies of TRAM-34 (0 vs. 5 μ M) and radiation (5x 0 vs. 5x 4 Gy) treated SMA-560 cells in DMEM + 10% FCS or NSC medium as determined by limited dilution assays. Shown are individual values of 4 independent experiments and means \pm sem (from Stransky *et al.* (2023)⁸⁰, modified).

As extensive prior work established K_{Ca}3.1's role in glioma cell migration⁵⁶⁻⁵⁸, we analyzed *in vivo* growth patterns and developed a scoring system for tumor growth (Figure 9a, b). Most animals in the control (but also irradiation only group) developed small (score 2) or medium-to-large-sized tumors (score 3). One animal in the control group showed only signs of gliosis (score 1), whereas one animal in the IR group showed no changes as compared to the contralateral healthy hemisphere (score 0). Both findings could hint towards technical issues during tumor cell injection, tumor rejection or clearance by treatment (only in treated animals). In the TRAM-34 or TRAM-34 and radiation-treatment groups, more animals presented with no changes or only gliosis, potentially caused by the respective treatment. However, direct comparisons are to be made cautiously, as not the whole brains of all mice were analyzed immunohistochemically. Therefore, one cannot exclude that deeper brain sections may contain larger tumor areas.

Apart from the region of tumor cell injection (Figure 9c, indicated by an arrow), several mice developed multiple satellite tumors, indicating cancer cell invasion into other brain areas (indicated by an arrowhead). Interestingly, such satellite tumors developed in 80% of brains of mice in the radiation treatment group, whereas no animal (0/6) of the combined radiation and TRAM-34 treatment group developed satellite tumors. An irradiation-induced hypermigration of glioma cells has been described by others^{76,93} and may explain the modest effect of radiation treatment alone on mouse survival. In general, satellite tumor formation (also called multifocal glioblastoma) has been associated with worse prognosis in glioma⁹⁴ and may counteract tumor growth inhibiting effects of irradiation to some extent. Hence, TRAM-34 may synergize with radiation treatment and prolong survival of the animals by inhibiting the irradiation-induced hyperinvasion of SMA-560 cells.

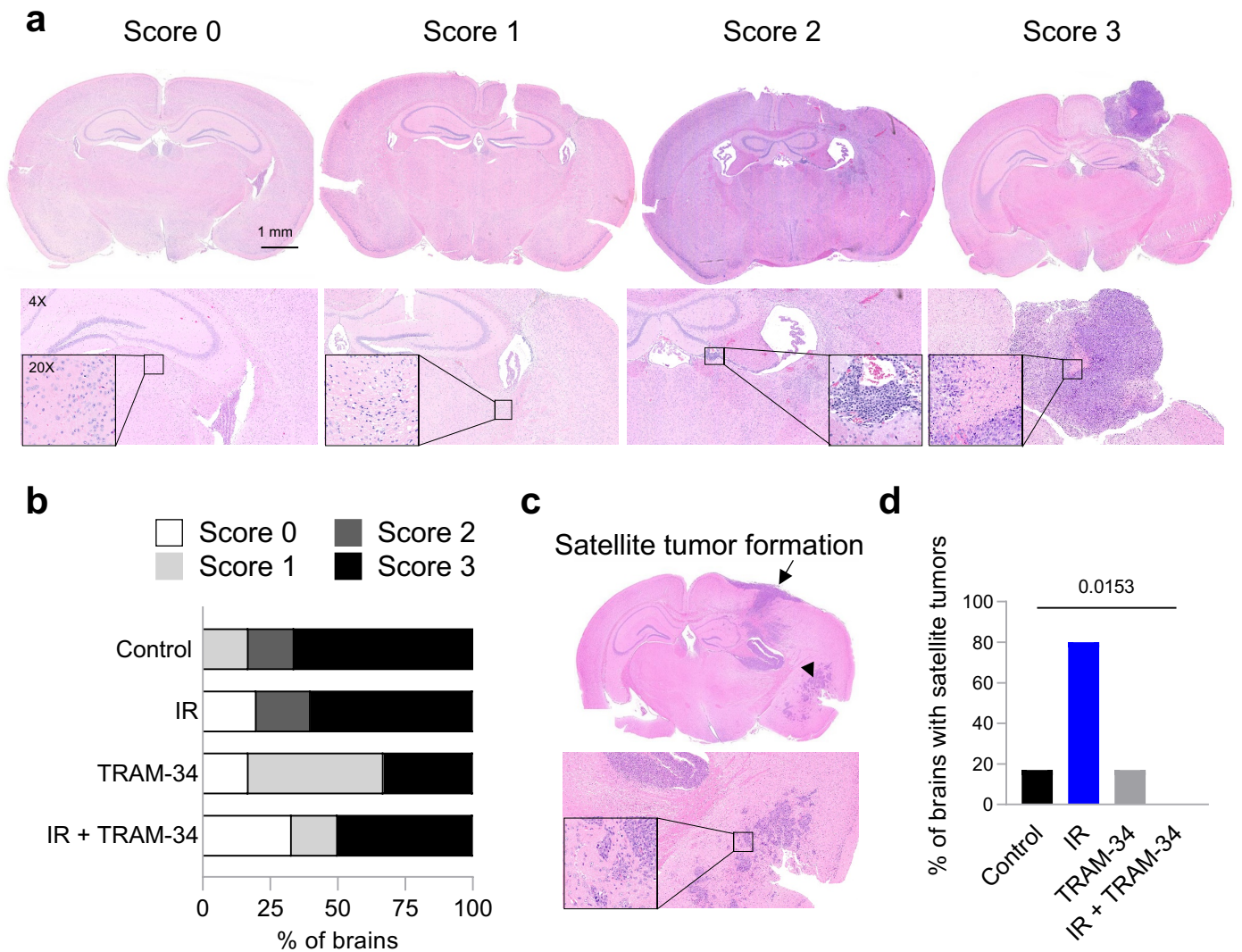


Figure 9: TRAM-34 inhibits irradiation-induced hypermigration in the SMA-560 VM/Dk glioma model. **a**, Representative images of each score at 1X, 4X and 20X magnification as indicated. **b**, Percentage of animals presenting with each respective score in each treatment group. **c**, Several animals developed multiple satellite tumors (indicated by arrowhead) apart from the main tumor in the area of tumor cell injection (indicated by an arrow). **d**, Depicted is the percentage of animals of each treatment arm which showed signs of satellite tumor formation. Results are from 5-6 animals per treatment arm. Number indicates *P* value as calculated by two-tailed Fisher's Exact test. Histological stainings were performed by Leticia Quintanilla-Martinez and Irene Gonzalez-Menendez (from Stransky *et al.* (2023)⁸⁰, modified).

In contrast to our *in vivo* findings, *in vitro* migration assays (wound healing and transwell migration assays) in SMA-560 cells did not delineate irradiation-induced or TRAM-34-sensitive migration velocities (Figure 10a, b). This might hint towards changes of invasive, rather than migratory processes induced by irradiation *in vivo*. Accordingly, irradiation triggered the secretion of TGF- β 1 in SMA-560 cells, coinciding with an upregulation of the Matrix metalloproteinase 9 (*MMP-9*) expression, which was

inhibited by concomitant TRAM-34 application (Figure 10c, d). MMP-9 is a well-known contributor to the degradation of extracellular matrix and hence facilitates the invasion of glioma cells^{95,96}.

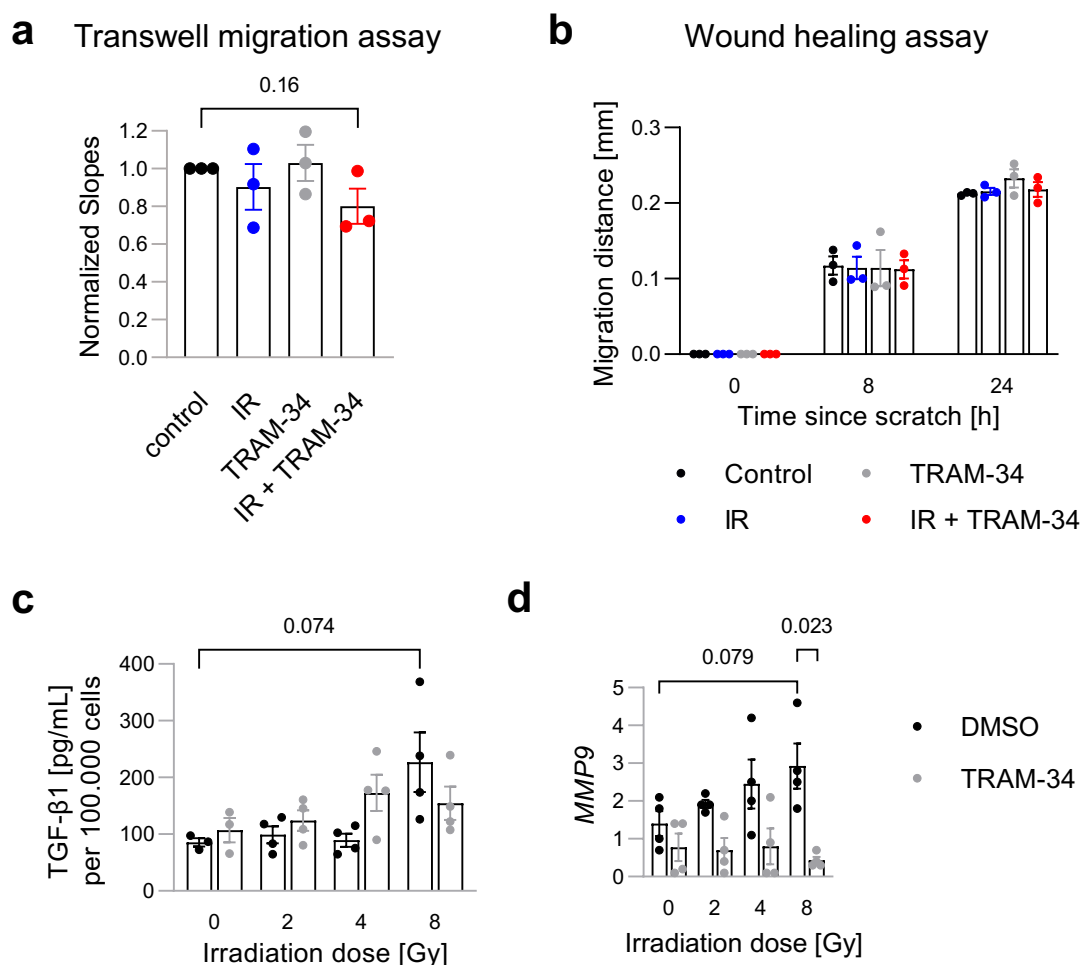


Figure 10: Irradiation induces TRAM-34 sensitive *MMP9* expression, which does not translate into increased migration velocities in SMA-560 cells *in vitro*. **a**, Normalized slopes of mean impedance increase (as a measure of transwell migration) after TRAM-34 (0 or 5 μ M) and radiation (0 vs. 2 Gy) co-treatment. **b**, Migration distances after TRAM-34 (0 or 5 μ M) and radiation (0 vs. 2 Gy) treatment as determined in wound healing assay. **c**, TGF- β 1 secretion after TRAM-34 (0 or 5 μ M) and radiation (0 vs. 2 Gy) treatment as determined by enzyme-linked immunosorbent assay. **d**, *MMP9* mRNA abundance (normalized to housekeepers *GAPDH* and *Pdhh1*) after TRAM-34 (0 or 5 μ M) and radiation treatment as determined in quantitative reverse-transcriptase PCR. Individual data points of 3-4 independent experiments and means \pm sem are shown. Numbers indicate *P* values as calculated by Welch-corrected two-tailed t-tests (from Stransky *et al.* (2023)⁸⁰, modified).

However, on a more general note, the development of invasion/metastasis-pathway-targeting drugs (such as MMP inhibitors) has mostly resulted in negative late stage clinical trials^{97,98}. The underlying reason may arguably be the early invasion of cancer cells even before the initial diagnosis has been made⁹⁹. For example, evidence of

whole brain invasion exists for IDH-mutated gliomas¹⁰⁰, potentially making anti-invasive therapies futile in later disease stages. Compared to the clinical situation, treatment in preclinical cancer models can be started at very early stages (7 days after tumor inoculation in our study), when invasion-inhibiting effects may still confer large differences in outcome. Hence, the results of the aforementioned randomized controlled trials at least question the translational potential of drugs, mostly targeting invasive processes in cancer cells.

Next, we analyzed effects of the combined treatment on the tumor microenvironment. To compare animals from the different treatment groups, scoring systems for each immunohistochemistry marker were defined with the help of Leticia Quintanilla-Martinez and Irene Gonzalez-Menendez (Institute of Pathology and Neuropathology, University of Tübingen). In short, scores of 0 indicate no difference as compared to the contralateral healthy hemisphere. Scores 1 and 2 indicate increasing amounts of positive cells of each respective staining. As the tumor mass in glioblastoma is made up of high proportions of tumor-associated macrophages/microglia (TAMs)¹⁰¹, we analyzed the composition of activated TAMs. We found a pronounced increase in Iba1⁺ macrophages in or nearby the tumor (Figure 11a), with larger tumors associated with higher amounts of Iba1⁺ cells. Very large tumors showed pseudopalisading TAMs at the edges of the tumor mass (as shown in Supplementary Figure S8 in Stransky *et al.* (2023)⁸⁰). In addition, we analyzed another macrophage marker, CD68, which correlated well with the Iba1 staining, with generally lower amounts of CD68⁺ cells (Figure 11b). This is expected, as Iba1 is commonly referred to as a pan-macrophage marker, whereas CD68 is more specific for phagocytic macrophages¹⁰². Treatment showed little effect on the general composition of activated TAMs.

As mentioned in the introduction, K_{Ca}3.1's role in immune cell function is well documented. Hence, we analyzed T cell infiltration and found high-moderate increases of CD3⁺ T cells (Figure 11c), a moderate increase of CD8⁺ cytotoxic T cells (Figure 11d) and a mostly low presence of FoxP3⁺ regulatory T cells (Figure 11e) in the tumor-bearing hemisphere. T cell numbers were not different among the four treatment arms. Overall, these results indicate little effects of radiation, TRAM-34 or their combination on the general composition of the tumor microenvironment in the SMA-560 VM/Dk glioma model. Importantly, our results are not able to differentiate macrophage subtypes, as has been performed by Grimaldi *et al.*⁶³.

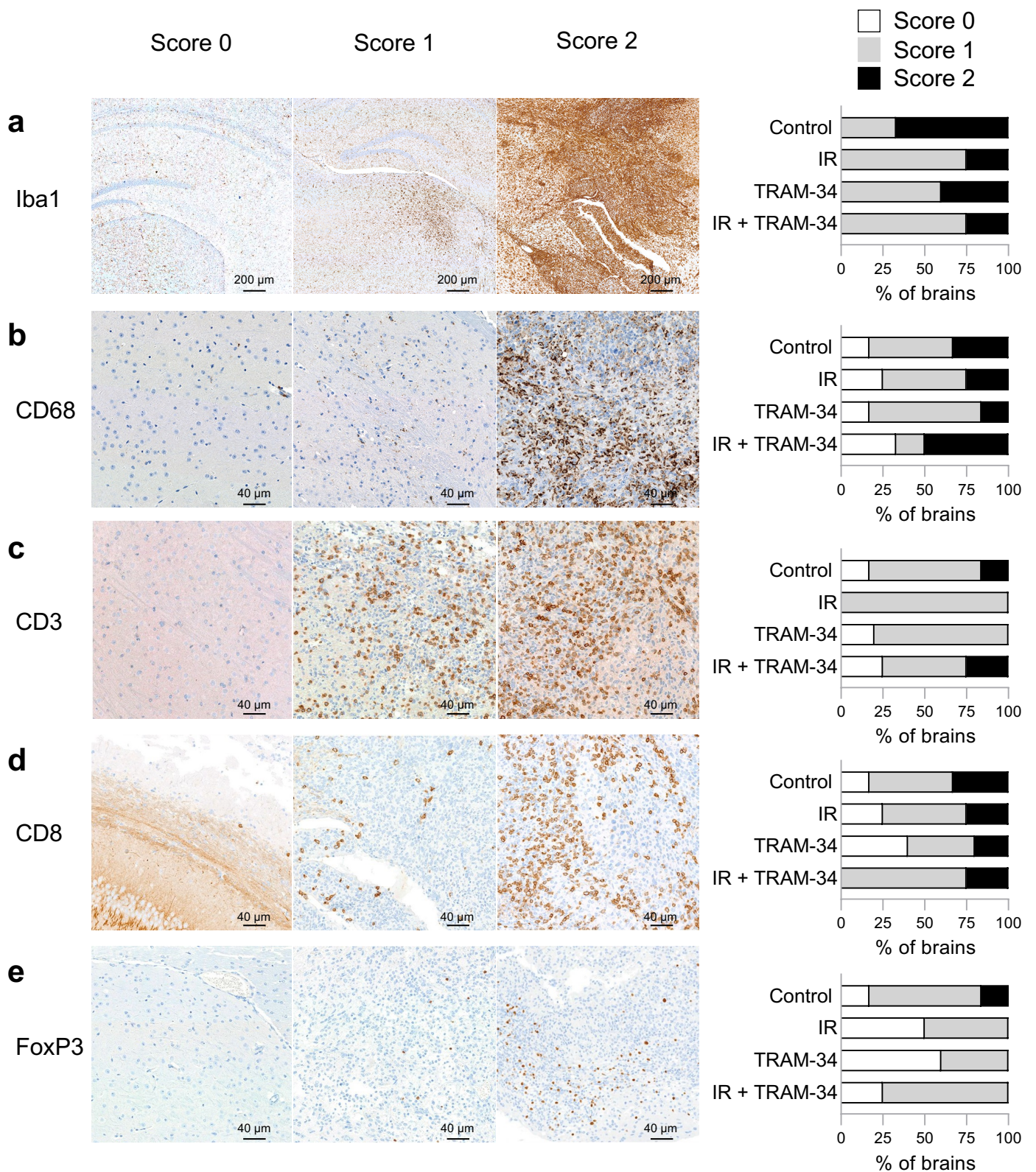


Figure 11: Radiation and/or TRAM-34 treatment do not exert changes in the tumor microenvironment in the SMA-560 VM/Dk glioma model. Representative micrographs of brains of each score of, **a**, Iba1, **b**, CD68, **c**, CD3, **d**, CD8 and, **e**, FoxP3. Additionally depicted is the percentage of animals presenting with each score (right side,

respectively). Of note, the brain parenchyma showed a non-specific staining with the anti-CD8 antibody, which did, however, not interfere with the identification of CD8⁺ T cells in the tumor. Number of animals: control (6 animals), IR only (4 animals), TRAM-34 only (5 animals) and IR + TRAM-34 (4 animals). Histological stainings were performed by Leticia Quintanilla-Martinez and Irene Gonzalez-Menendez (from Stransky *et al.* (2023)⁸⁰, modified).

Nevertheless, our data suggest against a decreased invasion of CD8⁺ T cells into the tumor tissue by the inhibition of K_{Ca}3.1, which could have been expected from earlier research¹⁰³. This was of particular concern, as the infiltration of CD8⁺ T cells has been found to represent an independent predictor for effective radiotherapy in several cancer models^{104,105}, and, also, a more general favorable prognostic factor in glioblastoma patients^{106,107}.

Last, to assess the tolerability of the combined treatment, weight changes as well as changes of blood counts were analyzed. All animals lost weight during the therapy, most likely due to the stress induced by daily injections or anesthesia (necessary for the radiation treatment), but, importantly, irrespective of treatment group (Figure 12a). Larger bounds of variations at later time points are largely explained because not all animals were weighed daily at these timepoints, reducing the number of animals analyzed and, hence, increasing the resulting standard errors. White blood counts, lymphocytes, neutrophils, red blood counts and hemoglobin concentration were determined as additional proxies for toxicity and, more specifically, because K_{Ca}3.1 plays an important role for volume regulation in erythrocytes⁷². White blood counts remained more or less stable before and after treatment (Figure 12c). There was a slight numerical reduction in lymphocytes at later timepoints in every treatment group as compared to animals from the control group (Figure 12d). The number of neutrophils increased after treatment in all animals, potentially also indicating increased stress (Figure 12e). Both red blood counts and hemoglobin levels increased slightly at later time points, irrespective of treatment group (Figure 12f, g). At best, hemoglobin levels in treated animals were slightly below those of control animals at later timepoints. Overall, these results indicate few treatment-specific adverse events, corroborating previous findings of *KCNN4* knockout mice^{72,73} and few adverse events of the K_{Ca}3.1 blocker senicapoc in a phase III study of sickle cell patients⁷⁴.

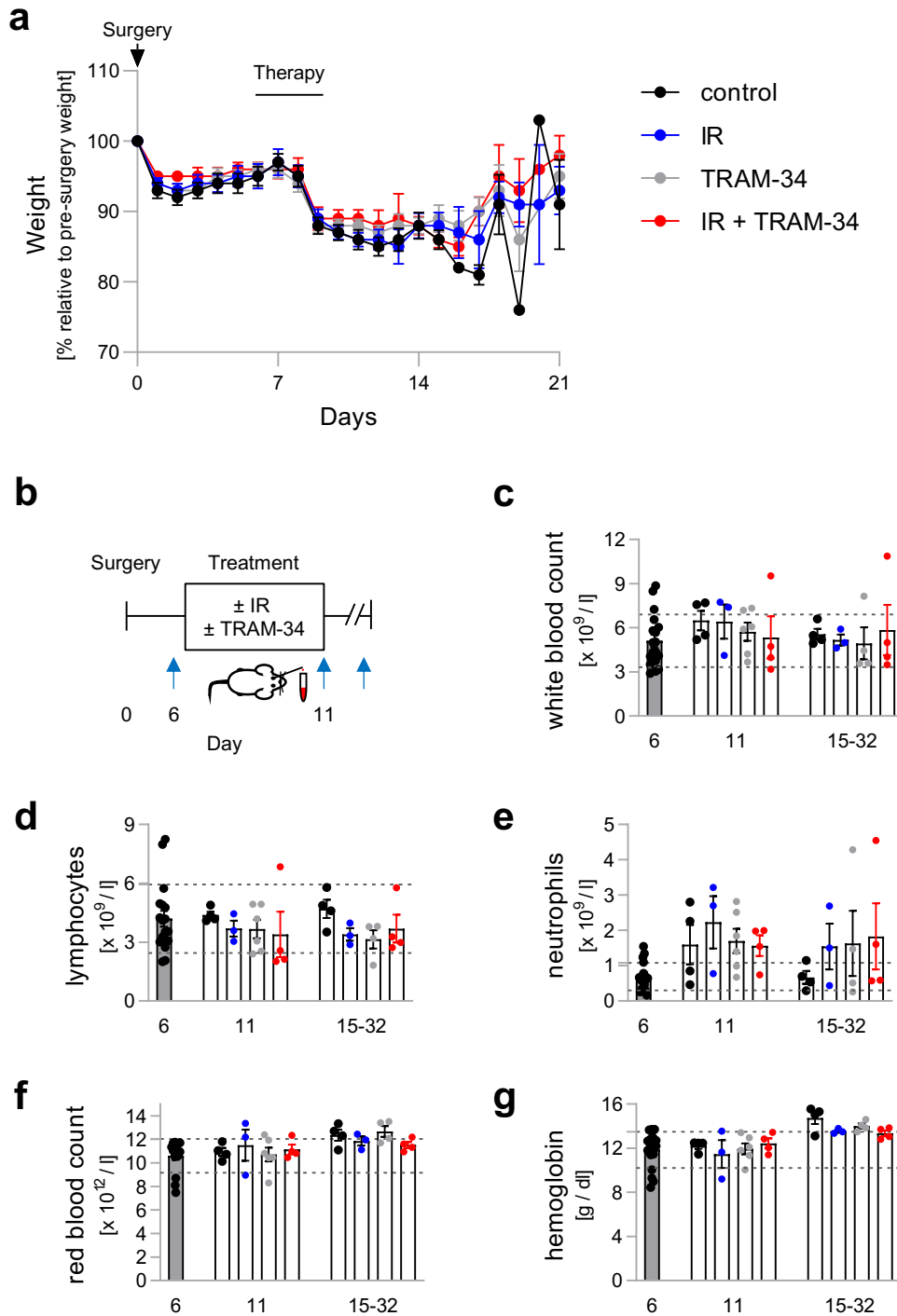


Figure 12: No treatment-specific adverse effects were detected. **a**, Weight change of animals relative to the weight before surgery of all animals depicted as mean \pm sem ($n = 15-19$ animals per treatment group). **b**, Time points of blood draw are indicated by blue arrows. **c-g**, Blood counts of different cell lines and hemoglobin concentration on day 6 (day before start of the treatment), day 11 (shortly after the last treatment) and days 15-32 (medium-term after treatment). All data points are representative of one animals. Additionally depicted are the means \pm sem. Dashed lines indicate 'normal' ranges, defined as mean values \pm 1 standard deviation of the mice before the treatment was initiated (from Stransky *et al.* (2023)⁸⁰, modified).

Overall, although TRAM-34 led to decreased clonogenicity or increased temozolomide-sensitivity in U-87MG and U-251MG cells in NSC medium, the overall *in vitro* effects of TRAM-34 were modest in our studies. Results observed in the SMA-560 VM/Dk glioma model hint towards synergistic effects of TRAM-34 to irradiation, probably by inhibiting irradiation-induced hyperinvasion of cancer cells. However, as described above, experience with other metastasis/invasion-pathway-inhibiting drugs questions the translatability of these effects to the clinics.

Finally, focusing on or selectively reporting the few beneficial effects of interventions, such as the cell lines and conditions in which TRAM-34 worked best in our studies, may produce an overly positive picture of new treatment approaches. Our further work¹⁰⁸ to analyze repurposing efforts in oncology may, arguably, hint towards this phenomenon. In our analysis, we found preclinical evidence of anti-cancer effects for 81 of the 100 most-often prescribed drugs, which are approved for non-cancer indications. In an additional analysis (not reported in the original manuscript), reports of anti-glioma effects were found for 47 of the 100 most-often prescribed drugs (Figure 13a). Both numbers are surprisingly high, especially given the lack of concordant clinical evidence of repurposed drugs' efficacy against cancer. Moreover, we assessed the methodological quality of the manuscripts. As such, the reporting quality of several items, such as cell type or animal species used, was moderate to good. However, few to none articles mentioned the usage of bias-reducing methods, such as blinding, preregistration or power calculations, a finding, which concurs with prior research¹⁰⁹. Only animals were randomized to the respective treatment groups in 58% of the *in vivo* studies (Figure 13b, c), which is a higher ratio than found by previous analyses^{109,110}. Nevertheless, the lack of blinding, preregistration or prior power calculations may bias the research findings towards higher effect sizes^{4,77,111}, ultimately leading to an abundance of false-positive findings¹¹².

A commonly discussed reason for this phenomenon is the academic reward system, which rewards high numbers of published articles, preferably in high-impact journals^{113,114}. To achieve this, researchers may choose to focus on the cell lines, in which the interventions work best, while simultaneously neglecting the application of bias-reducing methods. Both factors contribute to publication bias^{115,116} and, potentially also to the very low successful translation rates of both *de novo* and repurposed drug candidates in oncology^{117–119}.

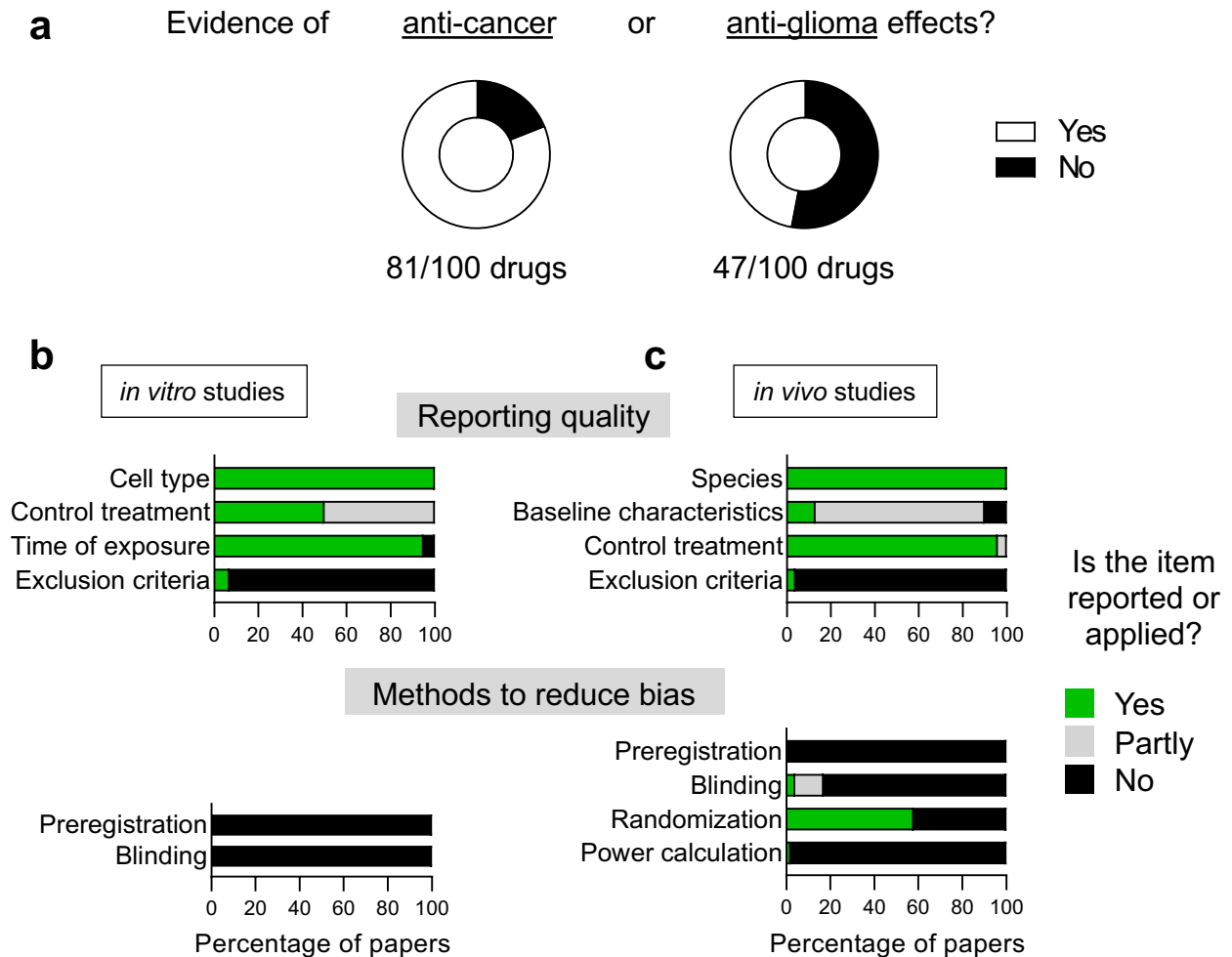


Figure 13: There exists preclinical evidence for anti-cancer or anti-glioma effects for a high number of often-prescribed drugs, which are approved for other indications. **a**, Number of often-prescribed drugs for which preclinical anti-cancer or anti-glioma effects were identified. For anti-glioma effects, an additional search strategy, according to the methods as described in the main manuscript¹⁰⁸, was conducted (<Name of drug> AND [glioblastoma OR glioma]). **b**, **c**, Methodological quality of articles, as indicated by the usage or application of respective item in **(b)** 50 *in vitro* and **(c)** 41 *in vivo* studies (from Stransky *et al.* (2021)¹⁰⁸, modified).

In contrast to the necessary long-term changes in the reward system, there are potential ‘quick-fixes’, which may alleviate the lack of new treatment options in the short-to-medium-term. First, increases in the numbers of clinical trial participants, which are especially low in glioma patients^{120,121}. Second, performing platform trials, which can reduce the bureaucratic hurdles and, hence, also reduce times until efficacy (or futility) of a new treatment candidate is established¹²². One currently conducted platform trial in glioblastoma patients is the GBM AGILE trial¹²³, which recently announced the lacking efficacy of regorafenib¹²⁴ after the aforementioned positive results from the phase II trial REGOMA. Third, high-throughput screenings to establish

cancer cell vulnerabilities guiding patient-individual treatment selection¹²⁵, and hence overcome challenges caused by inter- (but also intra-) tumor heterogeneity. Fourth, higher rates of adherence to methods to reduce biases in preclinical research, such as power calculations, randomization, blinding and preregistration – all of which are commonly used in later-stage research to ensure high methodological rigor and increase the rates of reproducibility. Last, there exist exciting new treatment options, for example, antibody-cytokine conjugates⁴⁴, multi-valent chimeric antigen receptor (CAR) T cells^{126,127} or CAR NK cells¹²⁸, all of which may ultimately circumvent glioma's immunosuppressive and heterogenous nature.

In conclusion, prior work on the $K_{Ca}3.1$ blocker TRAM-34 has elucidated its potential efficacy as an anti-glioblastoma treatment. Most notably, anti-invasive effects were reported in several reports, in addition to its potential synergism to other standard treatments of glioblastoma patients. Our findings increase the confidence in the potential translatability of TRAM-34 only marginally, as we found pronounced differences of its efficacy against different glioma cell lines. Whether the new findings of $K_{Ca}3.1$'s role in inter-tumor communication networks⁶⁵ may further invigorate this line of research, remains an open question.

List of references

1. Stupp, R. *et al.* Effect of Tumor-Treating Fields Plus Maintenance Temozolomide vs Maintenance Temozolomide Alone on Survival in Patients With Glioblastoma: A Randomized Clinical Trial. *JAMA* **318**, 2306 (2017).
2. Stupp, R. *et al.* Radiotherapy plus Concomitant and Adjuvant Temozolomide for Glioblastoma. *The New England Journal of Medicine* **10** (2005).
3. Herrlinger, U. *et al.* Lomustine-temozolomide combination therapy versus standard temozolomide therapy in patients with newly diagnosed glioblastoma with methylated MGMT promoter (CeTeG/NOA-09): a randomised, open-label, phase 3 trial. *The Lancet* **393**, 678–688 (2019).
4. Button, K. S. *et al.* Power failure: why small sample size undermines the reliability of neuroscience. *Nature Reviews Neuroscience* **14**, 365–376 (2013).
5. Weller, M. *et al.* EANO guidelines on the diagnosis and treatment of diffuse gliomas of adulthood. *Nat Rev Clin Oncol* **18**, 170–186 (2021).
6. Weller, M. *et al.* Rindopepimut with temozolomide for patients with newly diagnosed, EGFRvIII-expressing glioblastoma (ACT IV): a randomised, double-blind, international phase 3 trial. *Lancet Oncol* **18**, 1373–1385 (2017).
7. Lassman, A. B. *et al.* Depatuxizumab mafodotin in EGFR-amplified newly diagnosed glioblastoma: A phase III randomized clinical trial. *Neuro Oncol* **25**, 339–350 (2023).
8. Omuro, A. *et al.* Radiotherapy combined with nivolumab or temozolomide for newly diagnosed glioblastoma with unmethylated MGMT promoter: An international randomized phase III trial. *Neuro Oncol* **25**, 123–134 (2022).
9. Weller, M. & Le Rhun, E. How did lomustine become standard of care in recurrent glioblastoma? *Cancer Treat Rev* **87**, 102029 (2020).
10. Wick, W. *et al.* Lomustine and Bevacizumab in Progressive Glioblastoma. *N Engl J Med* **377**, 1954–1963 (2017).
11. Tsien, C. *et al.* ACTR-32. NRG ONCOLOGY RTOG 1205: RANDOMIZED PHASE II TRIAL OF CONCURRENT BEVACIZUMAB AND RE-IRRADIATION VS. BEVACIZUMAB ALONE AS TREATMENT FOR RECURRENT GLIOBLASTOMA. *Neuro Oncol* **21**, vi20 (2019).
12. Reardon, D. A. *et al.* Effect of Nivolumab vs Bevacizumab in Patients With Recurrent Glioblastoma: The CheckMate 143 Phase 3 Randomized Clinical Trial.

JAMA Oncology **6**, 1003–1010 (2020).

13. Stupp, R. *et al.* NovoTTF-100A versus physician's choice chemotherapy in recurrent glioblastoma: a randomised phase III trial of a novel treatment modality. *Eur. J. Cancer* **48**, 2192–2202 (2012).
14. Cloughesy, T. F. *et al.* A randomized controlled phase III study of VB-111 combined with bevacizumab vs bevacizumab monotherapy in patients with recurrent glioblastoma (GLOBE). *Neuro Oncol* **22**, 705–717 (2020).
15. Lombardi, G. *et al.* Regorafenib compared with lomustine in patients with relapsed glioblastoma (REGOMA): a multicentre, open-label, randomised, controlled, phase 2 trial. *Lancet Oncol* **20**, 110–119 (2019).
16. Westphal, M. *et al.* Adenovirus-mediated gene therapy with sitimagene ceradenovec followed by intravenous ganciclovir for patients with operable high-grade glioma (ASPECT): a randomised, open-label, phase 3 trial. *Lancet Oncol* **14**, 823–833 (2013).
17. Batchelor, T. T. *et al.* Phase III randomized trial comparing the efficacy of cediranib as monotherapy, and in combination with lomustine, versus lomustine alone in patients with recurrent glioblastoma. *J Clin Oncol* **31**, 3212–3218 (2013).
18. Chinot, O. L. *et al.* Bevacizumab plus radiotherapy-temozolomide for newly diagnosed glioblastoma. *N Engl J Med* **370**, 709–722 (2014).
19. Gilbert, M. R. *et al.* A randomized trial of bevacizumab for newly diagnosed glioblastoma. *N Engl J Med* **370**, 699–708 (2014).
20. Stupp, R. *et al.* Cilengitide combined with standard treatment for patients with newly diagnosed glioblastoma with methylated MGMT promoter (CENTRIC EORTC 26071-22072 study): a multicentre, randomised, open-label, phase 3 trial. *Lancet Oncol* **15**, 1100–1108 (2014).
21. Blumenthal, D. T. *et al.* A Phase III study of radiation therapy (RT) and O⁶-benzylguanine + BCNU versus RT and BCNU alone and methylation status in newly diagnosed glioblastoma and gliosarcoma: Southwest Oncology Group (SWOG) study S0001. *Int J Clin Oncol* **20**, 650–658 (2015).
22. Westphal, M. *et al.* A randomised, open label phase III trial with nimotuzumab, an anti-epidermal growth factor receptor monoclonal antibody in the treatment of newly diagnosed adult glioblastoma. *Eur J Cancer* **51**, 522–532 (2015).
23. Kong, D.-S. *et al.* Phase III randomized trial of autologous cytokine-induced killer cell immunotherapy for newly diagnosed glioblastoma in Korea. *Oncotarget* **8**, 7003–

7013 (2017).

24. Narita, Y. *et al.* A randomized, double-blind, phase III trial of personalized peptide vaccination for recurrent glioblastoma. *Neuro Oncol* **21**, 348–359 (2019).
25. Cloughesy, T. F. *et al.* Effect of Vocimagene Amiretrorepvec in Combination With Flucytosine vs Standard of Care on Survival Following Tumor Resection in Patients With Recurrent High-Grade Glioma: A Randomized Clinical Trial. *JAMA Oncol* **6**, 1939–1946 (2020).
26. Lim, M. *et al.* Phase III trial of chemoradiotherapy with temozolomide plus nivolumab or placebo for newly diagnosed glioblastoma with methylated MGMT promoter. *Neuro Oncol* **24**, 1935–1949 (2022).
27. Liao, L. M. *et al.* Association of Autologous Tumor Lysate-Loaded Dendritic Cell Vaccination With Extension of Survival Among Patients With Newly Diagnosed and Recurrent Glioblastoma: A Phase 3 Prospective Externally Controlled Cohort Trial. *JAMA Oncol* **9**, 112–121 (2023).
28. Pushpakom, S. *et al.* Drug repurposing: progress, challenges and recommendations. *Nat Rev Drug Discov* **18**, 41–58 (2019).
29. Yongjun, Y. *et al.* Atorvastatin suppresses glioma invasion and migration by reducing microglial MT1-MMP expression. *Journal of Neuroimmunology* **260**, 1–8 (2013).
30. Arrieta, O. *et al.* Blockage of angiotensin II type I receptor decreases the synthesis of growth factors and induces apoptosis in C6 cultured cells and C6 rat glioma. *Br J Cancer* **92**, 1247–1252 (2005).
31. Zhong, S. *et al.* Disulfiram in glioma: Literature review of drug repurposing. *Front Pharmacol* **13**, 933655 (2022).
32. Zirjacks, L. *et al.* Repurposing Disulfiram for Targeting of Glioblastoma Stem Cells: An In Vitro Study. *Biomolecules* **11**, 1561 (2021).
33. Kast, R. E., Karpel-Massler, G. & Halatsch, M.-E. CUSP9* treatment protocol for recurrent glioblastoma: aprepitant, artesunate, auranofin, captopril, celecoxib, disulfiram, itraconazole, ritonavir, sertraline augmenting continuous low dose temozolomide. *Oncotarget* **5**, 8052–8082 (2014).
34. Halatsch, M.-E. *et al.* In Vitro and Clinical Compassionate Use Experiences with the Drug-Repurposing Approach CUSP9v3 in Glioblastoma. *Pharmaceuticals (Basel)* **14**, 1241 (2021).
35. Ashburn, T. T. & Thor, K. B. Drug repositioning: identifying and developing new

- uses for existing drugs. *Nat Rev Drug Discov* **3**, 673–683 (2004).
36. Palumbo, A. *et al.* Thalidomide for treatment of multiple myeloma: 10 years later. *Blood* **111**, 3968–3977 (2008).
 37. Friesen, C., Roscher, M., Alt, A. & Miltner, E. Methadone, commonly used as maintenance medication for outpatient treatment of opioid dependence, kills leukemia cells and overcomes chemoresistance. *Cancer Res* **68**, 6059–6064 (2008).
 38. Friesen, C. *et al.* Cell death sensitization of leukemia cells by opioid receptor activation. *Oncotarget* **4**, 677–690 (2013).
 39. Friesen, C. *et al.* Opioid receptor activation triggering downregulation of cAMP improves effectiveness of anti-cancer drugs in treatment of glioblastoma. *Cell Cycle* **13**, 1560–1570 (2014).
 40. deutschlandfunk.de. Über Krebs und Hoffnung - Der Fall Methadon. *Deutschlandfunk* <https://www.deutschlandfunk.de/ueber-krebs-und-hoffnung-der-fall-methadon-100.html>.
 41. Theile, D. & Mikus, G. Methadone against cancer: Lost in translation. *International Journal of Cancer* **143**, 1840–1848 (2018).
 42. Vatter, T. *et al.* Against Repurposing Methadone for Glioblastoma Therapy. *Biomolecules* **10**, 917 (2020).
 43. Lin, K. *et al.* Mechanism-based design of agents that selectively target drug-resistant glioma. *Science* **377**, 502–511 (2022).
 44. Look, T. *et al.* Targeted delivery of tumor necrosis factor in combination with CCNU induces a T cell-dependent regression of glioblastoma. *Sci Transl Med* **15**, eadf2281 (2023).
 45. Wulff, H. *et al.* Design of a potent and selective inhibitor of the intermediate-conductance Ca²⁺-activated K⁺ channel, IKCa1: A potential immunosuppressant. *Proc Natl Acad Sci U S A* **97**, 8151–8156 (2000).
 46. Brown, B. M., Pressley, B. & Wulff, H. KCa3.1 Channel Modulators as Potential Therapeutic Compounds for Glioblastoma. *Curr Neuropharmacol* **16**, 618–626 (2018).
 47. Schilling, T. & Eder, C. TRAM-34 inhibits nonselective cation channels. *Pflugers Arch* **454**, 559–563 (2007).
 48. Khalid, M. H., Shibata, S. & Hiura, T. Effects of clotrimazole on the growth, morphological characteristics, and cisplatin sensitivity of human glioblastoma cells in vitro. *Journal of Neurosurgery* **90**, 918–927 (1999).
 49. Khalid, M. H., Tokunaga, Y., Caputy, A. J. & Walters, E. Inhibition of tumor

growth and prolonged survival of rats with intracranial gliomas following administration of clotrimazole. *Journal of Neurosurgery* **103**, 79–86 (2005).

50. Fioretti, B. *et al.* NPPB block of the intermediate-conductance Ca²⁺-activated K⁺ channel. *Eur J Pharmacol* **497**, 1–6 (2004).

51. Sciaccaluga, M. *et al.* CXCL12-induced glioblastoma cell migration requires intermediate conductance Ca²⁺-activated K⁺ channel activity. *Am J Physiol Cell Physiol* **299**, C175-184 (2010).

52. Kast, R. E. Profound Blockage of Cxcr4 Signaling at Multiple Points Using the Synergy Between Plerixafor, Mirtazapine, and Clotrimazole as a New Glioblastoma Treatment Adjunct. *Turkish Neurosurgery* **20**,

53. Kast, R. E. *et al.* A conceptually new treatment approach for relapsed glioblastoma: Coordinated undermining of survival paths with nine repurposed drugs (CUSP9) by the International Initiative for Accelerated Improvement of Glioblastoma Care. *Oncotarget* **4**, (2013).

54. Catacuzzeno, L. *et al.* Serum-activated K and Cl currents underlay U87-MG glioblastoma cell migration. *J Cell Physiol* **226**, 1926–1933 (2011).

55. Ruggieri, P. *et al.* The Inhibition of KCa3.1 Channels Activity Reduces Cell Motility in Glioblastoma Derived Cancer Stem Cells. *PLOS ONE* **7**, e47825 (2012).

56. D'Alessandro, G. *et al.* KCa3.1 channels are involved in the infiltrative behavior of glioblastoma in vivo. *Cell Death Dis* **4**, e773 (2013).

57. Cuddapah, V. A., Turner, K. L., Seifert, S. & Sontheimer, H. Bradykinin-induced chemotaxis of human gliomas requires the activation of KCa3.1 and ClC-3. *J Neurosci* **33**, 1427–1440 (2013).

58. Turner, K. L., Honasoge, A., Robert, S. M., McFerrin, M. M. & Sontheimer, H. A pro-invasive role for the Ca²⁺-activated K⁺ channel KCa3.1 in malignant glioma. *Glia* **62**, 971–981 (2014).

59. Catacuzzeno, L. & Franciolini, F. Role of KCa3.1 Channels in Modulating Ca²⁺ Oscillations during Glioblastoma Cell Migration and Invasion. *International Journal of Molecular Sciences* **19**, 2970 (2018).

60. Abdullaev, I. F., Rudkouskaya, A., Mongin, A. A. & Kuo, Y.-H. Calcium-Activated Potassium Channels BK and IK1 Are Functionally Expressed in Human Gliomas but Do Not Regulate Cell Proliferation. *PLOS ONE* **5**, e12304 (2010).

61. McFerrin, M. B., Turner, K. L., Cuddapah, V. A. & Sontheimer, H. Differential role of IK and BK potassium channels as mediators of intrinsic and extrinsic apoptotic

- cell death. *Am J Physiol Cell Physiol* **303**, C1070–C1078 (2012).
62. D'Alessandro, G. *et al.* KCa3.1 channel inhibition sensitizes malignant gliomas to temozolomide treatment. *Oncotarget* **7**, 30781–30796 (2016).
63. Grimaldi, A. *et al.* KCa3.1 inhibition switches the phenotype of glioma-infiltrating microglia/macrophages. *Cell Death & Disease* **7**, e2174–e2174 (2016).
64. Stegen, B. *et al.* Ca²⁺-Activated IK K⁺ Channel Blockade Radiosensitizes Glioblastoma Cells. *Molecular Cancer Research* **13**, 1283–1295 (2015).
65. Hausmann, D. *et al.* Autonomous rhythmic activity in glioma networks drives brain tumour growth. *Nature* **613**, 179–186 (2023).
66. Feske, S., Wulff, H. & Skolnik, E. Y. Ion Channels in Innate and Adaptive Immunity. *Annual Review of Immunology* **33**, 291–353 (2015).
67. Di, L. *et al.* Inhibition of the K⁺ channel KCa3.1 ameliorates T cell-mediated colitis. *Proc Natl Acad Sci U S A* **107**, 1541–1546 (2010).
68. Strøbæk, D. *et al.* NS6180, a new KCa3.1 channel inhibitor prevents T-cell activation and inflammation in a rat model of inflammatory bowel disease. *Br J Pharmacol* **168**, 432–444 (2013).
69. Girodet, P.-O. *et al.* Ca²⁺-Activated K⁺ Channel-3.1 Blocker TRAM-34 Attenuates Airway Remodeling and Eosinophilia in a Murine Asthma Model. *Am J Respir Cell Mol Biol* **48**, 212–219 (2013).
70. Chen, Y.-J., Lam, J., Gregory, C. R., Schrepfer, S. & Wulff, H. The Ca²⁺-Activated K⁺ Channel KCa3.1 as a Potential New Target for the Prevention of Allograft Vasculopathy. *PLoS One* **8**, e81006 (2013).
71. Massenzio, F. *et al.* In vivo morphological alterations of TAMs during KCa3.1 inhibition—by using in vivo two-photon time-lapse technology. *Front Cell Neurosci* **16**, 1002487 (2022).
72. Begenisich, T. *et al.* Physiological Roles of the Intermediate Conductance, Ca²⁺-activated Potassium Channel Kcnn4*. *Journal of Biological Chemistry* **279**, 47681–47687 (2004).
73. Henríquez, C. *et al.* The calcium-activated potassium channel KCa3.1 plays a central role in the chemotactic response of mammalian neutrophils. *Acta Physiologica* **216**, 132–145 (2016).
74. Ataga, K. I. *et al.* Improvements in haemolysis and indicators of erythrocyte survival do not correlate with acute vaso-occlusive crises in patients with sickle cell disease: a phase III randomized, placebo-controlled, double-blind study of the Gardos

- channel blocker senicapoc (ICA-17043). *Br. J. Haematol.* **153**, 92–104 (2011).
75. Klumpp, L., Sezgin, E. C., Skardelly, M., Eckert, F. & Huber, S. M. KCa3.1 Channels and Glioblastoma: In Vitro Studies. *Curr Neuropharmacol* **16**, 627–635 (2018).
76. D'Alessandro, G. *et al.* Radiation Increases Functional KCa3.1 Expression and Invasiveness in Glioblastoma. *Cancers (Basel)* **11**, 279 (2019).
77. Holman, L., Head, M. L., Lanfear, R. & Jennions, M. D. Evidence of Experimental Bias in the Life Sciences: Why We Need Blind Data Recording. *PLOS Biology* **13**, e1002190 (2015).
78. Stransky, N., Ganser, K., Naumann, U., Huber, S. M. & Ruth, P. Tumoricidal, Temozolomide- and Radiation-Sensitizing Effects of KCa3.1 K⁺ Channel Targeting In Vitro Are Dependent on Glioma Cell Line and Stem Cell Fraction. *Cancers (Basel)* **14**, 6199 (2022).
79. Chen, Y.-J., Raman, G., Bodendiek, S., O'Donnell, M. E. & Wulff, H. The KCa3.1 Blocker TRAM-34 Reduces Infarction and Neurological Deficit in a Rat Model of Ischemia/Reperfusion Stroke. *J Cereb Blood Flow Metab* **31**, 2363–2374 (2011).
80. Stransky, N. *et al.* Efficacy of combined tumor irradiation and KCa3.1-targeting with TRAM-34 in a syngeneic glioma mouse model. *Sci Rep* **13**, 20604 (2023).
81. Stegen, B. *et al.* K⁺ channel signaling in irradiated tumor cells. *Eur Biophys J* **45**, 585–598 (2016).
82. Zhou, H.-M., Zhang, J.-G., Zhang, X. & Li, Q. Targeting cancer stem cells for reversing therapy resistance: mechanism, signaling, and prospective agents. *Sig Transduct Target Ther* **6**, 1–17 (2021).
83. Chen, J. *et al.* A restricted cell population propagates glioblastoma growth after chemotherapy. *Nature* **488**, 522–526 (2012).
84. Becker, A. P., Sells, B. E., Haque, S. J. & Chakravarti, A. Tumor Heterogeneity in Glioblastomas: From Light Microscopy to Molecular Pathology. *Cancers* **13**, 761 (2021).
85. Patel, A. P. *et al.* Single-cell RNA-seq highlights intratumoral heterogeneity in primary glioblastoma. *Science* **344**, 1396–1401 (2014).
86. Schneider, H. *et al.* Age-associated and therapy-induced alterations in the cellular microenvironment of experimental gliomas. *Oncotarget* **8**, 87124–87135 (2017).
87. Pilkington, G. J., Darling, J. L., Lantos, P. L. & Thomas, D. G. Tumorigenicity of

- cell lines (VMDk) derived from a spontaneous murine astrocytoma. Histology, fine structure and immunocytochemistry of tumours. *J. Neurol. Sci.* **71**, 145–164 (1985).
88. Serano, R. D., Pegram, C. N. & Bigner, D. D. Tumorigenic cell culture lines from a spontaneous VM/Dk murine astrocytoma (SMA). *Acta Neuropathologica* **51**, 53–64 (1980).
89. Ganser, K. *et al.* Patient-individual phenotypes of glioblastoma stem cells are conserved in culture and associate with radioresistance, brain infiltration and patient prognosis. *Int J Cancer* **150**, 1722–1733 (2022).
90. Silginer, M. *et al.* Immunological and tumor-intrinsic mechanisms mediate the synergistic growth suppression of experimental glioblastoma by radiotherapy and MET inhibition. *Acta Neuropathol Commun* **11**, 41 (2023).
91. Tran, T.-T. *et al.* Inhibiting TGF- β signaling restores immune surveillance in the SMA-560 glioma model. *Neuro Oncol* **9**, 259–270 (2007).
92. Schneider, H. *et al.* Novel TIE-2 inhibitor BAY-826 displays in vivo efficacy in experimental syngeneic murine glioma models. *Journal of Neurochemistry* **140**, 170–182 (2017).
93. Wild-Bode, C., Weller, M., Rimner, A., Dichgans, J. & Wick, W. Sublethal Irradiation Promotes Migration and Invasiveness of Glioma Cells: Implications for Radiotherapy of Human Glioblastoma¹. *Cancer Research* **61**, 2744–2750 (2001).
94. Farhat, M. *et al.* Multifocal and multicentric glioblastoma: Imaging signature, molecular characterization, patterns of spread, and treatment. *Neuroradiol J* 19714009231193162 (2023) doi:10.1177/19714009231193162.
95. Nakada, M., Okada, Y. & Yamashita, J. The role of matrix metalloproteinases in glioma invasion. *FBL* **8**, 261–269 (2003).
96. Oishi, T., Koizumi, S. & Kurozumi, K. Molecular Mechanisms and Clinical Challenges of Glioma Invasion. *Brain Sciences* **12**, 291 (2022).
97. Esposito, M., Ganesan, S. & Kang, Y. Emerging strategies for treating metastasis. *Nat Cancer* **2**, 258–270 (2021).
98. Winer, A., Adams, S. & Mignatti, P. Matrix Metalloproteinase Inhibitors in Cancer Therapy: Turning Past Failures Into Future Successes. *Mol Cancer Ther* **17**, 1147–1155 (2018).
99. Gerstberger, S., Jiang, Q. & Ganesh, K. Metastasis. *Cell* **186**, 1564–1579 (2023).
100. Sahm, F. *et al.* Addressing Diffuse Glioma as a Systemic Brain Disease With

Single-Cell Analysis. *Archives of Neurology* **69**, 523–526 (2012).

101. Broekman, M. L. *et al.* Multidimensional communication in the microenvirons of glioblastoma. *Nature Reviews Neurology* **14**, 482–495 (2018).

102. Walker, D. G. & Lue, L.-F. Immune phenotypes of microglia in human neurodegenerative disease: challenges to detecting microglial polarization in human brains. *Alzheimers Res Ther* **7**, 56 (2015).

103. Chimote, A. A., Gawali, V. S., Newton, H. S., Wise-Draper, T. M. & Conforti, L. A Compartmentalized Reduction in Membrane-Proximal Calmodulin Reduces the Immune Surveillance Capabilities of CD8+ T Cells in Head and Neck Cancer. *Front Pharmacol* **11**, 143 (2020).

104. Gupta, A. *et al.* Radiotherapy promotes tumor-specific effector CD8+ T cells via dendritic cell activation. *J Immunol* **189**, 558–566 (2012).

105. Liang, H. *et al.* Radiation-induced equilibrium is a balance between tumor cell proliferation and T cell-mediated killing. *J Immunol* **190**, 5874–5881 (2013).

106. Han, S. *et al.* Tumour-infiltrating CD4+ and CD8+ lymphocytes as predictors of clinical outcome in glioma. *Br J Cancer* **110**, 2560–2568 (2014).

107. Mauldin, I. S. *et al.* Proliferating CD8+ T Cell Infiltrates Are Associated with Improved Survival in Glioblastoma. *Cells* **10**, 3378 (2021).

108. Stransky, N., Ruth, P., Schwab, M. & Löffler, M. W. Can Any Drug Be Repurposed for Cancer Treatment? A Systematic Assessment of the Scientific Literature. *Cancers (Basel)* **13**, 6236 (2021).

109. Macleod, M. R. *et al.* Risk of Bias in Reports of In Vivo Research: A Focus for Improvement. *PLOS Biology* **13**, e1002273 (2015).

110. Wieschowski, S. *et al.* Preclinical efficacy studies in investigator brochures: Do they enable risk–benefit assessment? *PLOS Biology* **16**, e2004879 (2018).

111. Kaplan, R. M. & Irvin, V. L. Likelihood of Null Effects of Large NHLBI Clinical Trials Has Increased over Time. *PLOS ONE* **10**, e0132382 (2015).

112. Ioannidis, J. P. A. Why Most Published Research Findings Are False. *PLoS Medicine* **2**, 6 (2005).

113. Holst, M. R., Faust, A. & Strehl, D. Do German university medical centres promote robust and transparent research? A cross-sectional study of institutional policies. *Health Research Policy and Systems* **20**, 39 (2022).

114. Rice, D. B., Raffoul, H., Ioannidis, J. P. A. & Moher, D. Academic criteria for promotion and tenure in biomedical sciences faculties: cross sectional analysis of

- international sample of universities. *BMJ* m2081 (2020) doi:10.1136/bmj.m2081.
115. Korevaar, D. A., Hooft, L. & Ter Riet, G. Systematic reviews and meta-analyses of preclinical studies: Publication bias in laboratory animal experiments. *Lab Anim* **45**, 225–230 (2011).
116. Tsilidis, K. K. *et al.* Evaluation of Excess Significance Bias in Animal Studies of Neurological Diseases. *PLOS Biology* **11**, e1001609 (2013).
117. Hay, M., Thomas, D. W., Craighead, J. L., Economides, C. & Rosenthal, J. Clinical development success rates for investigational drugs. *Nat Biotechnol* **32**, 40–51 (2014).
118. Seyhan, A. A. Lost in translation: the valley of death across preclinical and clinical divide – identification of problems and overcoming obstacles. *Translational Medicine Communications* **4**, 18 (2019).
119. Wong, C. H., Siah, K. W. & Lo, A. W. Estimation of clinical trial success rates and related parameters. *Biostatistics* **20**, 273–286 (2019).
120. Kim, Y., Armstrong, T. S., Gilbert, M. R. & Celiku, O. A critical analysis of neuro-oncology clinical trials. *Neuro Oncol* **25**, 1658–1671 (2023).
121. Vanderbeek, A. M. *et al.* The clinical trials landscape for glioblastoma: is it adequate to develop new treatments? *Neuro Oncol* **20**, 1034–1043 (2018).
122. Berry, S. M., Connor, J. T. & Lewis, R. J. The Platform Trial: An Efficient Strategy for Evaluating Multiple Treatments. *JAMA* **313**, 1619–1620 (2015).
123. Alexander, B. M. *et al.* Adaptive Global Innovative Learning Environment for Glioblastoma: GBM AGILE. *Clin Cancer Res* **24**, 737–743 (2018).
124. Wen, P. *et al.* CTNI-85. GBM AGILE PLATFORM TRIAL FOR NEWLY DIAGNOSED AND RECURRENT GBM: RESULTS OF FIRST EXPERIMENTAL ARM, REGORAFENIB. *Neuro-Oncology* **25**, v97–v98 (2023).
125. Charbonneau, M. *et al.* The development of a rapid patient-derived xenograft model to predict chemotherapeutic drug sensitivity/resistance in malignant glial tumors. *Neuro-Oncology* **25**, 1605–1616 (2023).
126. Bielamowicz, K. *et al.* Trivalent CAR T cells overcome interpatient antigenic variability in glioblastoma. *Neuro-Oncology* **20**, 506–518 (2018).
127. Schmidts, A. *et al.* Tandem chimeric antigen receptor (CAR) T cells targeting EGFRvIII and IL-13R α 2 are effective against heterogeneous glioblastoma. *Neuro-Oncology Advances* **5**, vdac185 (2023).
128. Burger, M. C. *et al.* Intracranial injection of NK cells engineered with a HER2-

targeted chimeric antigen receptor in patients with recurrent glioblastoma. *Neuro Oncol* noad087 (2023) doi:10.1093/neuonc/noad087.

Acknowledgments

I want to thank both of my thesis advisers, Peter Ruth and Stephan Huber, for their unwavering support. From the beginning of this project, I could always count on their critical feedback, helpful tips but also kind words in moments of disappointment. This project would not have been possible without them.

It goes without saying to also thank the whole Huber lab, which did not just teach me all the basics of cell culture, but also became dear friends, who I do not want to miss anymore: Andreas Riedel, Anna-Lena Müller, Christian Dieter, Katrin Ganser and Lukas Klumpp. I also want to thank Heidrun Faltin, which we all deeply miss and will keep only in the best memory. I am grateful for working with so many other good friends in the last couple of years: Alexander Kempf, Janina Palm, Lisa Groß (Zirjacks), Lukas Prause, Ranran Ji and Tayeb Abed.

I am obliged to my partner Laura Riza, who was a constant support since the early days and helped me keep my head up during the difficult days. I should probably also apologize for forcing her to read the very first drafts of many texts I wrote during the last couple of years. 😊

Last but not least, I am deeply grateful for the constant support from my parents, Carolin and Rainer, which enabled me to follow my passion. You are the reason for my curiosity.

Appendix

a) Akzeptierte Publikationen



OPEN

Efficacy of combined tumor irradiation and $K_{Ca}3.1$ -targeting with TRAM-34 in a syngeneic glioma mouse model

Nicolai Stransky^{1,2}, Katrin Ganser¹, Leticia Quintanilla-Martinez^{3,4}, Irene Gonzalez-Menendez^{3,4}, Ulrike Naumann^{5,6}, Franziska Eckert^{1,7}, Pierre Koch⁸, Stephan M. Huber¹✉ & Peter Ruth²

The intermediate-conductance calcium-activated potassium channel $K_{Ca}3.1$ has been proposed to be a new potential target for glioblastoma treatment. This study analyzed the effect of combined irradiation and $K_{Ca}3.1$ -targeting with TRAM-34 in the syngeneic, immune-competent orthotopic SMA-560/VM/Dk glioma mouse model. Whereas neither irradiation nor TRAM-34 treatment alone meaningfully prolonged the survival of the animals, the combination significantly prolonged the survival of the mice. We found an irradiation-induced hyperinvasion of glioma cells into the brain, which was inhibited by concomitant TRAM-34 treatment. Interestingly, TRAM-34 did neither radiosensitize nor impair SMA-560's intrinsic migratory capacities in vitro. Exploratory findings hint at increased TGF- β 1 signaling after irradiation. On top, we found a marginal upregulation of *MMP9* mRNA, which was inhibited by TRAM-34. Last, infiltration of CD3⁺, CD8⁺ or FoxP3⁺ T cells was not impacted by either irradiation or $K_{Ca}3.1$ targeting and we found no evidence of adverse events of the combined treatment. We conclude that concomitant irradiation and TRAM-34 treatment is efficacious in this preclinical glioma model.

Glioblastoma patients face a poor prognosis. Median survival times are in the range of 15–18 months in clinical trial settings¹, with only around 7% of patients surviving longer than 5 years². Several potential new therapeutics failed to prolong survival in recent randomized controlled trials: anti-VEGF antibody bevacizumab³, integrin inhibitor cilengitide⁴, EGFRvIII vaccination rindopepimut⁵ or anti-PD-1 antibody nivolumab^{6,7}. Except for the implementation of Tumor Treating Fields electrotherapy⁸, the glioblastoma treatment protocol has not changed substantially in the last 15 years. It still comprises surgical resection, radiotherapy plus concomitant and adjuvant temozolomide chemotherapy⁹. Identifying new potential treatment targets may be an important step to overcome this standstill.

As such, one potential target may be the intermediate-conductance, calcium-activated potassium channel $K_{Ca}3.1$ (also known as IK, IK_{Ca} , or Gardos channel) encoded by the *KCNN4* gene. Promising results of the brain-penetrant^{10,11} $K_{Ca}3.1$ channel inhibitor TRAM-34 in glioma cells, suggesting radiation-^{12–14} or temozolomide-sensitizing¹⁵ effects, were reported previously. Recent work of our group also elucidated radiation- and temozolomide-sensitizing effects (as well as direct tumoricidal effects) of TRAM-34¹⁶. However, these findings were only seen in certain glioma cell lines under specific cell culture conditions, questioning the general applicability of this potential treatment strategy. Beyond its proposed radio- and chemoresistance-conferring actions, $K_{Ca}3.1$'s role in cell migration and invasion is well documented^{17–19}, and $K_{Ca}3.1$ targeting therapies were

¹Department of Radiation Oncology, University of Tübingen, Hoppe-Seyler-Str. 3, 72076 Tübingen, Germany. ²Department of Pharmacology, Toxicology and Clinical Pharmacy, Institute of Pharmacy, University of Tübingen, 72076 Tübingen, Germany. ³Institute of Pathology and Neuropathology, Comprehensive Cancer Center, Eberhard Karls University of Tübingen, 72076 Tübingen, Germany. ⁴Cluster of Excellence iFIT (EXC 2180) "Image-Guided and Functionally Instructed Tumor Therapies", Eberhard Karls University, Tübingen, Germany. ⁵Molecular Neurooncology, Hertie Institute for Clinical Brain Research and Center Neurology, University of Tübingen, 72076 Tübingen, Germany. ⁶Faculty of Medicine University, Gene and RNA Therapy Center (GRTC), Tübingen, Germany. ⁷Department of Radiation Oncology, Comprehensive Cancer Center, Medical University Vienna, AKH, Wien, Austria. ⁸Department of Pharmaceutical/Medicinal Chemistry II, Institute of Pharmacy, University of Regensburg, 93040 Regensburg, Germany. ✉email: stephan.huber@uni-tuebingen.de

found to decrease glioma cell migration and invasion both in vitro and in vivo^{10,20,21}. Last, new findings hint towards $K_{Ca}3.1$'s important role in intertumoral communication networks, ultimately boosting tumor growth and potentially explaining TRAM-34's glioma growth-inhibiting effects²².

Thorough assessments of $K_{Ca}3.1$ targeting in glioma also need to study its off-tumor effects. While some reports found increased expression of $K_{Ca}3.1$ in glioma cells compared to healthy tissues of the brain¹⁹, $K_{Ca}3.1$ is also expressed in several normal cells, such as epithelia, endothelia or fibroblasts²³, but also astrocytes or neurons^{24,25}. Most importantly, it is functionally expressed in several immune cells and mediates important functions, such as T cell migration, activation and proliferation, or cytokine production and chemotaxis of macrophages^{26,27}. Several studies tested TRAM-34 as an immunosuppressive, anti-inflammatory agent in autoimmune-like diseases, such as colitis²⁸, asthma²⁹ or allograft vasculopathy³⁰. Additionally, recent findings in head and neck cancer patients showed that the immunosuppressing effects of immune checkpoints were (partly) driven by inhibition of $K_{Ca}3.1$ channel activity³¹. Other reports indicate the important function of $K_{Ca}3.1$ in CD8⁺ cytotoxic T cells' infiltration into tumors³². All of the just-mentioned effects could potentially limit TRAM-34's use as an anti-cancer therapeutic. However, two studies, testing TRAM-34 in immunocompetent mouse glioma models, found some evidence for potential immune-modulating (anti-tumor) effects^{33,34}.

In the present study, we set out to test the effect of TRAM-34 in combination with fractionated irradiation on survival, glioma cell invasion and the tumor immune microenvironment in an immune-competent glioma model. We provide evidence of an irradiation-induced hyperinvasion of glioma cells, which was blunted by TRAM-34 and coincided with prolonged survival times. Furthermore, we did not detect differences of either treatment on the tumor immune microenvironment or blood counts of immune cells.

Results

$K_{Ca}3.1$ targeting has been proposed to radiosensitize glioblastoma cells^{12,13} and to inhibit dissemination of glioblastoma cells in the brain²⁰. Since $K_{Ca}3.1$ is also highly expressed in immune cells^{26,27}, this targeted therapy might interfere with the anti-glioblastoma immune response. We, therefore, studied the effect of $K_{Ca}3.1$ targeting on the survival of tumor-transplanted mice, on the tumor dissemination in the brain, and on the immune-microenvironment in a syngeneic orthotopic glioma mouse model. To this end, we injected 5×10^3 SMA-560 cells into the right striatum of VM/Dk mice (Fig. 1a). SMA-560 cells functionally express TRAM-34-sensitive $K_{Ca}3.1$ channels in vitro (Supplemental Fig. S1, S2, S3), which is retained after tumor formation in VM/Dk mice (Supplemental Fig. S4). Gliomas were then treated by fractionated irradiation (5×0 or 5×4 Gy) concomitant to the systemic application of TRAM-34 (0 or 120 mg/kg b.w. in miglyol intraperitoneally [i.p.]; Fig. 1a) on five consecutive days.

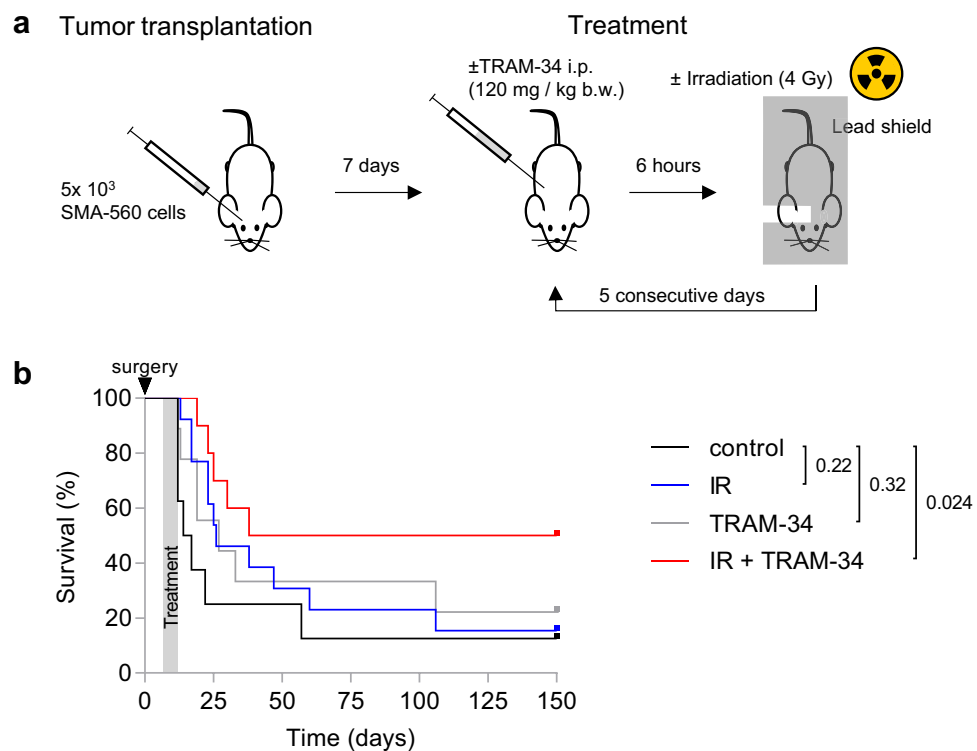


Figure 1. Combined irradiation + TRAM-34 therapy increases survival in the SMA-560 VM/Dk glioma model. (a), Schematic of tumor transplantation and subsequent treatment. (b), Kaplan–Meier estimator started on the day of tumor cell injection into the right striatum. Arrowhead depicts day of surgery; the treatment period is shaded in grey. Animals in the control group (N = 8) are shown in black, in the irradiation group (N = 13) in blue, in the TRAM-34 only (N = 10) group in grey and in the combined irradiation + TRAM-34 group (N = 9) in red. Numbers in (b) indicate *P* values as calculated by log-rank Mantel-Cox test.

Almost all animals, irrespective of treatment groups, lost weight during treatment (most notably starting on day 3 of the treatment). Weight loss may be due to daily intraperitoneal injections, daily isoflurane anesthesia or daily transport of the animals to the linear accelerator, all of which could ultimately elicit a stress response in the animals (see Supplemental Fig. S5). On the other hand, we detected no differences in weight loss between the treatment groups, which suggests no severe toxicity of the treatment.

In the control group, the tumor-transplanted mice exhibited a median survival of 16 days, which is comparable to other reports (16–27.5 days^{35–37}). Neither irradiation only, nor TRAM-34 only did meaningfully affect the survival of the animals (median survival times: 26 and 27 days, respectively). Combined IR + TRAM-34, however, significantly prolonged the survival of the mice (median survival 38 days; Fig. 1b).

To identify potential mechanisms underlying the prolonged survival of the combined irradiation + TRAM-34 treated mice, we first determined the effect of $K_{Ca}3.1$ channel blockade on the radiosensitivity of SMA-560 cells in vitro. Irradiation (2 Gy) increased TRAM-34-sensitive channel activity of $K_{Ca}3.1$ in SMA-560 cells (see Supplemental Figures S1 and S2), which conferred radioresistance in other glioblastoma models^{12,38}. A recent in vitro study of our group, however, concluded that TRAM-34 neither impairs clonogenic survival nor radioresistance in SMA-560 cells when treated with single-dose irradiation¹⁶. To exclude differential effects of TRAM-34 after fractionated irradiation protocols, we analyzed clonogenic survival of SMA-560 cells treated with fractionated irradiation (ranging from 5×0 to 5×4 Gy) and TRAM-34 (0 or $5 \mu\text{M}$). Notably, fractionated irradiation with 5×4 Gy led to strong decreases in survival fraction. On the other hand, we did not detect meaningful effects of additional TRAM-34 treatment in standard (DMEM; Fig. 2) or glioblastoma stem-cell-enriching NSC medium (see Supplemental Fig. S6). This led us to assume that effects other than radiosensitization are responsible for the prolonged survival after combined IR + TRAM-34 treatment.

Mesenchymal subpopulations of primary glioblastoma cells exhibit a highly invasive behavior in vitro and show an upregulation of $K_{Ca}3.1$ ³⁹. Moreover, $K_{Ca}3.1$ targeting delayed glioblastoma brain invasion in an orthotopic *xenograft* mouse model¹⁰ and after previous radiation therapy²¹. Hence, we analyzed the tumor growth morphology after up to 14 days after the end of treatment (Fig. 3). As soon as the first animal became symptomatic (Score ≥ 5 , see methods), all animals of a simultaneously tumor-challenged batch of mice were sacrificed and brains were extracted. Some animals (especially in the TRAM-34 or combined IR + TRAM-34 treatment group) showed no signs of residual tumor (histological Score 0) or only gliosis (Score 1), whereas most animals presented with small (Score 2) to medium-large-sized tumors with necrosis (Score 3). Several animals developed satellite tumors, i.e. tumor cell clusters that were distant from the main tumor (Fig. 3c). Satellite tumors were frequently found in the IR only group (4/5 animals). In comparison, only 1/6 animals in the control and TRAM-34 only groups, and none (0/6 animals) in the combined IR + TRAM-34 treatment arm developed satellite tumors (Fig. 3d). Combined, these results point towards an irradiation-induced hyperinvasion of SMA-560 cells, which was completely blocked by TRAM-34 treatment in vivo.

To identify potential underlying processes, the effects of irradiation (1×0 Gy or 1×2 Gy) and TRAM-34 (0 or $5 \mu\text{M}$ TRAM-34) on migration velocity of SMA-560 cells was tested in vitro by transwell migration and wound healing assays (Fig. 4). Low irradiation doses were chosen due to findings of other authors, indicating increased invasion velocity of SMA-560 cells after low dose irradiation (2 Gy) compared to no increases after high irradiation doses (8 Gy)³⁵. Overall, neither of the two assays disclosed an irradiation-induced hypermigration in vitro. Moreover, we did not observe any difference in transwell migration (Fig. 4a–c) and wound healing (Fig. 4d–f) between the four experimental arms. Only the combined treatment (1×2 Gy + $5 \mu\text{M}$ TRAM-34) showed a slight

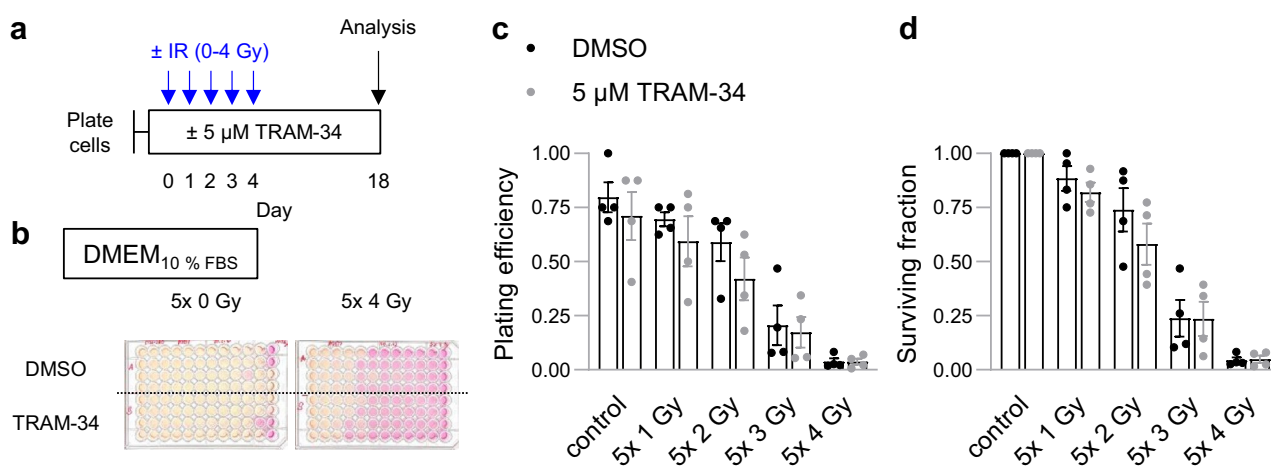


Figure 2. TRAM-34 does not affect clonogenic survival after fractionated irradiation in SMA-560 cells in vitro. The results shown are for SMA-560 cells grown in 10% FBS-containing DMEM. **a**, Scheme depicting the time course of the experiment. **(b)**, Representative image of limited dilution assay on day 18 of cells treated with DMSO (upper wells) or $5 \mu\text{M}$ TRAM-34 (lower wells) and irradiation (left: 5×0 Gy; right: 5×4 Gy). **(c)**, Plating efficiency and, **(d)**, surviving fraction of cells after fractionated irradiation (5×0 , 1, 2, 3 or 4 Gy) and TRAM-34 treatment (0 or $5 \mu\text{M}$). **(c, d)**, Individual values of 4 independent experiments and mean values \pm standard error of the mean (sem) are depicted.

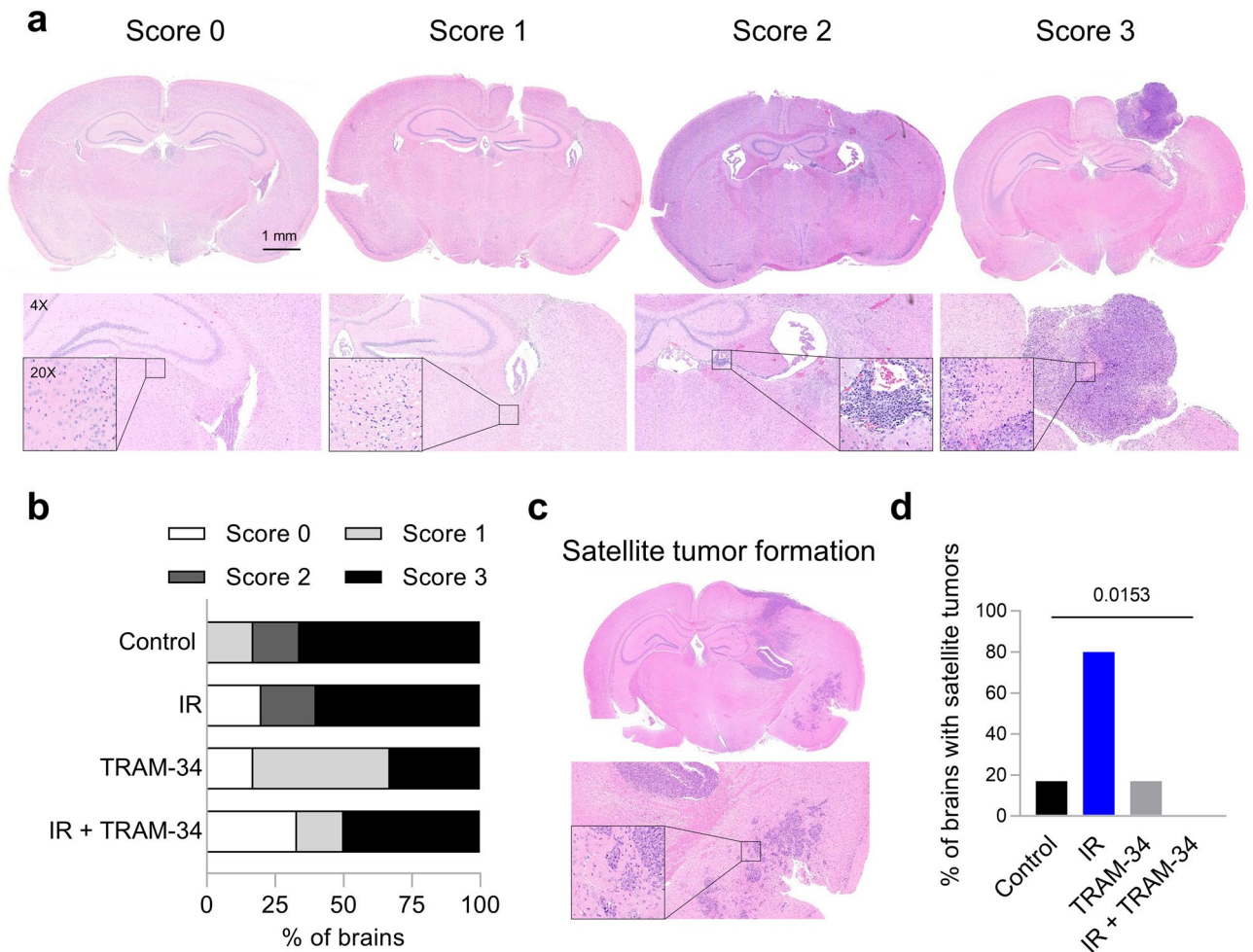


Figure 3. Irradiation-induced micro-satellite formation of SMA-560 gliomas is inhibited by TRAM-34. (a), Representative images of each score to subclassify tumor growth morphology in lowest (1x, top row), 4x (bottom row) or 20x magnification (bar indicates 1 mm). Brains were classified as showing no difference to the contralateral hemisphere (Score 0), gliosis (Score 1), small diffuse tumors (Score 2) or medium-large solid tumor formation with necrosis (Score 3). (b), Quantification of each category among the four treatment arms (control: N = 6 animals; IR only: N = 5 animals; TRAM-34 only: N = 6 animals; IR + TRAM-34: N = 6 animals). (c, d), Satellite tumor formation was mostly found in animals from the irradiation only group, whereas no (0/6) animal from the combined IR + TRAM-34 treatment group exhibited this glioblastoma growth morphology. Number indicates *P* value as calculated by two-tailed Fisher's Exact test (d).

tendency ($P=0.16$) towards lower transwell migration velocity (Fig. 4b,c). Together, these data suggest that satellite tumor formation after irradiation (Fig. 3c) is not due to an increase in intrinsic cell motility of SMA-560 cells.

Next, we analyzed further factors that might promote TRAM-34-sensitive radiogenic formation of SMA-560 microsattellites in vivo. Among those, we focused on auto-/paracrine TGF- β 1 signaling, the interaction between CD44 and extracellular hyaluronic acid, and matrix metalloproteinases (MMP)-mediated remodeling of the tumor microenvironment⁴⁰. Irradiation has previously been demonstrated to stimulate TGF- β signaling in orthotopic SMA-560 gliomas³⁵, whereas pharmacological TGF- β targeting was shown to block invasion of SMA-560 cells in Boyden chamber experiments in vitro as well as microsattellite formation in vivo³⁶. In our experiments, single-dose irradiation (Fig. 5a) induced a non-significant ($P=0.074$) increase in TGF- β 1 protein release at the highest irradiation dose in DMEM-grown SMA-560 cells. This trend was not observed when TRAM-34 was co-applied (Fig. 5b). In stem-cell-enriched SMA-560 cultures (NSC medium), single-dose (8 Gy; Supplemental Fig. S7a) or fractionated irradiation (5×4 Gy; Supplemental Fig. S7b) induced a profound ($p < 0.005$) but TRAM-34-insensitive increase in TGF- β 1 protein release into the medium. Additionally, 8 Gy single-dose irradiation induced a non-significant ($P=0.079$) rise in MMP-9 mRNA abundance, which was blunted by TRAM-34 co-application. In contrast, no irradiation- or TRAM-34-modulated change in TGF- β receptor-1 (*TGFBR1*), MMP-2, or CD44 mRNA abundance was apparent after single-dose irradiation (Fig. 5c). Similar trends were observed when DMEM-grown SMA-560 cells were subjected to fractionated irradiation, except for an additional TRAM-34-insensitive rise in CD44 mRNA only after 5×4 Gy irradiation ($P=0.017$; Fig. 5d-f). Combined, these explorative experiments might hint at a radiogenic upregulation of auto-/paracrine TGF- β 1 signaling and a TRAM-34-sensitive MMP-9-mediated remodeling of the tumor microenvironment.

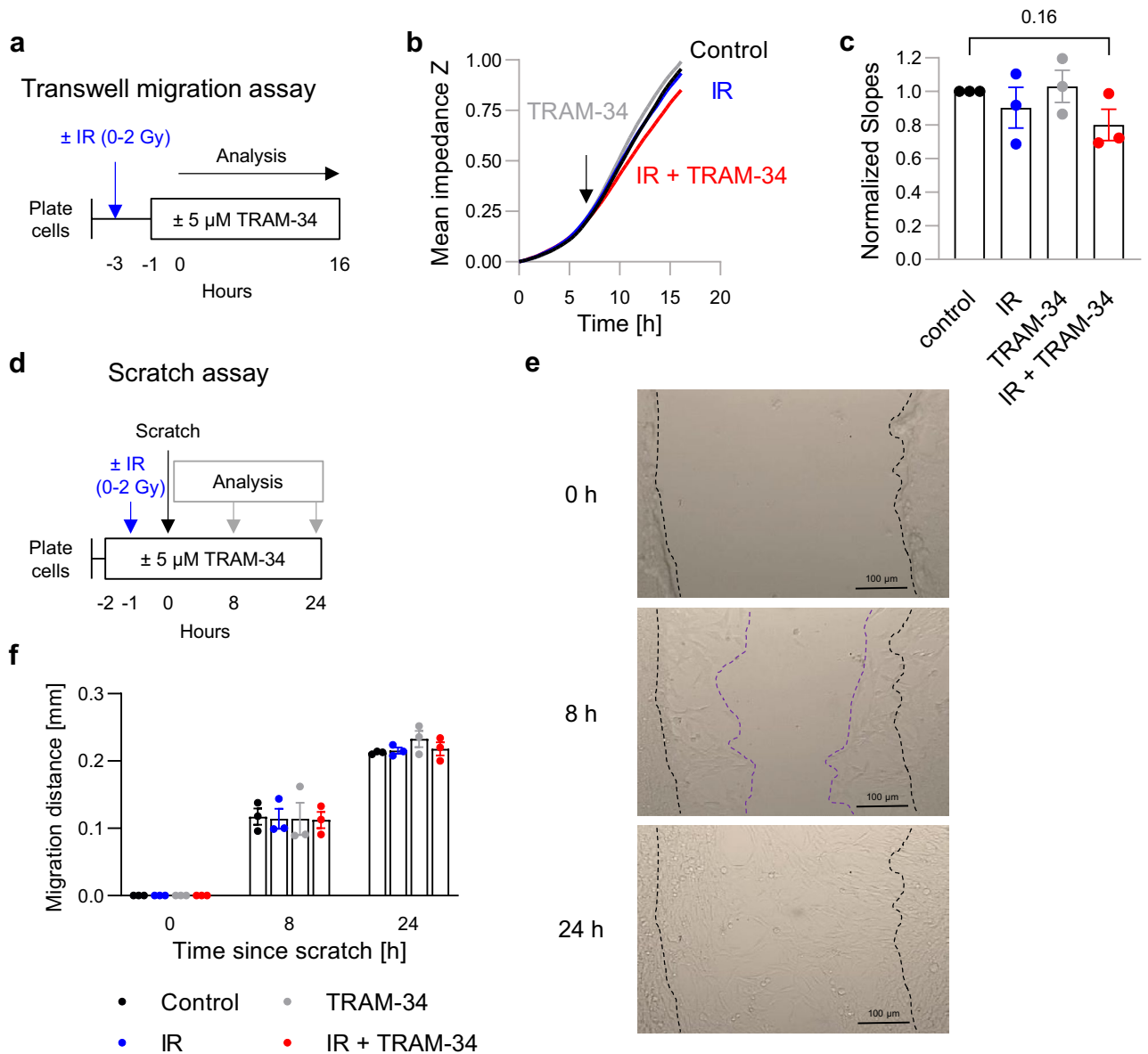


Figure 4. Combined single-dose irradiation (0 or 2 Gy) + TRAM-34 (0 or 5 μM) treatment does not affect SMA-560 cell migration in vitro. (a–c), Transwell migration assay with SMA-560 cells cultured in DMEM medium. (a), Scheme depicting time course of transwell migration assay. (b), Mean impedance (as a measure of number of trans-migrated cells) over time averaged from three independent experiments. Arrow indicates the time point after which a linear course was assumed and the slope of the time-dependent impedance-increase calculated. (c), Normalized slopes were not significantly different between treatment arms. Depicted are individual and mean values ± sem. (d–f), Scratch Assay with SMA-560 cells cultured in DMEM medium. (d), Scheme depicting time course of scratch assay. (e), Representative images of scratches 0, 8 and 24 h after the scratch. The dashed black line shows the original distance of scratch, whereas the dashed purple line represents the scratch distance after 8 h. (f), Quantification of migration distance in all four treatment arms. Depicted are individual values from 3 independent experiments and means ± sem. Number indicates *P* value as calculated by two-tailed one-sample *t*-test against 1.0 (c).

Since TGF-β has also been reported to exert several immuno-suppressive functions⁴¹ and K_{Ca}3.1 has been proposed to exert pivotal functions in the anti-cancer immune response^{31,32} or T cell migration²⁷ on its own, we next analyzed the effects of fractionated irradiation and K_{Ca}3.1 targeting on the immune microenvironment of the SMA-560 glioma mouse model. As expected, an increase in the number of Iba1⁺ reactive microglia cells in or around the tumor (Score 1; ‘gliosis’) was detected in the majority of animals as compared to the healthy contralateral hemisphere. We found a moderate to prominent Iba1⁺ macrophage reaction in larger solid tumors (Score 2, Fig. 6a), including macrophage pseudopalising in several animals (Supplemental Fig. S8). Additionally, we used another macrophage activation marker, CD68. In general, we found less CD68⁺ than Iba1⁺ macrophages with little differences among the treatment groups (Fig. 6b). The amount of Iba1⁺ and CD68⁺ cells correlated with each other and the tumor size, i.e., bigger tumors contained more Iba1⁺ and more CD68⁺ macrophages.

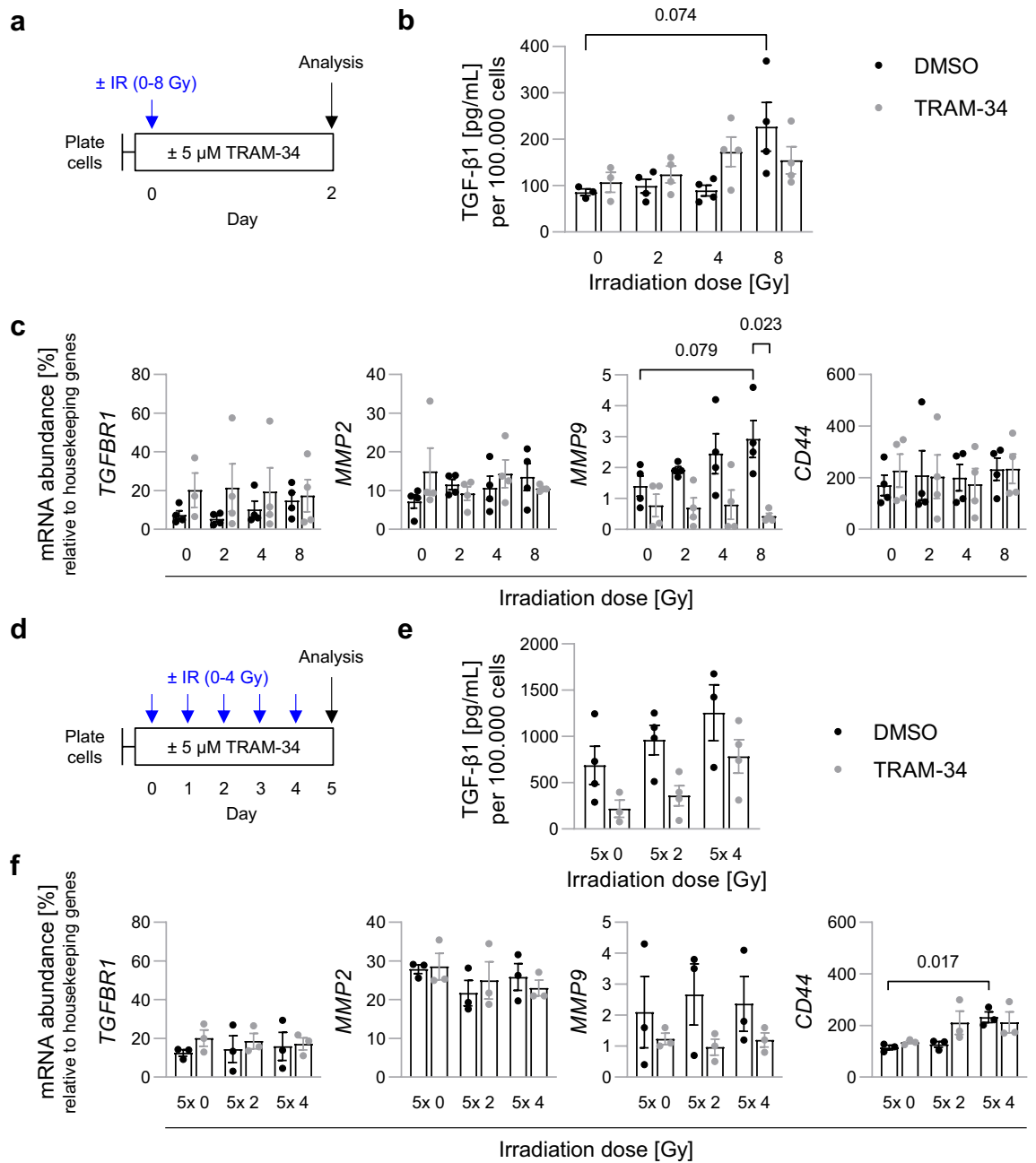


Figure 5. Irradiation increases TGF-β1 signaling and TRAM-34-sensitive *MMP9* mRNA abundance. (a–c), Effects of single-dose irradiation in SMA-560 cells cultured in DMEM medium. (a), Scheme depicting time course. (b), TGF-β1 secretion per 100,000 cells trends towards irradiation-induced increases at high irradiation doses as measured by ELISA with mixed effects of concomitant TRAM-34 treatment. c, mRNA abundance of *TGFBR1*, *MMP2*, *MMP9* and *CD44* as measured with RT qPCR relative to housekeeper genes. *MMP9* abundance is slightly increased after irradiation, whereas TRAM-34 consistently decreases *MMP9* expression. (d–f), Effects of fractionated irradiation in SMA-560 cells cultured in DMEM medium. (d), Scheme depicting time course. (e), Fractionated irradiation marginally increases TGF-β1 secretion per 100,000 cells (non-significant; n.s.), which is blunted by TRAM-34 (n.s.). (f), mRNA abundance of *TGFBR1*, *MMP2*, *MMP9* and *CD44* as measured with RT qPCR relative to housekeeper genes. Depicted are individual values from 3–4 independent experiments and mean values ± sem. Numbers indicate *P* values as calculated by Welch-corrected two-tailed t-tests (b, c, f).

Furthermore, most animals presented with a mild-moderate amount of CD3⁺ T cells (Score 1), while 2 animals displayed a prominent presence of CD3⁺ T cells (Score 2; Fig. 6c, right), mostly at the tumor periphery

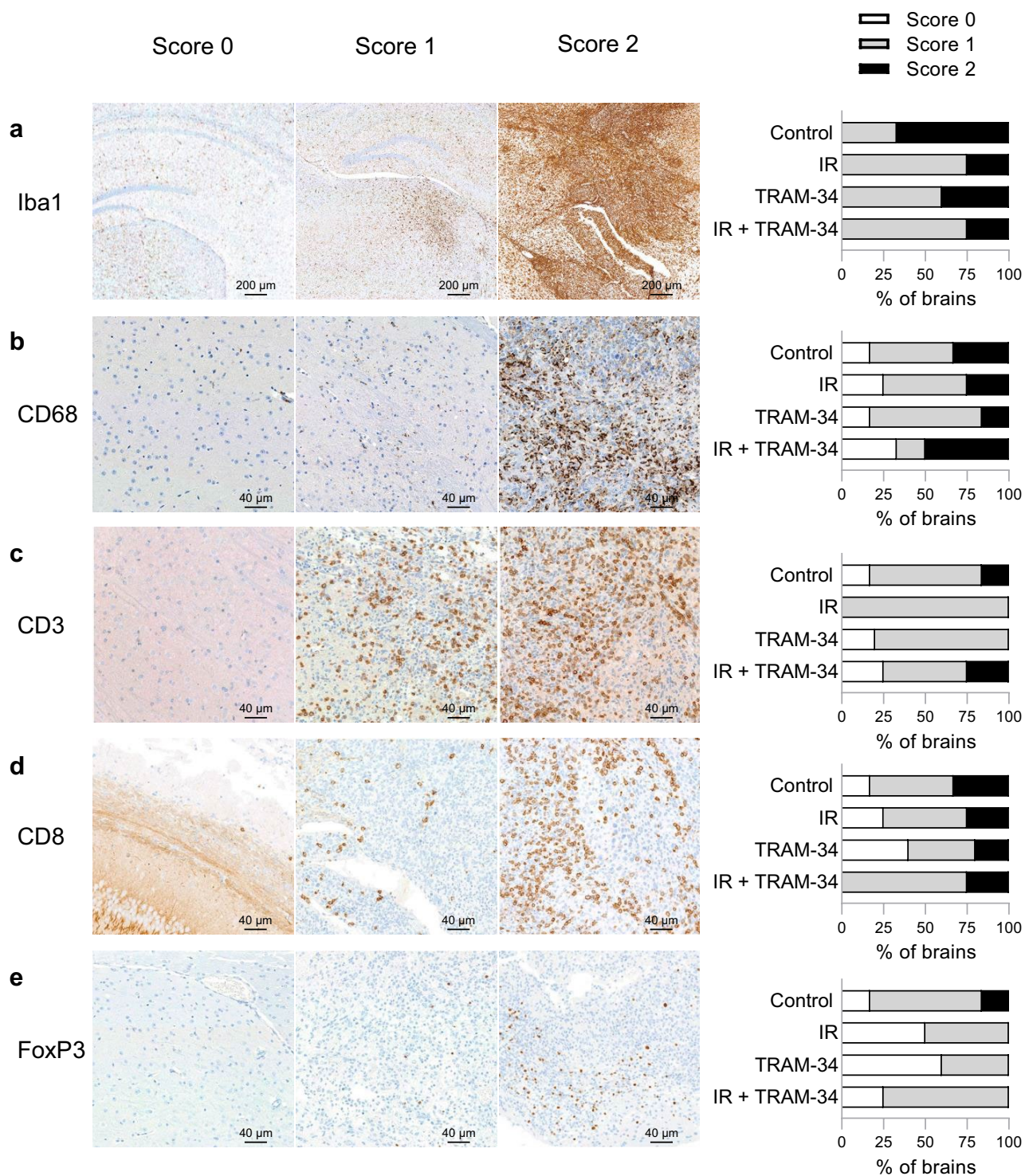


Figure 6. Immunohistochemical stains show no difference between treatment arms in the tumor-microenvironment. A scoring system to compare effects of the treatments was developed for, (a), Iba1⁺ reactive macrophages, (b), CD68⁺ reactive macrophages, (c), CD3⁺ T cells, (d), CD8⁺ cytotoxic T cells and e, FoxP3⁺ regulatory T cells. No animal with an H&E score of >0 displayed an Iba1 Score of 0. Additionally depicted is the share of animals per treatment group displaying each score (right side; control: N=6 animals; irradiation only: N=4 animals; TRAM-34 only: N=5 animals; IR + TRAM-34: N=4 animals).

(Supplemental Fig. S8). No differences were detected regarding the CD8 (Fig. 6d) and FoxP3 positive T cells (Fig. 6e) among the treatment groups.

Combined, these data indicate that neither fractionated radiation nor $K_{Ca}3.1$ targeting with TRAM-34 nor their combination, induced pronounced changes in the abundance of $Iba1^+$ or $CD68^+$ reactive microglia and $CD3^+$, $CD8^+$ cytotoxic or $FoxP3^+$ regulatory T cells in the SMA-560 VM/Dk glioma model.

To analyze treatment-dependent systemic changes of the immune system, we finally determined the counts of total white blood cells (WBC), lymphocytes and neutrophils, shortly before (day 6), as well as directly (day 11) and 0.5–3 weeks (days 15–32) after the end of treatment (Fig. 7a). In addition, blood hemoglobin concentration and red cell count were used as markers of treatment-associated adverse events, as $K_{Ca}3.1$ has previously been shown to be important for volume regulation in erythrocytes^{42,43}. Blood counts of animals were well balanced at the time of randomization (see Supplemental Fig. S9) and were used to calculate ‘normal blood count ranges’ for the VM/Dk mice (as defined by mean values ± 1 standard deviation of all mice before treatment; indicated in Fig. 7 by dotted grey lines). According to this ‘normal range’, white blood count (Fig. 7b) and lymphocytes (Fig. 7c) remained unchanged after the treatments, at most displaying slight reductions of WBC after combined IR + TRAM-34 or of lymphocytes after irradiation only, TRAM-34 only or combined IR + TRAM-34 treatment (all n.s., ordinary one-way ANOVA followed by Tukey’s multiple comparisons test). We observed an increase in neutrophil counts in each treatment group on day 11, whereas neutrophil counts at later time points varied considerably between the animals (Fig. 7d). Both red blood cell count (Fig. 7e) and hemoglobin concentration (Fig. 7f) remained unchanged at day 11 and appeared to slightly increase at later time points irrespective of treatment group. Overall, except for increases in neutrophil counts, arguably due to increased stress during the treatment, we found little to no effect of our treatment regimens on blood counts.

Discussion

Our study provides evidence that fractionated tumor irradiation combined with systemic application of the $K_{Ca}3.1$ blocker TRAM-34 prolongs the survival of VM/Dk mice with orthotopically transplanted syngeneic SMA-560 cells. In contrast, fractionated irradiation alone (5×4 Gy, corresponding to an equivalent dose in 2 Gy fractions [EQD2] of 23.3 Gy assuming an alpha/beta ratio of 10 Gy) did not meaningfully affect the survival of the animals (see Fig. 1b). These in vivo results are in line with other reports after single-dose irradiation with 12 Gy (EQD2 = 22 Gy), which also reported no meaningfully prolonged survival in this glioma model^{35,44}. This contrasts findings of our in vitro experiments, showing 80–90% reductions in clonogenic survival of SMA-560 cells after 5×4 Gy irradiation treatment (see Fig. 2C, S4). Explanations for the discrepant in vivo and in vitro results may comprise hypoxic tumor cores in vivo, a well-known contributor to increased radioresistance^{45,46}, or

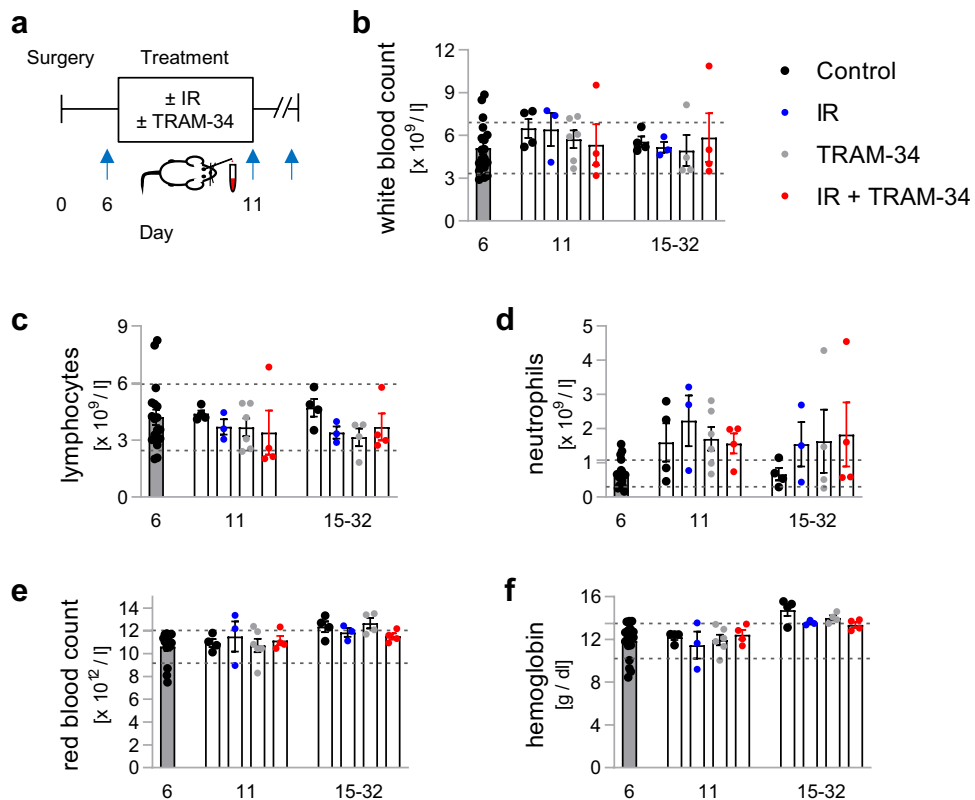


Figure 7. Fractionated irradiation and/or TRAM-34 have little effect on blood counts in the SMA-560 VM/Dk glioma model. (a), Scheme depicting time course of sample collection as indicated by blue arrows. (b–f), Depicted are individual values from 3 to 6 animals and mean values \pm sem. Additionally, a ‘normal range’ of values (defined as the range of mean value \pm standard deviation of all animals before the start of treatment) are outlined by dashed lines representing the upper and lower limit.

reciprocal interactions of SMA-560 glioma cells with the tumor microenvironment and stroma cells^{47,48}. This may also be supported by increased radioresistance of stem-cell-enriched SMA-560 cells (NSC medium) compared to normal DMEM culture conditions¹⁶.

While TRAM-34 applied concomitantly to fractionated irradiation resulted in prolonged mouse survival (see Fig. 1b), the $K_{Ca}3.1$ blocker did not radiosensitize SMA-560 cells in vitro in the present (see Fig. 2c, S6) or our recent study¹⁶. Radiosensitizing effects of TRAM-34 have been reported previously in different in vitro and ectopic mouse glioma models^{12,14}. Hence, one might speculate that SMA-560 cells acquire a TRAM-34-sensitive radioresistant phenotype in an orthotopic microenvironment in vivo. Intriguingly and similarly to our results, targeting HGF/MET in combination with tumor irradiation (but not tumor irradiation alone) prolonged survival in the SMA-560 glioma model but did not affect radiosensitivity in vitro³⁵. From our data, we cannot distinguish whether the blockade of mitochondrial⁴⁹ or of plasmalemmal $K_{Ca}3.1$ channels, or of both, contributed to these findings.

Our histological analysis provides evidence of a hyperinvasion of SMA-560 cells in the brain after irradiation (see Fig. 3c,d). This has been reported previously in vitro and in vivo in other glioma models^{14,21,50,51}. As the occurrence of multifocal glioblastoma is associated with a worse prognosis⁵², this might also explain the lacking efficacy of radiation treatment alone in this glioma model. While irradiation will most likely reduce tumor growth in the irradiation field, this beneficial effect on mouse survival appears to be counteracted by a co-occurring hyperinvasion of cancer cells. Overall, a balance of both effects might result in similar survival times as compared to animals in the control arm.

Importantly, the concomitant application of TRAM-34 abolished the radiogenic hyperinvasion in the present study (see Fig. 3c,d). This might suggest that radiation treatment only resulted in meaningful survival benefits when radiogenic tumor spreading was inhibited by TRAM-34. $K_{Ca}3.1$ has been demonstrated in various in vitro and in vivo models to be required for migration and brain invasion of glioblastoma cells^{10,17,19–21}. Consistently, $K_{Ca}3.1$ (*KCNN4*) mRNA abundance of primary glioblastoma stem cells correlated with mesenchymal marker expression and in vitro matrix invasion capability in our previous work^{13,39}. In contrast, we found no irradiation-induced or TRAM-34-sensitive transfilter migration or wound healing of DMEM-grown SMA-560 cells in vitro (see Fig. 4). Hence, one might speculate that $K_{Ca}3.1$ regulates 3D invasion (secretion of matrix metalloproteinases, etc., see next paragraph) rather than migration mechanics in SMA-560 cells.

Auto-/paracrine TGF- β signaling might be a potential pathway involved in this process (albeit a significant radiogenic stimulation of TGF- β 1 secretion was only found in stem-cell-enriched NSC cultures in vitro and was not TRAM-34 sensitive, see Fig. 5b–e, S7). Previous work has demonstrated that radiation indeed stimulates TGF- β signaling in the orthotopic SMA-560 glioma model via hepatocyte growth factor (HGF) and its receptor MET³⁵. Matrix metalloproteinases (MMPs) are TGF- β downstream targets and are reportedly involved in glioblastoma brain invasion^{53,54}. In the present study, a single dose (8 Gy) of irradiation led to a doubling of *MMP9* ($P = 0.079$) but not of *MMP2* mRNA abundance in DMEM-grown SMA-560 cells (see Fig. 5c). Importantly, TRAM-34 co-treatment decreased *MMP9* mRNA abundance after either single dose or fractionated irradiation treatment (Fig. 5c–f). This might hint at an activation of $K_{Ca}3.1$ by irradiation, ultimately leading to TGF- β release, *MMP9* expression and increased cell invasion.

As mentioned above, immune cell function, e.g., migration or proliferation of T cells, may critically depend on $K_{Ca}3.1$ channel activity^{26,27}. In the present study, we detected no detrimental effects on immune cell infiltration or blood counts of TRAM-34 treatment +/- irradiation (see Figs. 6 and 7). Reassuringly, the invasion of cytotoxic CD8⁺ T cells was not blunted by irradiation and/or TRAM-34 treatment. On top, we detected no increase in immunosuppressive FoxP3⁺ regulatory T cells, in contrast to other authors' conclusion that regulatory T cells may be more radioresistant and hence may accumulate after irradiation⁵⁵. It appears tempting to speculate whether the prolongation of survival may partly be also due to TRAM-34's immunomodulating effects in glioma as described elsewhere^{33,34}. In this line, other authors concluded that not intrinsic radioresistance of cancer cells, but rather factors of the host immune system may correlate with the efficacy of radiotherapy⁵⁶. In particular, the authors identified CD8⁺ T cells as essential contributors for successful radiotherapy in a murine breast cancer model, a conclusion similar to other work⁵⁷. Our immunohistochemical analyses did by and large not identify differences in intratumoral CD8⁺ T cells between the treatment arms (see Fig. 6d), even though there exist multiple studies associating higher CD8⁺ counts with prolonged survival of glioblastoma patients^{58–60}. New studies may try to elucidate immune cell subpopulations predictive of efficacious irradiation treatment in primary brain tumors.

Last, we did not detect safety signals when combining TRAM-34 with radiation treatment (see Fig. 7 and S5). This builds on previous evidence on the tolerability of $K_{Ca}3.1$ targeting: both *KCNN4*^{-/-} animal models (except impaired volume control of erythrocytes and lymphocytes^{42,43}), as well as clinical data on the structurally-related $K_{Ca}3.1$ blocker sennicapoc in patients with sickle cell disease did not detect serious adverse effects⁶¹.

There are several limitations to our work. We could not delineate the precise molecular mechanism driving the synergism of radiation + TRAM-34 treatment. Our results point towards irradiation-induced TGF-beta secretion, followed by hyperinvasion of tumor cells into the brain parenchyma, which might be inhibited by TRAM-34. However, one may debate whether the anti-invasive action of drugs is generally likely to translate into clinical efficacy. Most glioblastoma patients—even after complete macroscopic tumor resections—will ultimately relapse⁶². This finding hints at an early spreading of tumor cells, likely before the initial diagnosis has been made. Evidence of a whole brain invasion of glioma cells exists for *IDH*-mutated gliomas⁶³. Similar explanations may apply to the failure of metastatic pathway targeting therapeutics (such as MMP inhibitors) in nearly all large randomized controlled trials in solid tumors so far^{64,65}. Whereas treatment in preclinical tumor models may be started at a very early stage, this does not apply to cancer patients with visible primary tumors, arguably months or years after the metastatic (or invasive) process has started⁶⁶. On a more general note, we only used one syngeneic glioma model limiting the generalizability of the results. Further experiments in other syngeneic glioma models, such as GL-261/C57BL/6 or CT-2A/C57BL/6⁶⁷, are needed. Along those lines, acute inflammatory processes elicited

by transplanting syngeneic glioma cells in the brains of immunocompetent mice differ substantially from longer-lasting immune editing processes occurring in glioblastoma patients⁶⁸. Here, genetically induced glioma animal models might bring further insights^{69–71}.

To conclude, $K_{Ca}3.1$ targeting with TRAM-34 seems to inhibit invasion of irradiated SMA-560 glioma cells *in vivo*. Most importantly, these effects are relevant for the survival of the glioma mice and are not associated with apparent immune cell alterations. Due to lacking TRAM-34 effects in our *in vitro* experiments, it is tempting to speculate that the TRAM-34 sensitive phenotype is only acquired in the orthotopic syngeneic brain environment.

Material and methods

All sections henceforth are written in accordance with MeRIT (Method Reporting with Initials for Transparency)⁷².

Cell culture Murine glioma cells SMA-560 were originally derived from a spontaneous murine astrocytoma in VM/Dk mice^{73,74}. The cells were cultivated in DMEM medium (ThermoFisher, #41965-039) supplemented with 10% fetal bovine serum (FBS) in a 10% CO₂ atmosphere if not otherwise specified. In experiments assessing the migratory properties of cells, FBS levels were lowered to 0.1–1% to reduce proliferative capacity while ensuring the viability of cells. To enrich SMA-560 stem cells (see Supplementary Figures S6, S7), SMA-560 cells were grown as spheroids in FBS-free human NeuroCult NS-A Proliferation Medium (including 10 ng/mL rhFGF, 20 ng/mL rhEGF, 2 µg/mL Heparin; STEMCELL Technologies, #05751, #78003, #78006.2, #07980) at 37 °C and 5% CO₂.

Adherent cells were detached (DMEM medium) or cells separated from spheroids (NSC medium) with Trypsin–EDTA 0.05% (ThermoFisher, #25300054) and manually counted with Hemocytometer Chips (Neubauer improved).

Drug treatment TRAM-34 was synthesized in house by P.K. using the synthetic strategy reported by Wulff et al.⁷⁵ The chemical purity and identity of TRAM-34 was confirmed by high-performance liquid chromatography (HPLC) and ¹H-NMR (HPLC and NMR spectra can be found in the Supplementary Appendix). For *in vitro* experiments, TRAM-34 was dissolved in DMSO at concentrations of 1 or 10 mmol/L and used at final concentrations of 200 nM or 1 µM (patch clamp experiments) or 5 µM (all other experiments) with same volumes of DMSO serving as vehicle control. TRAM-34 concentrations used for *in vitro* experiments are in the same range as previously found in brain tissue of up to 1.3 µM in mice¹⁰ or up to 2.5 µM in rats¹¹. 1-EBIO (1-ethylbenzimidazolone, Sigma-Aldrich) was prepared from 200 mM stock solution in DMSO and used at final concentrations of 200 µmol/L for patch clamp experiments. For *in vivo* experiments, TRAM-34 was dissolved in miglyol-812 (Caesar & Loretz, PZN1115805) at a concentration of 12 mg/mL (34,8 mmol/L) before sterile filtration (Millex – FG 0.20 µm, SLFG025LS, Merck) resulting in injection volumes of 10 µL per gram of bodyweight. Accordingly, equal volumes of miglyol-812 were used as vehicle control. Except for patch clamp experiments, all experiments were conducted in a blinded fashion until data visualization or statistical analysis. Sketches depicting exact treatment times can be found in respective figures or in the following paragraphs.

Irradiation. Photon irradiation was performed by NS or KG with a 6 MV linear accelerator (LINAC SL25 Philips) at room temperature. The applied dose rate for *in vitro* experiments was 5 Gy/min. Equivalent dose in 2 Gy fractions (EQD2) was calculated with an online tool <http://www.eqd2.de/> assuming an alpha/beta ratio of 10 Gy for SMA-560 cells.

Limited dilution assays. To assess the effect of fractionated irradiation in combination with 5 µM TRAM-34 on plating efficiency and survival fractions, limited dilution assays were performed by NS. Cells were plated in 96 well plates in serial dilutions (2048–1 cell per well). 4 h after plating the cells, TRAM-34 or vehicle (DMSO) was added. Irradiation treatment (0, 1, 2, 3 or 4 Gy) was started 1 h after addition of the drug, and repeated for another 4 consecutive days. 14 days after the last day of irradiation, numbers needed to retain culture (defined as cell colonies or spheroids consisting of at least 50 cells) were determined. Results of 4 wells per treatment group were averaged for each independent experiment. Plating efficiency and surviving fraction were calculated as follows:

$$\text{Plating efficiency} = \frac{1}{\text{Number of cells needed to retain culture}}$$

$$\text{Survival fraction} = \frac{\text{Plating efficiency (treatment group X at Y Gy)}}{\text{Plating efficiency (treatment group X at 0 Gy)}}$$

Of note, determining numbers needed to retain culture at other time points (e.g. 7 days, 21 or 28 days after the last day of irradiation) led to negligible differences in plating efficiency or survival fraction results (data not shown).

Transwell migration. The transwell migration of SMA-560 cells was measured using the Real-Time Cell Analyzer DP (xCELLigence, Roche, Mannheim, Germany) and performed by NS. After irradiation of cells (0 or 2 Gy), cells were detached and 40.000 cells in DMEM/1% FBS, further containing 5 µM TRAM-34 or vehicle (DMSO) alone, were pipetted into filter inserts forming the upper chambers of a CIM-Plate-16. The lower chambers were filled with DMEM/10% FBS to produce a chemoattractant transfilter gradient. Upon plugging the filter inserts into the lower chambers, the electrical impedance between gold electrodes at the outer face of the filter membrane and the bottom of the lower chamber was continuously recorded. Transfilter migration and subsequent cell settling on the gold electrodes of the filter membrane results in an increase in this impedance. As a measure of migration velocity, the slope of the time-dependent impedance increase was analyzed as soon as this slope became linear. Due to high inter-experimental scattering, recorded slopes had to be normalized to that of the respective control arm (vehicle, 0 Gy) to become comparable between independent experiments.

Scratch assay (wound healing assay) The scratch assay was performed by NS as previously described⁷⁶. Briefly, 75,000 SMA-560 cells were plated into 96 well plates and let adhere overnight. To minimize proliferation of cells, 0.1% FBS-containing DMEM was used as culture medium. One hour after 5 μ M TRAM-34 or vehicle (DMSO) was added, cells were irradiated (0 or 2 Gy). After another hour of incubation, a scratch was created by using 20 μ L pipette tips (Biosphere® plus, 70.1116.210). Pictures of the scratch were recorded at time points 0, 8 and 24 h after the scratch. The width of scratch was quantified with FIJI (version 2.9.0/1.53t⁷⁷). In general, results of 5 wells per treatment group were averaged for each independent experiment. Migration distance was calculated as follows:

$$\text{Migration distance} = \frac{\text{Distance of scratch}(\text{time } 0) - \text{Distance of scratch}(\text{time } X)}{2}$$

TGF- β 1 ELISA. Measuring released TGF- β 1 in cell culture supernatants was performed by NS using Mouse TGF- β 1 DuoSet ELISA, DuoSet ELISA Ancillary Reagent Kit 1 and Sample Activation Kit 1 (all R&D Systems, DY1679-05, DY007B, DY010) according to the manufacturer's instruction. Samples were prepared by plating 187,500 cells/1 mL medium (single-dose irradiation) or 62,500 cells/1 mL medium (fractionated irradiation; lower cell concentrations due to longer incubation periods). Medium used was 0.1% FBS-containing DMEM to reduce the proliferation of cells and avoid cross-contamination of results by bovine TGF- β 1 present in FBS. 5 μ M TRAM-34 or vehicle (DMSO) was added 4 h after plating of cells. For single-dose irradiation treatment, cells were irradiated (0, 2, 4 or 8 Gy) and supernatants collected 48 h after the irradiation. For fractionated irradiation, cells were irradiated for 5 consecutive days (0, 2 or 4 Gy) and supernatants collected 24 h after the last irradiation. Additionally, cells were detached, counted to correct for residual cell proliferation and used for further RT-PCR measurements.

RNA isolation and RT-PCR Sample preparation was described in the previous paragraph. RNA of samples was isolated using the NucleoSpin RNA isolation kit (Macherey–Nagel, #740955.250) according to the manufacturer's instructions. 20 ng of RNA (as measured by a NanoDrop ND-100 spectrometer) were used for one-step SYBR Green-based reverse transcriptase PCR using the 1 Step RT PCR Green ROX L Kit (highQu) according to the manufacturer's instruction. Specific fragments (all Quantitect Primer Assay, Qiagen) used, were *KCNN4* (*K_{Ca}3.1*; QT00105672), *TGFBR1* (QT00135828), *MMP2* (QT00116116), *MMP9* (QT00108815) and *CD44* (QT00173404). Results were normalized to the mean abundance of housekeeper genes *GAPDH* (QT01658692) and *PDHB* (QT00163366). Measurements and other steps were performed by NS on a LightCycler480 device (Roche). Crossing point values and melting curves were analyzed using LightCycler 480 software (Roche, version 1.5.0).

Immunoblotting Standard protocols were used for SDS polyacrylamide gel electrophoresis (SDS-PAGE) and immunoblotting. In short, cells were lysed with NP-40-based lysis buffer (including protease- and phosphatase-inhibitors), proteins separated by 12% SDS-Page, blotted, and probed against *K_{Ca}3.1* and against beta-actin as a loading control using a rabbit anti-*K_{Ca}3.1* antibody (1:1000 in 1% BSA/PBS, Alomone labs, APC-064) and mouse anti-beta-actin antibody (1:20,000 in 1% BSA/PBS, Sigma Aldrich, #A554). Antibody binding was detected with fluorescent anti-rabbit (1:5000 in 1% BSA/PBS, 926–68071, LI-COR Biosciences) or anti-mouse (1:5000 in 1% BSA/PBS, 926–32350, LI-COR Biosciences) secondary antibodies and a LI-COR ODYSSEY FC detection system (LI-COR Biosciences). For blocking specific epitope binding of the anti-*K_{Ca}3.1* antibody, the antibody was pre- (1 h) and co-incubated with its specific blocking peptide (2 μ g blocking peptide per 1 μ g of antibody; Alomone labs, BLP-PC064).

Patch-clamp recording. Macroscopic on-cell (cell-attached) and whole-cell currents from DMEM medium-grown irradiated (0 or 2 Gy, 90–240 min post-irradiation) SMA-560 cells were recorded by SMH in voltage-clamp mode (10 kHz sampling rate) and 3 kHz low-pass-filtered by an EPC-9 patch-clamp amplifier (Heka, Lambrecht, Germany) using Pulse software (Heka) and an ITC-16 Interface (Instrutech, Port Washington, NY, USA). Borosilicate glass pipettes (~5 M Ω pipette resistance; GC150 TF-10, Clark Medical Instruments, Pangbourne, UK) manufactured by a microprocessor-driven DMZ puller (Zeitz, Augsburg, Germany) were used in combination with an STM electrical micromanipulator (Lang, Gießen, Germany). Cells were continuously superfused at 37 °C with NaCl solution (in mM: 125 NaCl, 32 *N*-2-hydroxyethylpiperazine-*N*-2-ethanesulfonic acid (HEPES), 5 KCl, 5 D-glucose, 1 MgCl₂, 5 CaCl₂, titrated with NaOH to pH 7.4) additionally containing 0 or 200 μ M of the *K_{Ca}3.1* K⁺ channel activator 1-EBIO and 0 or 1 μ M of TRAM-34. The pipette solution contained in on-cell-mode (in mM) 130 KCl, 32 HEPES, 5 D-glucose, 1 MgCl₂, 5 CaCl₂, titrated with KOH to pH 7.4. and in whole-cell mode (in mM) 140 K-D-gluconate, 5 HEPES, 5 MgCl₂, 1 K₂-EGTA, 1 K₂-ATP, titrated with KOH to pH 7.2.

Currents were elicited by 41 voltage square pulses (700 ms each) from 0 mV holding potential to voltages between –100 mV and +100 mV (on-cell) or +75 mV (whole-cell) delivered in 5 mV increments. Clamp voltages refer to the cytosolic face of the plasma membrane and were not corrected (on-cell) or corrected by adding –10 mV (whole cell) for the liquid junction potential between pipette and bath solution. For analysis, macroscopic on-cell currents were averaged between 100 and 700 ms of each voltage sweep. Inward currents are defined as influx of cations into the cells (or efflux of anions out of the cell), depicted as downward deflections of the current tracings, and defined as negative currents in the current voltage relationships. Macroscopic on-cell conductance was calculated for the inward currents between –100 mV and +25 mV clamp voltage. The 1-EBIO-stimulated and TRAM-34-sensitive increase in macroscopic on-cell conductance and the associated change in current reversal potential were used as a measure of functional *K_{Ca}3.1* channel expression in the plasma membrane. For single channel analysis, currents were continuously on-cell recorded (10 kHz sampling rate, 3 kHz low-pass-filtering) for several seconds at clamp voltages between –100 mV and +100 mV (10 mV increments) and unitary current transitions were analyzed as a measure of channel amplitude. In addition, single channel activity was assessed during wash-in and wash-out of TRAM-34 (1 μ M).

Animal model. All animal experiments were performed in accordance to the laboratory animal research guidelines, authorized by the local ethics committee for Animal Research (Regierungspräsidium Tübingen, Germany) with the registration code R13/18G and performed by NS or KG. This manuscript complies with the ARRIVE guidelines 2.0⁷⁸. VM/Dk mice were kept under standard SPF conditions on a dark–light cycle of 12 h with humidity of $55 \pm 10\%$, temperatures of $22 \pm 2^\circ\text{C}$, and ad libitum food and water supply.

Tumor transplantation Two-to-six-month-old male and female mice (60% male; mean body weight: 26.6 g, standard deviation: 4.5 g) were anaesthetized using fentanyl (0.05 mg/kg b.w. [body weight]), midazolam (5 mg/kg b.w.) and medetomidine (0.5 mg/kg b.w.) intraperitoneally. Body temperature was stabilized via external heating mats. Mice were placed in a stereotactic fixation device (Stoelting) and a burr hole was drilled 2 mm lateral of the bregma to ensure transplantation into the right striatum as described previously³⁶. After ensuring no excess bleeding from the burr hole, the needle of a Hamilton syringe was inserted to a depth of 3 mm from the level of the skull surface, after which it was pulled out 0.5 mm to ensure a final depth of injection of 2.5 mm. 5×10^3 SMA-560 cells in phosphate-buffered saline were injected slowly over 1 min. After the injection and an additional waiting period of 2 min, the syringe was slowly withdrawn. Tissue adhesive (Histoacryl®, B. Braun) was used for closing the burr hole and the skin sutured. After the procedure, antidotes naloxone (1.2 mg/kg b.w.), flumazenil (0.5 mg/kg b.w.) and atipamezole (0.5 mg/kg b.w.) were administered subcutaneously to end anesthesia. Carprofen analgesic treatment (0.5 mg/kg b.w.) was administered subcutaneously right before the surgical intervention started and for three additional days after it. All drugs (except for fentanyl, which was purchased separately: Fentadon 50 µg/mL, Eurovet Animal Health B.V.) were provided by the facility of animal welfare of the University of Tübingen.

Afterwards, the animals were observed and weighed daily for the first 7 days after the injection or if any sign of distress was present. Otherwise, monitoring frequency was twice weekly. Criteria of experiment termination were defined as reaching a cumulative animal observation score of 5 or higher (see Supplementary Table S1 for short descriptions of all components of the score). Long-term surviving animals from the overall survival experiments were taken off the experiment after a maximum of 150 days. Animals were sacrificed using CO₂ asphyxia in their cages. Afterwards, the brains of the animals were extracted and fixated in phosphate-buffered 4.5% formalin solution. All steps were performed by NS or KG.

For power calculations in the orthotopic SMA-560 glioma mouse model, we estimated approximately 5% of animals surviving more than 7 weeks, as has been reported previously³⁶. Required mouse numbers per treatment group were estimated for alpha and beta errors of 5% and 20%, respectively, and a treatment-associated increase in ≥ 7 -weeks-survivors from 5 to 20%. Such quadruplication of “long-term” survivors was considered scientifically relevant when extrapolating to the clinical situation of glioblastoma patients. The sample size calculation led us to aim for 12 animals per treatment group (excluding 20% reserve animals for the substitution of animals with failed tumor cell engraftment). In the end, we slightly fell short of 12 animals per treatment group due to changes at the beginning of the study. In detail, we initially planned to deliver 10 fractions of 2 Gy irradiation, which was not feasible as most animals reached the stopping criteria before the end of treatment. To compensate, we initially lowered the number of injected tumor cells (5×10^2) which led to inconsistent tumor engraftment. Hence, we changed back to injecting 5×10^3 cells and treating animals with 5×4 Gy of irradiation. Moreover, we excluded one batch of 8 animals from further analyses as none of the animals showed any sign of tumor development, hinting at technical issues during the surgery. One animal (TRAM-34 group) was excluded as bleeding from the burr hole at the time of tumor cell injection potentially interfered with tumor engraftment. Exclusion criteria were not stated a priori.

Treatment of animals Treatment of the animals started on day 7 after tumor cell injection and was performed by NS or KG. Experimental mouse batches, i.e., animals transplanted in one session, were randomized (<https://www.randomizer.org/>) to one of the following treatments, that were administered daily for five consecutive days (days 7–11): control (5×0 Gy and $5 \times$ miglyol intraperitoneally), irradiation (IR) only (5×4 Gy and $5 \times$ miglyol i.p.), TRAM-34 only (5×0 Gy and 5×120 mg/kg b.w. TRAM-34 in miglyol i.p.) or combined IR + TRAM-34 treatment (5×4 Gy and 5×120 mg/kg b.w. TRAM-34 in miglyol i.p.). TRAM-34 or vehicle (miglyol) was injected 6 h before irradiation of the animals. As mentioned previously, experiments were blinded in regard to drug treatment. Irradiation was conducted as previously described¹⁴. In short, all animals were anaesthetized with isoflurane (Isofluran CP®, CP-Pharma). Animals from the irradiation only or IR + TRAM-34 groups were placed under the linear accelerator and body parts, except for parts of the right hemisphere, were protected by a lead shield (Fig. 1a, right; for target volume and dose distribution, see Edalat et al.¹⁴). Irradiation was performed with a 6 MV linear accelerator (LINAC SL25 Philips) at room temperature and a dose rate of 3.5 Gy/min.

Immunohistochemistry. All brains of an experimental batch (see above) were extracted on the same day by NS. Time of extraction was planned as of 14 days after the last day of treatment or as soon as the first animal within a batch reached the termination criteria (range: 3–14 days post-treatment). 4 animals (1 per group) were only injected with 5×10^2 SMA-560 cells due to an earlier protocol (all animals developed a visible tumor). H&E and immunohistochemical stainings were performed by IGM and LQM. For histology, 3–5 µm-thick sections were cut and stained with haematoxylin and eosin (H&E). Immunohistochemistry was performed on brains of animals displaying an H&E-Score ≥ 1 on an automated immunostainer (Ventana Medical Systems, Inc.) according to the company's protocols for open procedures with slight modifications. The slides were stained with the antibodies Iba1 (Abcam, Cambridge, UK), CD68 (ab125212, Abcam, Cambridge, UK) CD3 (clone SP7, DCS Innovative Diagnostik-Systeme GmbH u. Co. KG, Hamburg, Germany), CD8 (clone C8/144B; Dako, Glostrup, Denmark) and FoxP3 (236A/E7, Abcam, Cambridge, UK). Appropriate positive and negative controls were used to confirm the adequacy of the staining. All samples were scanned with the Ventana DP200 (Roche, Basel, Switzerland) and processed with the Image Viewer MFC Application. Final image preparation was performed with Adobe Photoshop CS6. The tumor histology and the tumor microenvironment were scored as follows:

H&E: Score 0: no tumor or histological alterations were detected; Score 1: gliosis, no tumor or necrosis detected; Score 2: small tumors without clear tumor borders accompanied by gliosis, but no necrosis detected; Score 3: medium to large tumors with clear tumor borders accompanied by gliosis and necrosis in the tumor core. Additional occurrence of multiple satellite tumors (foci of tumor not connected to the main body tumor, related to invasiveness) were scored separately.

Iba1: Score 0: no alterations, the microglia showed few and thin ramifications; Score 1: mild increase of the reactive microglia (shorter and thicker ramifications) and; Score 2: moderate to prominent reactive microglia accompanied by phagocytic microglia (loss of the ramification and globular inflated cells body) in the tumor core. Some animals presented with macrophage pseudopalisading around the tumor.

CD68: Score 0: no alterations were detected, the microglia present showed few and thin ramifications; Score 1: mild focal increase of the CD68 + macrophages; Score 2: moderate to prominent increase of CD68 + macrophages. Pseudopalisading of the macrophages around the tumor is present in some tumors.

CD3: Score 0: no presence of CD3 positive cells; Score 1: mild to moderate presence of CD3 positive cells; Score 2: prominent presence of CD3 positive cells.

CD8 and FoxP3: Score 0: no presence of positive cells; Score 1: mild presence of positive cells; Score 2: moderate presence of positive cells.

Blood counts Blood samples were collected from tail vein or retro-orbital sinus in isoflurane anesthesia (for the latter one) by NS. Time points of sample collection were: first, for a baseline measurement on the day before treatment initiation (day 6 post-surgery); second, after the last round of irradiation treatment (day 11 post-surgery); and lastly, 3 weeks after the last day of treatment or if the stopping criteria for individual animals were reached (day 15–32 post-surgery). Blood samples were analyzed with a Hematology Analyzer HM5 (Abaxis) right after sample collection.

Data visualization and statistical analysis Data visualization and statistical tests were performed using Graph-Pad Prism (version 9.4.1) by NS and SMH. Statistical tests were performed using (mean) values of independent experiments (in vitro) or animals (in vivo experiments). Specifics are given in the respective figure legend.

Data availability

Data is available upon reasonable request from the corresponding author.

Received: 24 May 2023; Accepted: 15 November 2023

Published online: 23 November 2023

References

- Wen, P. Y. *et al.* Glioblastoma in adults: A Society for Neuro-Oncology (SNO) and European Society of Neuro-Oncology (EANO) consensus review on current management and future directions. *Neuro Oncol.* **22**, 1073–1113. <https://doi.org/10.1093/neuonc/noaa106> (2020).
- Miller, K. D. *et al.* Brain and other central nervous system tumor statistics, 2021. *CA A Cancer J. Clin.* **71**, 381–406. <https://doi.org/10.3322/caac.21693> (2021).
- Chinot, O. L. *et al.* Bevacizumab plus radiotherapy-temozolomide for newly diagnosed glioblastoma. *N. Engl. J. Med.* **370**, 709–722. <https://doi.org/10.1056/NEJMoal308345> (2014).
- Stupp, R. *et al.* Cilengitide combined with standard treatment for patients with newly diagnosed glioblastoma with methylated MGMT promoter (CENTRIC EORTC 26071–22072 study): a multicentre, randomised, open-label, phase 3 trial. *Lancet Oncol.* **15**, 1100–1108. [https://doi.org/10.1016/s1470-2045\(14\)70379-1](https://doi.org/10.1016/s1470-2045(14)70379-1) (2014).
- Weller, M. *et al.* Rindopepimut with temozolomide for patients with newly diagnosed, EGFRvIII-expressing glioblastoma (ACT IV): A randomised, double-blind, international phase 3 trial. *Lancet Oncol.* **18**, 1373–1385. [https://doi.org/10.1016/s1470-2045\(17\)30517-x](https://doi.org/10.1016/s1470-2045(17)30517-x) (2017).
- Lim, M. *et al.* Phase III trial of chemoradiotherapy with temozolomide plus nivolumab or placebo for newly diagnosed glioblastoma with methylated MGMT promoter. *Neuro Oncol.* **24**, 1935–1949. <https://doi.org/10.1093/neuonc/noac116> (2022).
- Omuro, A. *et al.* Radiotherapy combined with nivolumab or temozolomide for newly diagnosed glioblastoma with unmethylated MGMT promoter: An international randomized phase III trial. *Neuro Oncol.* **25**, 123–134. <https://doi.org/10.1093/neuonc/noac099> (2023).
- Stupp, R. *et al.* Effect of tumor-treating fields plus maintenance temozolomide vs maintenance temozolomide alone on survival in patients with glioblastoma: A randomized clinical trial. *JAMA* **318**, 2306–2316. <https://doi.org/10.1001/jama.2017.18718> (2017).
- Stupp, R. *et al.* Radiotherapy plus concomitant and adjuvant temozolomide for glioblastoma. *N. Engl. J. Med.* **352**, 987–996. <https://doi.org/10.1056/NEJMoal43330> (2005).
- D'Alessandro, G. *et al.* KCa3.1 channels are involved in the infiltrative behavior of glioblastoma in vivo. *Cell Death Dis.* **4**, e773. <https://doi.org/10.1038/cddis.2013.279> (2013).
- Chen, Y.-J., Raman, G., Bodendiek, S., O'Donnell, M. E. & Wulff, H. The KCa3.1 blocker TRAM-34 reduces infarction and neurological deficit in a rat model of ischemia/reperfusion stroke. *J. Cereb. Blood Flow Metab.* **31**, 2363–2374. <https://doi.org/10.1038/jcbfm.2011.101> (2011).
- Stegen, B. *et al.* Ca²⁺-activated IK K⁺ channel blockade radiosensitizes glioblastoma cells. *Mol. Cancer Res.* **13**, 1283–1295. <https://doi.org/10.1158/1541-7786.Mcr-15-0075> (2015).
- Klumpp, L., Sezgin, E. C., Skardelly, M., Eckert, F. & Huber, S. M. KCa3.1 channels and glioblastoma: In vitro studies. *Curr. Neuropharmacol.* **16**, 627–635. <https://doi.org/10.2174/1570159x15666170808115821> (2018).
- Edalat, L. *et al.* BK K⁺ channel blockade inhibits radiation-induced migration/brain infiltration of glioblastoma cells. *Oncotarget* **7**, 14259–14278. <https://doi.org/10.18632/oncotarget.7423> (2016).
- D'Alessandro, G. *et al.* KCa3.1 channel inhibition sensitizes malignant gliomas to temozolomide treatment. *Oncotarget* **7**, 30781–30796. <https://doi.org/10.18632/oncotarget.8761> (2016).
- Stransky, N., Ganser, K., Naumann, U., Huber, S. M. & Ruth, P. Tumoricidal, temozolomide- and radiation-sensitizing effects of K(Ca)3.1 K(+) channel targeting in vitro are dependent on glioma cell line and stem cell fraction. *Cancers (Basel)* <https://doi.org/10.3390/cancers14246199> (2022).
- Sciacaluga, M. *et al.* CXCL12-induced glioblastoma cell migration requires intermediate conductance Ca²⁺-activated K⁺ channel activity. *Am. J. Physiol. Cell Physiol.* **299**, C175–184. <https://doi.org/10.1152/ajpcell.00344.2009> (2010).
- Catacuzzeno, L. *et al.* Serum-activated K and Cl currents underlay U87-MG glioblastoma cell migration. *J. Cell Physiol.* **226**, 1926–1933. <https://doi.org/10.1002/jcp.22523> (2011).

19. Ruggieri, P. *et al.* The inhibition of KCa3.1 channels activity reduces cell motility in glioblastoma derived cancer stem cells. *PLoS One* **7**, e47825. <https://doi.org/10.1371/journal.pone.0047825> (2012).
20. Turner, K. L., Honasoge, A., Robert, S. M., McFerrin, M. M. & Sontheimer, H. A proinvasive role for the Ca(2+) -activated K(+) channel KCa3.1 in malignant glioma. *Glia* **62**, 971–981. <https://doi.org/10.1002/glia.22655> (2014).
21. D'Alessandro, G. *et al.* Radiation increases functional KCa3.1 expression and invasiveness in glioblastoma. *Cancers (Basel)* <https://doi.org/10.3390/cancers11030279> (2019).
22. Hausmann, D. *et al.* Autonomous rhythmic activity in glioma networks drives brain tumour growth. *Nature* **613**, 179–186. <https://doi.org/10.1038/s41586-022-05520-4> (2023).
23. Jensen, B. S., Hertz, M., Christophersen, P. & Madsen, L. S. The Ca²⁺-activated K⁺ channel of intermediate conductance: A possible target for immune suppression. *Expert Opin. Ther. Targets* **6**, 623–636. <https://doi.org/10.1517/14728222.6.6.623> (2002).
24. Wei, T. *et al.* The potassium channel KCa3.1 represents a valid pharmacological target for astroglia-induced neuronal impairment in a mouse model of Alzheimer's disease. *Front. Pharmacol.* **7**, 528. <https://doi.org/10.3389/fphar.2016.00528> (2016).
25. Faragó, N. *et al.* Human neuronal changes in brain edema and increased intracranial pressure. *Acta Neuropathol. Commun.* **4**, 78. <https://doi.org/10.1186/s40478-016-0356-x> (2016).
26. Feske, S., Wulff, H. & Skolnik, E. Y. Ion channels in innate and adaptive immunity. *Annu. Rev. Immunol.* **33**, 291–353. <https://doi.org/10.1146/annurev-immunol-032414-112212> (2015).
27. Lin, Y. *et al.* Regulatory role of KCa3.1 in immune cell function and its emerging association with rheumatoid arthritis. *Front. Immunol.* <https://doi.org/10.3389/fimmu.2022.997621> (2022).
28. Di, L. *et al.* Inhibition of the K⁺ channel KCa3.1 ameliorates T cell-mediated colitis. *Proc. Natl. Acad. Sci.* **107**, 1541–1546. <https://doi.org/10.1073/pnas.0910133107> (2010).
29. Girodet, P. O. *et al.* Ca(2+)-activated K(+) channel-3.1 blocker TRAM-34 attenuates airway remodeling and eosinophilia in a murine asthma model. *Am. J. Respir. Cell Mol. Biol.* **48**, 212–219. <https://doi.org/10.1165/rcmb.2012-0103OC> (2013).
30. Chen, Y. J., Lam, J., Gregory, C. R., Schrepfer, S. & Wulff, H. The Ca²⁺-activated K⁺ channel KCa3.1 as a potential new target for the prevention of allograft vasculopathy. *PLoS One* **8**, e81006. <https://doi.org/10.1371/journal.pone.0081006> (2013).
31. Gawali, V. S. *et al.* Immune checkpoint inhibitors regulate K(+) channel activity in cytotoxic T lymphocytes of head and neck cancer patients. *Front. Pharmacol.* **12**, 742862. <https://doi.org/10.3389/fphar.2021.742862> (2021).
32. Chimote, A. A., Gawali, V. S., Newton, H. S., Wise-Draper, T. M. & Conforti, L. A compartmentalized reduction in membrane-proximal calmodulin reduces the immune surveillance capabilities of CD8(+) T cells in head and neck cancer. *Front. Pharmacol.* **11**, 143. <https://doi.org/10.3389/fphar.2020.00143> (2020).
33. Grimaldi, A. *et al.* KCa3.1 inhibition switches the phenotype of glioma-infiltrating microglia/macrophages. *Cell Death Dis.* **7**, e2174. <https://doi.org/10.1038/cddis.2016.73> (2016).
34. Massenzio, F. *et al.* In vivo morphological alterations of TAMs during KCa3.1 inhibition-by using in vivo two-photon time-lapse technology. *Front. Cell Neurosci.* **16**, 1002487. <https://doi.org/10.3389/fncel.2022.1002487> (2022).
35. Silgner, M. *et al.* Immunological and tumor-intrinsic mechanisms mediate the synergistic growth suppression of experimental glioblastoma by radiotherapy and MET inhibition. *Acta Neuropathol. Commun.* **11**, 41. <https://doi.org/10.1186/s40478-023-01527-8> (2023).
36. Tran, T. T. *et al.* Inhibiting TGF-beta signaling restores immune surveillance in the SMA-560 glioma model. *Neuro Oncol.* **9**, 259–270. <https://doi.org/10.1215/15228517-2007-010> (2007).
37. Friese, M. A. *et al.* MICA/NGG2D-mediated immunogene therapy of experimental gliomas. *Cancer Res.* **63**, 8996–9006 (2003).
38. Stegen, B. *et al.* K⁺ channel signaling in irradiated tumor cells. *Eur. Biophys. J.* **45**, 585–598. <https://doi.org/10.1007/s00249-016-1136-z> (2016).
39. Ganser, K. *et al.* Patient-individual phenotypes of glioblastoma stem cells are conserved in culture and associate with radioresistance, brain infiltration and patient prognosis. *Int. J. Cancer* **150**, 1722–1733. <https://doi.org/10.1002/ijc.33950> (2022).
40. Armento, A., Ehlers, J., Schötterl, S. & Naumann, U. In *Glioblastoma* (ed. De Vleeschouwer, S.). <https://doi.org/10.15586/codon.glioblastoma.2017> (Codon Publications, 2017).
41. Yang, L., Pang, Y. & Moses, H. L. TGF-beta and immune cells: An important regulatory axis in the tumor microenvironment and progression. *Trends Immunol.* **31**, 220–227. <https://doi.org/10.1016/j.it.2010.04.002> (2010).
42. Begegnich, T. *et al.* Physiological roles of the intermediate conductance, Ca²⁺-activated potassium channel Kcnn4. *J. Biol. Chem.* **279**, 47681–47687. <https://doi.org/10.1074/jbc.M409627200> (2004).
43. Henriquez, C. *et al.* The calcium-activated potassium channel KCa3.1 plays a central role in the chemotactic response of mammalian neutrophils. *Acta Physiol. (Oxf)* **216**, 132–145. <https://doi.org/10.1111/apha.12548> (2016).
44. Schneider, H. *et al.* Novel TIE-2 inhibitor BAY-826 displays in vivo efficacy in experimental syngeneic murine glioma models. *J. Neurochem.* **140**, 170–182. <https://doi.org/10.1111/jnc.13877> (2017).
45. Domènech, M., Hernández, A., Plaja, A., Martínez-Balibrea, E. & Balaña, C. Hypoxia: The cornerstone of glioblastoma. *Int. J. Mol. Sci.* <https://doi.org/10.3390/ijms22212608> (2021).
46. Jain, R. K. Antiangiogenesis strategies revisited: From starving tumors to alleviating hypoxia. *Cancer Cell* **26**, 605–622. <https://doi.org/10.1016/j.ccr.2014.10.006> (2014).
47. Calabrese, C. *et al.* A perivascular niche for brain tumor stem cells. *Cancer Cell* **11**, 69–82. <https://doi.org/10.1016/j.ccr.2006.11.020> (2007).
48. Arnold, C. R., Mangesius, J., Skvortsova, I.-I. & Ganswindt, U. The role of cancer stem cells in radiation resistance. *Front. Oncol.* <https://doi.org/10.3389/fonc.2020.00164> (2020).
49. Bachmann, M. *et al.* Pharmacological targeting of the mitochondrial calcium-dependent potassium channel KCa3.1 triggers cell death and reduces tumor growth and metastasis in vivo. *Cell Death Dis.* **13**, 1055. <https://doi.org/10.1038/s41419-022-05463-8> (2022).
50. Steinle, M. *et al.* Ionizing radiation induces migration of glioblastoma cells by activating BK K(+) channels. *Radiother. Oncol.* **101**, 122–126. <https://doi.org/10.1016/j.radonc.2011.05.069> (2011).
51. Wild-Bode, C., Weller, M., Rimmer, A., Dichgans, J. & Wick, W. Sublethal irradiation promotes migration and invasiveness of glioma cells: Implications for radiotherapy of human glioblastoma. *Cancer Res.* **61**(6), 2744–2750 (2001).
52. Farhat, M. *et al.* Multifocal and multicentric glioblastoma: Imaging signature, molecular characterization, patterns of spread, and treatment. *Neuroradiol. J.* <https://doi.org/10.1177/19714009231193162> (2023).
53. Nakada, M., Okada, Y. & Yamashita, J. The role of matrix metalloproteinases in glioma invasion. *Front. Biosci.* **8**, e261–269. <https://doi.org/10.2741/1016> (2003).
54. Oishi, T., Koizumi, S. & Kurozumi, K. Molecular mechanisms and clinical challenges of glioma invasion. *Brain Sci.* **12**, 291. <https://doi.org/10.3390/brainsci12020291> (2022).
55. Kachikwu, E. L. *et al.* Radiation enhances regulatory T cell representation. *Int. J. Radiat. Oncol. Biol. Phys.* **81**, 1128–1135. <https://doi.org/10.1016/j.ijrobp.2010.09.034> (2011).
56. Liang, H. *et al.* Radiation-induced equilibrium is a balance between tumor cell proliferation and T cell-mediated killing. *J. Immunol.* **190**, 5874–5881. <https://doi.org/10.4049/jimmunol.1202612> (2013).
57. Gupta, A. *et al.* Radiotherapy promotes tumor-specific effector CD8⁺ T cells via dendritic cell activation. *J. Immunol.* **189**, 558–566. <https://doi.org/10.4049/jimmunol.1200563> (2012).

58. Mauldin, I. S. *et al.* Proliferating CD8(+) T cell infiltrates are associated with improved survival in glioblastoma. *Cells* <https://doi.org/10.3390/cells10123378> (2021).
59. Lin, P. *et al.* Increased infiltration of CD8 T cells in recurrent glioblastoma patients is a useful biomarker for assessing the response to combined bevacizumab and lomustine therapy. *Int. Immunopharmacol.* **97**, 107826. <https://doi.org/10.1016/j.intimp.2021.107826> (2021).
60. Kmiecik, J. *et al.* Elevated CD3⁺ and CD8⁺ tumor-infiltrating immune cells correlate with prolonged survival in glioblastoma patients despite integrated immunosuppressive mechanisms in the tumor microenvironment and at the systemic level. *J. Neuroimmunol.* **264**, 71–83. <https://doi.org/10.1016/j.jneuroim.2013.08.013> (2013).
61. Ataga, K. I. *et al.* Improvements in haemolysis and indicators of erythrocyte survival do not correlate with acute vaso-occlusive crises in patients with sickle cell disease: A phase III randomized, placebo-controlled, double-blind study of the gardos channel blocker senicapoc (ICA-17043). *Br. J. Haematol.* **153**, 92–104. <https://doi.org/10.1111/j.1365-2141.2010.08520.x> (2011).
62. De Bonis, P. *et al.* The influence of surgery on recurrence pattern of glioblastoma. *Clin. Neurol. Neurosurg.* **115**, 37–43. <https://doi.org/10.1016/j.clineuro.2012.04.005> (2013).
63. Sahn, F. *et al.* Addressing diffuse glioma as a systemic brain disease with single-cell analysis. *Arch Neurol.* **69**, 523–526. <https://doi.org/10.1001/archneurol.2011.2910> (2012).
64. Esposito, M., Ganesan, S. & Kang, Y. Emerging strategies for treating metastasis. *Nat. Cancer* **2**, 258–270. <https://doi.org/10.1038/s43018-021-00181-0> (2021).
65. Winer, A., Adams, S. & Mignatti, P. Matrix metalloproteinase inhibitors in cancer therapy: Turning past failures into future successes. *Mol. Cancer Ther.* **17**, 1147–1155. <https://doi.org/10.1158/1535-7163.Mct-17-0646> (2018).
66. Gerstberger, S., Jiang, Q. & Ganesh, K. Metastasis. *Cell* **186**, 1564–1579. <https://doi.org/10.1016/j.cell.2023.03.003> (2023).
67. Oh, T. *et al.* Immunocompetent murine models for the study of glioblastoma immunotherapy. *J. Transl. Med.* **12**, 107. <https://doi.org/10.1186/1479-5876-12-107> (2014).
68. Gangoso, E. *et al.* Glioblastomas acquire myeloid-affiliated transcriptional programs via epigenetic immunoeediting to elicit immune evasion. *Cell* **184**, 2454–2470.e2426. <https://doi.org/10.1016/j.cell.2021.03.023> (2021).
69. Nunez, F. M. *et al.* Genetically engineered mouse model of brainstem high-grade glioma. *STAR Protoc.* **1**, 100165. <https://doi.org/10.1016/j.xpro.2020.100165> (2020).
70. Hicks, W. H. *et al.* Contemporary mouse models in glioma research. *Cells* <https://doi.org/10.3390/cells10030712> (2021).
71. Gargiulo, G. Next-generation in vivo modeling of human cancers. *Front. Oncol.* <https://doi.org/10.3389/fonc.2018.00429> (2018).
72. Nakagawa, S. *et al.* Method reporting with initials for transparency (MeRIT) promotes more granularity and accountability for author contributions. *Nat. Commun.* **14**, 1788. <https://doi.org/10.1038/s41467-023-37039-1> (2023).
73. Serano, R. D., Pegram, C. N. & Bigner, D. D. Tumorigenic cell culture lines from a spontaneous VM/Dk murine astrocytoma (SMA). *Acta Neuropathol.* **51**, 53–64. <https://doi.org/10.1007/bf00688850> (1980).
74. Pilkington, G. J., Darling, J. L., Lantos, P. L. & Thomas, D. G. T. Cell lines (VMDk) derived from a spontaneous murine astrocytoma: Morphological and immunocytochemical characterization. *J. Neurol. Sci.* **62**, 115–139. [https://doi.org/10.1016/0022-510X\(83\)90193-4](https://doi.org/10.1016/0022-510X(83)90193-4) (1983).
75. Wulff, H. *et al.* Design of a potent and selective inhibitor of the intermediate-conductance Ca²⁺-activated K⁺ channel, IKCa1: A potential immunosuppressant. *Proc. Natl. Acad. Sci.* **97**, 8151–8156. <https://doi.org/10.1073/pnas.97.14.8151> (2000).
76. Liang, C.-C., Park, A. Y. & Guan, J.-L. In vitro scratch assay: A convenient and inexpensive method for analysis of cell migration in vitro. *Nat. Protoc.* **2**, 329–333. <https://doi.org/10.1038/nprot.2007.30> (2007).
77. Schindelin, J. *et al.* Fiji: An open-source platform for biological-image analysis. *Nat. Methods* **9**, 676–682. <https://doi.org/10.1038/nmeth.2019> (2012).
78. Percie du Sert, N. *et al.* Reporting animal research: Explanation and elaboration for the ARRIVE guidelines 2.0. *PLOS Biol.* **18**, e3000411. <https://doi.org/10.1371/journal.pbio.3000411> (2020).

Acknowledgements

We thank Heidrun Faltin, Helga Pertsch and Claus Mayer for excellent technical assistance and Andreas Hönes for constructing the lead shieldings and mouse holders for irradiation treatment.

Author contributions

N.S., F.E., S.M.H. and P.R. conceptualized the work; N.S., K.G., I.G.M., L.Q.M. and S.M.H. performed experiments; N.S., I.G.M., L.Q.M. and S.M.H. were involved in data curation; N.S. and S.M.H. performed formal analysis; F.E., S.M.H. and P.R. acquired financial support; U.N., P.K., S.M.H. and P.R. provided resources and infrastructure; S.M.H. and P.R. supervised the project; N.S. and S.M.H. wrote the original draft. All authors critically reviewed the manuscript and provided feedback.

Funding

Open Access funding enabled and organized by Projekt DEAL. NS, KG, SMH and PR were funded by a grant from the German Cancer Aid (70112872, 70113144), FE by a grant from Gesellschaft für Kinderkrebsforschung. In addition, FE and SMH received funding from the German Research Foundation (DFG EC 575/2-1 and HU 781/7-1).

Competing interests

The authors declare no competing interests.

Additional information

Supplementary Information The online version contains supplementary material available at <https://doi.org/10.1038/s41598-023-47552-4>.

Correspondence and requests for materials should be addressed to S.M.H.

Reprints and permissions information is available at www.nature.com/reprints.

Publisher's note Springer Nature remains neutral with regard to jurisdictional claims in published maps and institutional affiliations.





Open Access This article is licensed under a Creative Commons Attribution 4.0 International License, which permits use, sharing, adaptation, distribution and reproduction in any medium or format, as long as you give appropriate credit to the original author(s) and the source, provide a link to the Creative Commons licence, and indicate if changes were made. The images or other third party material in this article are included in the article's Creative Commons licence, unless indicated otherwise in a credit line to the material. If material is not included in the article's Creative Commons licence and your intended use is not permitted by statutory regulation or exceeds the permitted use, you will need to obtain permission directly from the copyright holder. To view a copy of this licence, visit <http://creativecommons.org/licenses/by/4.0/>.

© The Author(s) 2023

Article

Tumoricidal, Temozolomide- and Radiation-Sensitizing Effects of $K_{Ca}3.1$ K^+ Channel Targeting In Vitro Are Dependent on Glioma Cell Line and Stem Cell Fraction

Nicolai Stransky ^{1,2} , Katrin Ganser ¹, Ulrike Naumann ³ , Stephan M. Huber ^{1,*} and Peter Ruth ²¹ Department of Radiation Oncology, University of Tübingen, 72076 Tübingen, Germany² Department of Pharmacology, Toxicology and Clinical Pharmacy, Institute of Pharmacy, University of Tübingen, 72076 Tübingen, Germany³ Molecular Neurooncology, Hertie Institute for Clinical Brain Research and Center Neurology, University of Tübingen, 72076 Tübingen, Germany* Correspondence: stephan.huber@med.uni-tuebingen.de or stephan.huber@uni-tuebingen.de; Tel.: +49-7071-29-82183; Fax: +49-7071-29-4944

Simple Summary: A potential new treatment for glioma patients is the blockade of $K_{Ca}3.1$ potassium channels. In our study, we performed experiments with the $K_{Ca}3.1$ blocker TRAM-34 in five glioma cell lines. To broaden our findings, effects on cultures enriched in glioma stem cells which are thought to be responsible for treatment failure and relapse were delineated in addition to standard culture conditions. Accordingly, stem-cell enriched cultures were found to be more resistant towards irradiation therapy. Effects of TRAM-34 were dependent on cell line and culture condition and included direct tumoricidal effects, but also temozolomide- and irradiation-sensitizing effects, showing its synergistic potential with current treatment strategies. TRAM-34 effects were mostly found in stem-cell enriched cultures. Overall, our results underline the importance of testing new interventions in several cell lines and different culture conditions to mimic in vivo inter- and intra-tumoral heterogeneity.



Citation: Stransky, N.; Ganser, K.; Naumann, U.; Huber, S.M.; Ruth, P. Tumoricidal, Temozolomide- and Radiation-Sensitizing Effects of $K_{Ca}3.1$ K^+ Channel Targeting In Vitro Are Dependent on Glioma Cell Line and Stem Cell Fraction. *Cancers* **2022**, *14*, 6199. <https://doi.org/10.3390/cancers14246199>

Academic Editor: Luis A. Pardo

Received: 20 September 2022

Accepted: 12 December 2022

Published: 15 December 2022

Publisher's Note: MDPI stays neutral with regard to jurisdictional claims in published maps and institutional affiliations.



Copyright: © 2022 by the authors. Licensee MDPI, Basel, Switzerland. This article is an open access article distributed under the terms and conditions of the Creative Commons Attribution (CC BY) license (<https://creativecommons.org/licenses/by/4.0/>).

Abstract: Reportedly, the intermediate-conductance Ca^{2+} -activated potassium channel $K_{Ca}3.1$ contributes to the invasion of glioma cells into healthy brain tissue and resistance to temozolomide and ionizing radiation. Therefore, $K_{Ca}3.1$ has been proposed as a potential target in glioma therapy. The aim of the present study was to assess the variability of the temozolomide- and radiation-sensitizing effects conferred by the $K_{Ca}3.1$ blocking agent TRAM-34 between five different glioma cell lines grown as differentiated bulk tumor cells or under glioma stem cell-enriching conditions. As a result, cultures grown under stem cell-enriching conditions exhibited indeed higher abundances of mRNAs encoding for stem cell markers compared to differentiated bulk tumor cultures. In addition, stem cell enrichment was paralleled by an increased resistance to ionizing radiation in three out of the five glioma cell lines tested. Finally, TRAM-34 led to inconsistent results regarding its tumoricidal but also temozolomide- and radiation-sensitizing effects, which were dependent on both cell line and culture condition. In conclusion, these findings underscore the importance of testing new drug interventions in multiple cell lines and different culture conditions to partially mimic the in vivo inter- and intra-tumor heterogeneity.

Keywords: glioma stem cells; colony formation assay; limited dilution assay; TRAM-34; temozolomide; ionizing radiation

1. Introduction

Patients with glioblastoma, the most common malignant primary brain tumor in adults [1], exhibit dismal median overall survival times of below two years after multimodal therapy. Standard therapy comprises surgical resection followed by radio-chemotherapy with the DNA-alkylating agent temozolomide and temozolomide maintenance therapy, and,

optionally, electrotherapy with tumor-treating fields [2]. One potential new drug target is the intermediate-conductance Ca^{2+} -activated potassium channel $\text{K}_{\text{Ca}3.1}$ (also known as IK, SK4, Gardos Channel or *KCNN4*; for reviews see [3,4]), which may be inhibited by TRAM-34 (1-[(2-Chlorophenyl)diphenylmethyl]-1H-pyrazole, for review see [5]). In the brain, early reports hypothesized $\text{K}_{\text{Ca}3.1}$ to be solely expressed on malignant cells; however, it is now well-established that normal brain tissues also express $\text{K}_{\text{Ca}3.1}$, such as brain-resident immune cells [6], astrocytes or neurons [7,8]. Importantly, $\text{K}_{\text{Ca}3.1}$ expression is reportedly highly upregulated in glioma stem cells [9] and its function has been demonstrated to regulate tumor cell proliferation [10,11] and spreading of glioma cells in the brain [9,12–16]. In addition, blocking $\text{K}_{\text{Ca}3.1}$ with TRAM-34 reportedly radio-sensitizes glioma cells both in vitro and in vivo [17]. Beyond that, $\text{K}_{\text{Ca}3.1}$ targeting has been shown to sensitize glioma cells to temozolomide [16]. Both findings underscore potential synergistic effects of $\text{K}_{\text{Ca}3.1}$ targeting to two main pillars of standard therapy. Finally, high abundance of $\text{K}_{\text{Ca}3.1}$ mRNA in glioblastoma resection specimens has been proposed to associate with poor survival times of glioblastoma patients in both the REMBRANDT [14] and TCGA patient cohorts [17], even though this type of analysis suffers from structural weaknesses (as discussed in [18]).

The aim of this work was to define the radio- and chemo-sensitizing effects of pharmacological $\text{K}_{\text{Ca}3.1}$ targeting in glioma cell lines that differ in genetic background or phenotype. As many earlier reports identified cancer stem cells as more therapy-resistant than “differentiated” cancer cells (for reviews see [19,20]), we compared bulk tumor-differentiating with glioma stem cell-enriching growth conditions in five glioma cell lines.

2. Material and Methods

2.1. Cell Culture

Three different murine glioma cell lines (SMA-560, SMA-540 and GL-261) and two human glioma cell lines (U-87MG and U-251MG) were studied. SMA-560 and SMA-540 cells originated from the same spontaneous mouse astrocytoma and are, hence, believed to be genetically related [21,22], whereas GL-261 cells were chemically induced by intracranial injection of 3-methylcholantrene in C57BL/6 mice [23]. Both human glioma cell lines were established several decades ago in Sweden [24]. Although several reports describe difficulties tracing back present cultures to original tumor tissues, analyses show glioma origin for both U-87MG and U-251MG cell lines [25,26]. To induce “differentiated” bulk tumor cells, the cell lines were grown in a DMEM medium (ThermoFisher, #41965-039, Austin, TX, USA) supplemented with 10 % fetal bovine serum (FBS) in a 10% CO_2 atmosphere. For glioblastoma stem cell enriching conditions, cells were cultivated in complete human NeuroCult NS-A Proliferation Medium (including 10 ng/mL rhFGF, 20 ng/mL rhEGF, 2 $\mu\text{g}/\text{mL}$ Heparin; STEMCELL Technologies, #05751, #78003, #78006.2, #07980) at 37 °C and 5% CO_2 .

To detach adherent cells or to dissociate cells from spheres, cells were incubated with Trypsin-EDTA 0.05 % (ThermoFisher, #25300054, Austin, TX, USA) for 5–10 min and cell numbers were determined using hemocytometer chips (Neubauer improved). The SMA-540 cells were kindly provided by Hans-Georg Wirsching (Department of Neurology, University Hospital Zurich, Switzerland), and the U-251MG cells were a gift from Dr. Luiz O. Penalva (Graduate School of Biomedical Sciences, UT Health San Antonio, TX, USA).

2.2. RNA Isolation and qPCR

mRNA was isolated with NucleoSpin RNA isolation kit (Macherey-Nagel, #740955.250) according to the manufacturer’s instruction. Resulting RNA concentrations were determined with a NanoDrop ND-100 spectrometer. A total of 20 ng of RNA was used for each sample. One step SYBR Green-based reverse transcriptase PCR was accomplished using the 1 Step RT PCR Green ROX L Kit (highQu) following the manufacturer’s instruction. Specific fragments used for murine cell lines were (all Quantitect Primer Assays, Qiagen): *ALDH1A3* (QT01077867), *CXCR4* (QT00249305), *Nestin* (QT00316799), *SOX2* (QT00249347), *KCNN4* ($\text{K}_{\text{Ca}3.1}$, QT00105672). mRNA abundances were normalized to the geometric means

of those of the housekeeper genes *GAPDH* (QT01658692) and *PDHB1* (QT00163366). Fragments used for human cell lines were (again all Quantitect Primer Assays, Qiagen): *KCNN4* (*K_{Ca}3.1*, QT00003780), *ALDH1A3* (QT00077588), *CXCR4* (QT00223188), *NES* (QT00235781) and *SOX2* (QT00237601). mRNA abundances were normalized to the geometric means of those of the housekeeper genes *GAPDH* (QT01192646) and *ACTB* (QT00095431).

Measurements were conducted on a LightCycler480 (Roche), and crossing point values and melting curves were analyzed using LightCycler 480 software (Roche, version 1.5.0).

2.3. Drug Treatment

TRAM-34 (Sigma Aldrich, T6700) was dissolved in DMSO (10 mM stock solution, Sigma Aldrich, D2650) and used at final concentrations of 1 μ M (patch-clamp) or 5 μ M (all other experiments). The *K_{Ca}3.1* channel opener 1-EBIO (1-ethyl-2-benzimidazolinone, 200 μ M; Sigma Aldrich, SML0034) was diluted from a 20 mM stock solution in DMSO. Temozolomide (Sigma Aldrich, T2577) was dissolved in DMSO (100 mM stock solution) and used at final concentrations of 30 μ M. Drugs were added to the cells 1 h before irradiation. Equivalent volumes of DMSO were used as control conditions. Except electrophysiology, all experiments were conducted in a blinded fashion until statistical analysis.

2.4. Ionizing Radiation

Irradiation with 6 MV photons of cells at indicated doses was accomplished using a linear accelerator (LINAC SL15, Philips) at a dose rate of 4 Gy/min at room temperature.

2.5. Patch-Clamp on-Cell Recording

Macroscopic on-cell (cell-attached) currents from NSC (10–14 d) and DMEM medium-grown SMA-540 mouse glioma cells were recorded in voltage-clamp mode (10 kHz sampling rate) and 3 kHz low-pass-filtered by an EPC-9 patch-clamp amplifier (Heka, Lambrrecht, Germany) using Pulse software (Heka) and an ITC-16 Interface (Instrutech, Port Washington, NY, USA). Borosilicate glass pipettes (~5 M Ω pipette resistance; GC150 TF-10, Clark Medical Instruments, Pangbourne, UK) manufactured by a microprocessor-driven DMZ puller (Zeitz, Augsburg, Germany) were used in combination with a STM electrical micromanipulator (Lang, Gießen, Germany). Cells were continuously superfused at 37 °C with NaCl solution (in mM: 125 NaCl, 32 N-2-hydroxyethylpiperazine-N-2-ethanesulfonic acid (HEPES), 5 KCl, 5 D-glucose, 1 MgCl₂, 1 CaCl₂, titrated with NaOH to pH 7.4) additionally containing the *K_{Ca}3.1* K⁺ channel activator 1-EBIO (0 or 200 μ M) and TRAM-34 (0 or 1 μ M). The pipette solution contained (in mM) 130 KCl, 32 HEPES, 5 D-glucose, 1 MgCl₂, 1 CaCl₂, titrated with KOH to pH 7.4. Currents were elicited by 41 voltage square pulses (700 ms each) from 0 mV holding potential to voltages between –100 mV and +100 mV delivered in 5 mV increments. Clamp voltages refer to the cytosolic face of the plasma membrane and were not corrected for the liquid junction potential between pipette and bath solution. For analysis, macroscopic on-cell currents were averaged between 100 and 700 ms of each voltage sweep. Inward currents are defined as influx of cations into the cells (or efflux of anions out of the cell), depicted as downward deflections of the current tracings, and defined as negative currents in the current voltage relationships. Macroscopic on-cell conductance was calculated for the inward currents between –75 mV and +25 mV clamp voltage. The 1-EBIO-stimulated and TRAM-34-sensitive increase in macroscopic on-cell conductance was used as a measure of functional *K_{Ca}3.1* channel expression in the plasma membrane.

2.6. Clonogenic Survival

Clonogenic survival after drug and/or irradiation treatment was tested using colony formation (attached cells) and limited dilution assays (floating spheres) due to different growth phenotypes of the cell lines (see Supplemental Figure S1). For delayed plating colony formation assays (SMA-560, SMA-540 and GL-261 cells), 600 cells were seeded per well in 6-well plates in a drug-free medium 24 h after irradiation (0–6 Gy). 60 min prior to

24 h after irradiation, cells were incubated with TRAM-34 (0 or 5 μM) and temozolomide (0 or 30 μM). For pre-plating colony formation assays (U-87MG and U-251MG cells), 300 cells were seeded per well. After 4 h of incubation period, cells were incubated with TRAM-34 (0 or 5 μM) and temozolomide (0 or 30 μM). Irradiation treatment was conducted 1 h after TRAM-34 or temozolomide were added. After 5–7 (SMA-560, SMA-540 and U-87MG), 11 (U-251MG) or 13–14 (GL-261) days, cells were fixated with 4.5% formaldehyde and stained with 0.05 % Coomassie blue. Resulting colonies, defined as cell clusters consisting of at least 50 cells, were counted. Plating efficiency was calculated by dividing the number of colonies by the number of plated cells. Survival fractions were calculated by dividing the plating efficiencies by the respective plating efficiency at 0 Gy of each treatment arm. All experiments consist of 3 experimental and 3–6 observational units each (for definitions of experimental and observational unit, see [27]).

For limited dilution assays, singularized cells were serially 1:2 diluted in 96-well plates resulting in cell numbers between 2048 and 1 cell per well. A total of 24 h after cell plating, cells were pretreated (60 min) and continuously post-treated before and after irradiation (0–8 Gy) with TRAM-34 (0 or 5 μM) and temozolomide (0 or 30 μM). After a further 5–7 (SMA-560, U-87MG), 11 (U-251MG) or 14 days (SMA-540, GL-261), minimal cell number to retain the culture was determined. Plating efficiency was defined as the reciprocal value of this minimal cell number. The survival fraction was calculated as mentioned above. All experiments consist of three experimental and four observational units each. Fitted curves were calculated according to the linear quadratic model [28] with the following equation:

$$\text{Survival Fraction} = e^{-(\alpha \cdot D + \beta \cdot D^2)}$$

with D = radiation dose, and α and β = cell-type specific parameters.

3. Results

To account for genetic, but also phenotypical differences, three different murine and two human glioma cell lines were grown in two different culture media, DMEM supplemented with 10% fetal bovine serum that should “differentiate” glioblastoma “bulk” cells [29,30], and a neural stem cell-enriching/inducing NSC medium. To assess the influence of these two incubation conditions on stem cell properties, the mRNA abundance of four established stem cell markers, *ALDH1A3* [31], *CXCR4* [32], *Nestin* [33] and *SOX2* [34] was determined (Figure 1A–D). All but U-87MG (SMA-560, SMA-540, GL-261 and U-251MG) showed statistically significant increases in mRNA abundance in one or more of the stem cell markers when grown in NSC medium (see Figure 1). For example, mRNA abundance of *ALDH1A3* was more than doubled ($p = 0.0183$), while mRNA abundance of *CXCR4* was more than 100 \times greater when SMA-540 cells were grown in NSC compared to standard DMEM culture. U-87MG cells were the only cell line for which no statistically significant increase in any of the four analyzed stem cell markers was observed, even though *Nestin* was upregulated on a low basal level ($p = 0.0883$). Combined, these data suggest that stem cell-enriching culture conditions indeed increased the expression of stem cell markers in all but one cell line studied.

Next, the effect of this stem cell enrichment on survival fractions after irradiation was analyzed. For “differentiated” cells grown in DMEM culture medium, colony formation assays (CFA) were performed. Since the cell lines formed floating or attached spheroids when cultured in NSC medium (Supplemental Figure S1), we used limited dilution assays (LDA) for NSC-grown cells. To exclude LDA vs. CFA inter-assay differences, SMA-560 cells, grown in DMEM medium, were tested both in CFAs and LDAs, which resulted in only negligible differences of clonogenicity (see Supplemental Figure S2) indicating inter-assay concordance.

Comparison of the two culturing media suggested that stem cell-enriching conditions led to higher survival fractions in irradiated SMA-560 and SMA-540 cells, as compared to “differentiated” DMEM-grown cells (Figure 2A,B). No differences were observed with

GL-261 cells (Figure 2C). In contrast, U-87MG cells cultured in DMEM medium exhibited higher numerical survival fractions, even though data largely overlapped between both culture media (Figure 2D). Last, human U-251MG cells showed a doubling in survival fraction when grown in stem cell-enriching NSC medium ($p = 0.056$, Figure 2E).

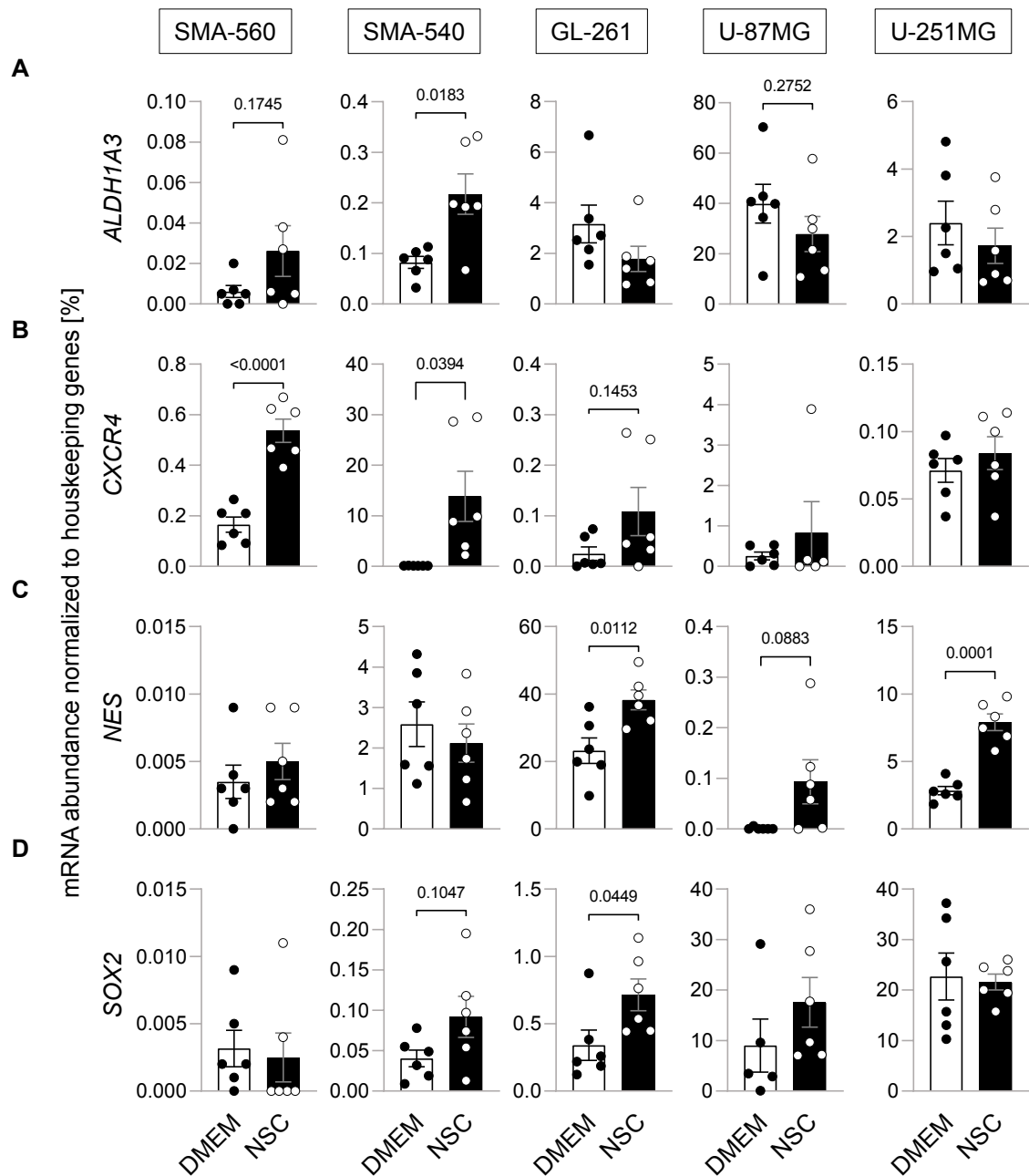


Figure 1. Enrichment of the glioblastoma stem cell fraction. (A–D). Culturing murine SMA-560, SMA-540 and GL-261 glioma cells and human U-251MG glioma cells in NSC medium (open circles) increased housekeeper-normalized mRNA abundances of stem cell markers as compared to DMEM medium (closed circles; in addition to the individual values, means \pm standard error of three experimental and two observational units each are depicted). The mRNA abundances of four different stem cell markers, (A) *ALDH1A3*, (B) *CXCR4*, (C) *Nestin* and (D) *SOX2* were determined by real-time RT-PCR. Numbers indicate error probability (p values) as calculated by Welch-corrected two-tailed t -test.

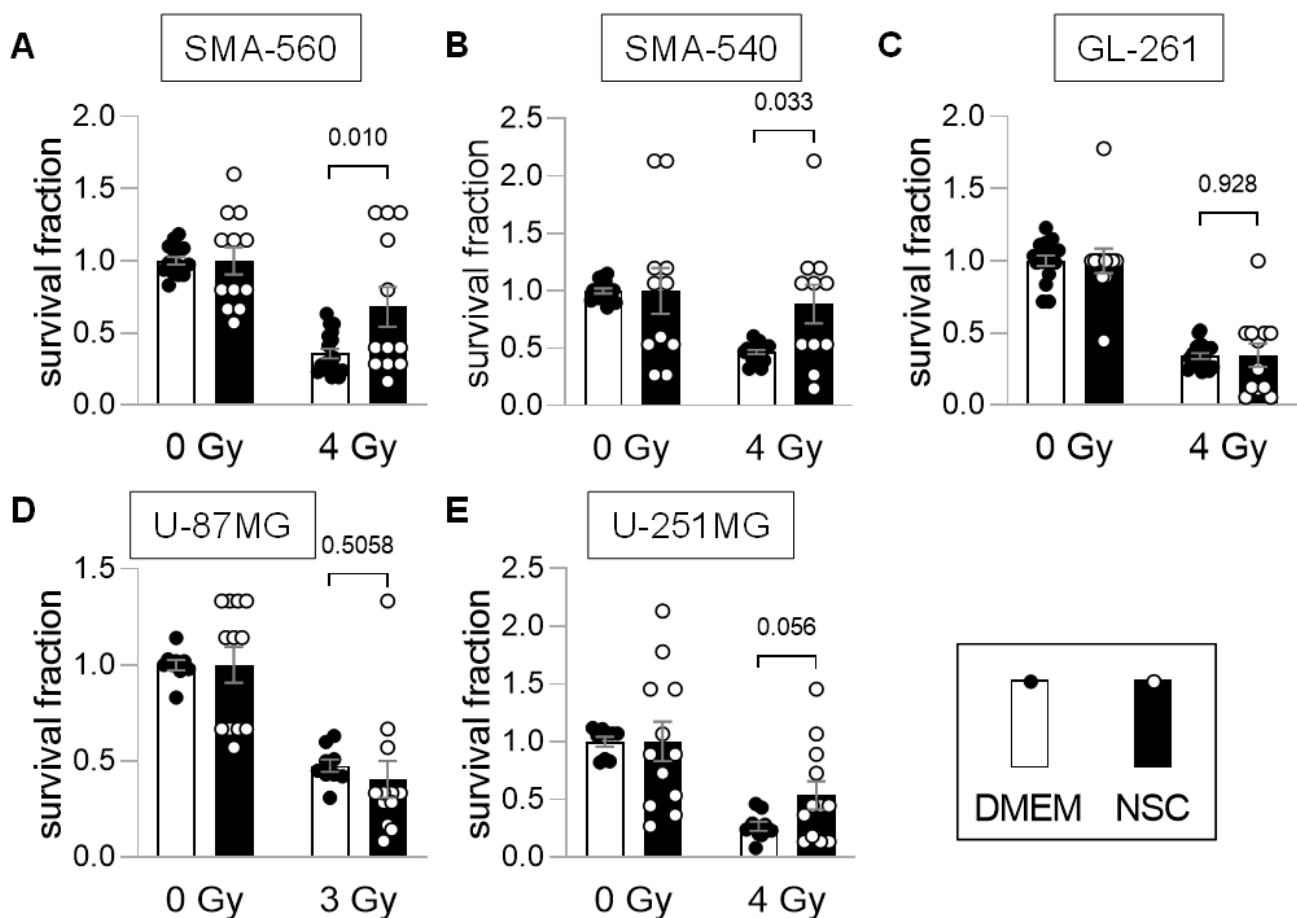


Figure 2. SMA-560, SMA-540 and U-251MG stem cell-enriched cultures are more radio-resistant than “differentiated” cultures. (A–E). Compared to standard culturing medium DMEM (closed circles; open bars), stem cell-inducing culture conditions with NSC medium (open circles; closed bars) increased clonogenic survival in (A) SMA-560, (B) SMA-540 and (E) (statistically non-significantly) U-251MG cells after irradiation. No statistically significant difference was observed in (C) GL-261 and (D) U-87MG cells (means \pm SE of 3 experimental units with 4–6 observational units each). Numbers indicate error probabilities (p values) as calculated by Welch-corrected two-tailed t -test.

To test the influence of stem-cell enriching culture conditions on $K_{Ca}3.1$ ($KCNN4$) mRNA, we performed real-time RT-PCR analyses for all five cell lines under both culture conditions. SMA-560 cells expressed $K_{Ca}3.1$ independently of culture conditions to a moderate-to-high extent (Figure 3A). In SMA-540 cells, $K_{Ca}3.1$ mRNA abundance was increased by twofold under stem cell enriching as compared to DMEM culture conditions, even though statistical significance was not reached (Figure 3B). Both murine GL-261 (Figure 3C) and human U-87MG cells did express $K_{Ca}3.1$ to a much lower extent, and this expression was not influenced by the culture condition (Figure 3D). U-251MG cells also expressed $K_{Ca}3.1$ on a low-to-moderate level; however, its expression almost doubled when cultured in NSC medium (Figure 3E). Irradiation of cells had no further systematic influence on mRNA abundances of stem cell-associated genes or $K_{Ca}3.1$ (Supplemental Figure S3) in all three murine cell lines.

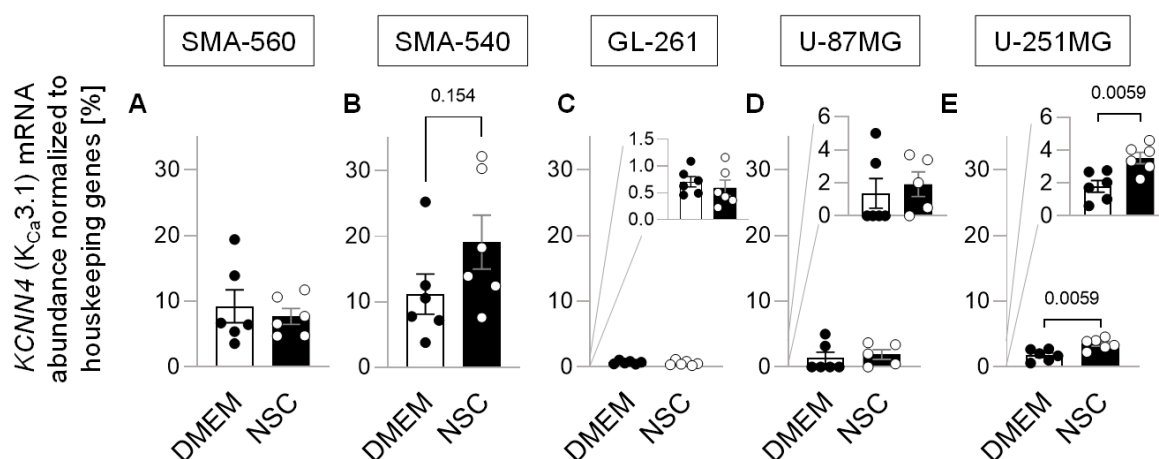


Figure 3. Effect of the enrichment of the glioblastoma stem cell fraction on $K_{Ca}3.1$ mRNA abundance. (A–C). Housekeeper-normalized mRNA abundance of $K_{Ca}3.1$ (*KCNN4*) in SMA-560 (A), SMA-540 (B), GL-261 (C), U-87 MG (D) and U-251MG (E) cells in both DMEM (closed circles) and NSC (open circles) medium (in addition to the individual values, means \pm standard error of three experimental and two observational units each are depicted; numbers in (B,E) indicate error probability (p value) as calculated by Welch-corrected two-tailed t -test.

To confirm functional expression of $K_{Ca}3.1$ K^+ channels in the plasma membrane of SMA-540 murine glioma cells and to identify its dependence on the culture conditions, macroscopic on-cell (cell-attached) currents as obtained with patch-clamp recordings in voltage-clamp mode were compared between cells grown in NSC medium and continuously DMEM medium-cultured sub-confluent monolayers. Macroscopic on-cell currents were recorded with KCl pipette and NaCl bath solution at clamp voltages between -100 and $+100$ mV. Maximal $K_{Ca}3.1$ K^+ channel activity was first induced by bath super-fusion with the $K_{Ca}3.1$ opener 1-EBIO (200 μ M) and then blocked by co-super-fusion of the $K_{Ca}3.1$ blocker TRAM-34 (1 μ M). The TRAM-34-sensitive current fraction was analyzed as a measure of functional $K_{Ca}3.1$ surface expression (Figure 4A,B).

In on-cell mode, the physiological membrane potential also applies to the electrically sealed membrane patch and contributes additively to the transmembrane voltage of the recorded membrane patch on top of the clamp voltage. With KCl pipette solution and with an assumed high intracellular K^+ concentration, the E_K electrochemical equilibrium potential for potassium across the recorded membrane patch can be expected to be around 0 mV transmembrane voltage, i.e., when the positive clamp voltage zeroes the negative physiological membrane potential. Since (further) activation of the $K_{Ca}3.1$ K^+ conductance by 1-EBIO is expected to hyperpolarize the membrane potential and $K_{Ca}3.1$ blockage by TRAM-34 to depolarize it, $K_{Ca}3.1$ activation and blockage should be paralleled by an increase and decrease, respectively, of the positive clamp voltage that is required to zero the physiological membrane potential. Assuming finally that the K^+ conductance is the largest conductance fraction in the plasma membrane of glioma cells and this fraction largely determines the membrane potential, the reversal potential (V_{rev}) of the recorded macroscopic current should to some extent represent E_K and thereby the negative value of the membrane potential.

In our experiments on SMA-540 cells, 1-EBIO induced an increase in the macroscopic on-cell inward currents and TRAM-34 the blockage of these currents (Figure 4B). Notably, on average, the 1-EBIO-induced increase in macroscopic on-cell inward current and TRAM-34-sensitive current fractions seemed to be larger in SMA-540 cells grown in NSC medium than in DMEM medium-cultivated cells (Figure 4C,D). As a matter of fact, a significant and almost significant higher number of NSC medium-grown and 1-EBIO-treated cells exhibited a large inward conductance and a high TRAM-34-sensitive conductance fraction, respectively, than 1-EBIO-treated DMEM medium cultivated cells. Moreover, and

in accordance with the above-mentioned assumptions, 1-EBIO induced a right shift (i.e., an increase) and TRAM-34 an left shift (i.e., decrease), respectively, in V_{rev} of the macroscopic on-cell current especially in NSC medium-grown SMA-540 cells (Figure 4C,F). In two-by-two contingency plots (Figure 4G), however, number of cells with high V_{rev} and large TRAM-34-induced V_{rev} decline were not significantly different between both culture conditions. Combined, this data indicate functional expression of $K_{Ca}3.1$ channels in SMA-540 murine glioma cells and suggest upregulation of $K_{Ca}3.1$ in the plasma membrane upon transferring SMA-540 from DMEM in NSC medium.

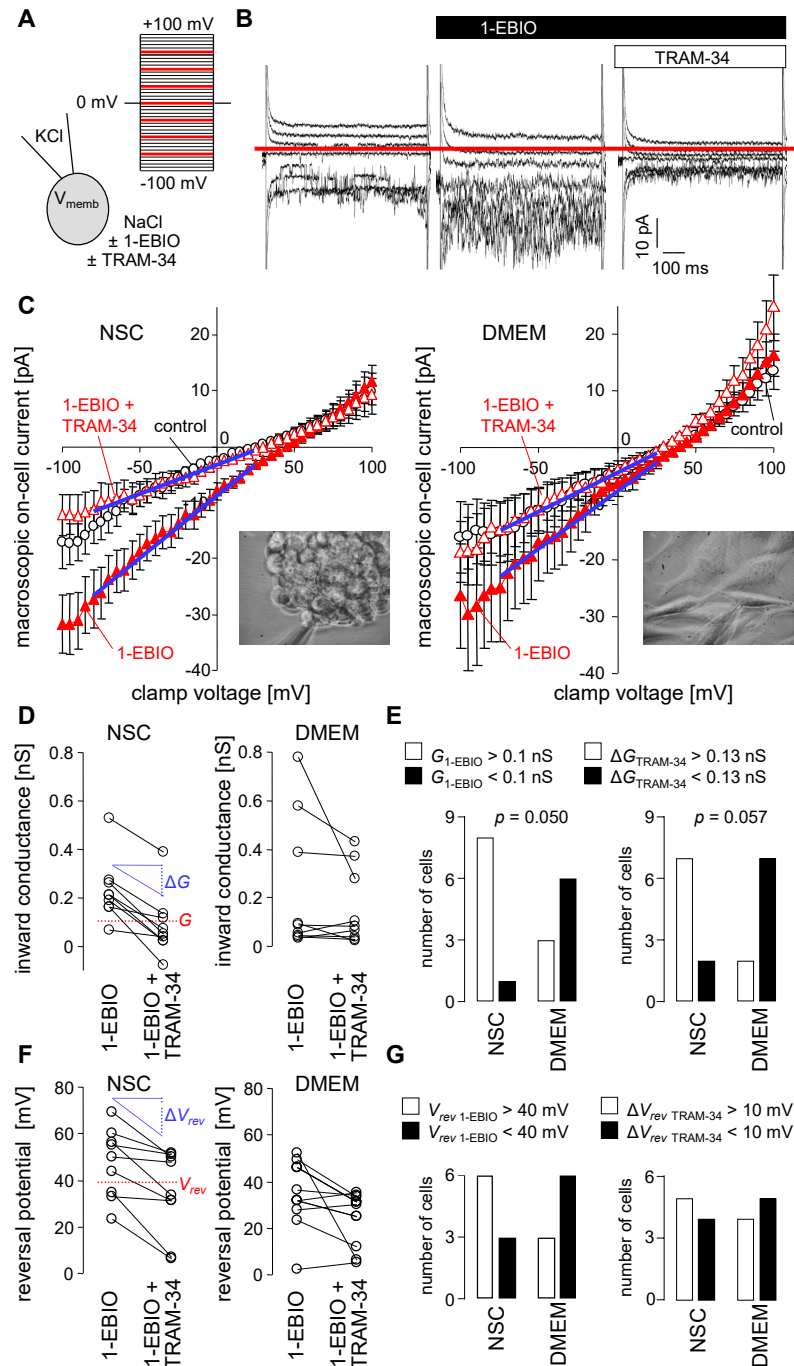


Figure 4. NSC culture conditions induce upregulation of $K_{Ca}3.1$ K^+ currents in the plasma membrane of SMA-540 mouse glioma cells (A,B). Ionic composition with channel modulators of pipette and

bath solution and applied voltage pulse protocol (A) used to record macroscopic on-cell (cell-attached) currents from an NSC-grown (10–14 d) SMA-540 cell. On-cell current tracings depicted in (B) were obtained before (left), during bath application of the $K_{Ca}3.1$ K^+ channel opener 1-EBIO (200 μ M) alone (middle) or in combination with the $K_{Ca}3.1$ inhibitor TRAM-34 (1 μ M, right). For better readability, only current tracings elicited by voltage square pulses to -75 , -50 , -25 , 0 , $+25$, $+50$, and $+75$ mV are shown; red line in (B) indicates 0 pA (C). Dependence of macroscopic on-cell currents on clamp voltage in NSC- (left) and DMEM-grown (right) SMA-540 cells recorded before (control, open black circles), during bath application of 1-EBIO (closed red triangles) and co-application of 1-EBIO and Tram-34 (open red triangles). Data are means \pm SE, $n = 9$; the inserts in the lower right corner of the plots show light micrographs of a SMA-540 spheroid (left) and a SMA-540 monolayer (right) during patch-clamp recording (D). Paired conductances as calculated for the inward currents from the data summarized in (C) in NSC- (left) and DMEM-grown (right) SMA-540 cells recorded successively with 1-EBIO and 1-EBIO/TRAM-34 in the bath solution. Given are individual values determined for that range of clamp voltage indicated in (C) by blue lines (E). Two-by-two contingency plots showing the number of NSC- and DMEM-grown SMA-540 cells with an on-cell inward conductance in 1-EBIO-containing bath solution (G_{1-EBIO}) of above (closed columns) and below (open columns) 0.1 nS (left) as well as with a TRAM-34-induced inward conductance decline ($\Delta G_{TRAM-34}$) of above (closed columns) and below (open columns) 0.13 nS (right). Data are from (D), indicated p values refer to the difference between the culture conditions and were calculated with chi square test (F). Paired reversal potentials ($V_{rev,S}$, individual values) as given for the data summarized in (C) in NSC- (left) and DMEM-grown (right) SMA-540 cells recorded successively with 1-EBIO and 1-EBIO/TRAM-34 in the bath solution (G). Two-by-two contingency plots showing the number of NSC- and DMEM-grown cells with a V_{rev} in 1-EBIO-containing bath solution ($V_{rev, 1-EBIO}$) of above (closed columns) and below (open columns) +40 mV (left) as well as with a TRAM-34-induced drop in V_{rev} ($\Delta V_{rev, TRAM-34}$) by above (closed columns) and below (open columns) 10 mV (right).

To test for the functional significance of $K_{Ca}3.1$ on clonogenic survival of DMEM cultured and stem-cell enriched (NSC culture) glioma cells after irradiation (0–8 Gy) and/or chemotherapy, we applied the $K_{Ca}3.1$ blocker TRAM-34 (0 or 5 μ M) in combination with temozolomide (0 or 30 μ M). As shown in Figure 5A–C, temozolomide or TRAM-34 alone hardly affected plating efficiency of SMA-560 cells in colony formation assay or limited dilution assay. TRAM-34, however, sensitized SMA-560 cells to temozolomide when grown in DMEM medium, while this trend was only numerical when grown in NSC medium. Furthermore, in DMEM-grown irradiated (0–6 Gy) SMA-560 cells, neither TRAM-34 nor temozolomide, nor their combination, decreased survival fraction in colony formation assay (Figure 5D), suggesting no radio-sensitizing action of both drugs alone or their combination in “differentiated” SMA-560 cells. In limited dilution assay with stem cell-enriched NSC-grown SMA-560 cells, temozolomide showed a trend ($p = 0.056$) towards radio-sensitization of the cells at high irradiation doses (Figure 5D). TRAM-34 alone, in contrast, did not exhibit any effect on survival fraction of irradiated stem cell-enriched SMA-560 cells (Figure 5E).

In SMA-540 cells, neither TRAM-34 nor temozolomide, nor their combination, decreased plating efficiency in both culture conditions (Figure 6A–C). However, while neither TRAM-34 nor TMZ affected survival fractions after irradiation in DMEM-cultured SMA-540 cells (Figure 6D), both agents (and their combination) did significantly reduce survival fractions at high irradiation doses in stem-cell enriched SMA-540 cells (Figure 6E).

In contrast to SMA-540 and SMA-560 cells, GL-261 cells were highly temozolomide-sensitive irrespective of culture conditions. Temozolomide reduced plating efficiency in colony formation assay and limited dilution assay by approximately 85% and 97%, respectively (Figure 7A–C; $p < 0.0001$). Further reductions by the addition of TRAM-34 were small and only numerical (Figure 7B,C). Due to temozolomide’s large effect on plating efficiency on its own, we subsequently only analyzed TRAM-34’s effects on survival fraction after irradiation. TRAM-34 had no effect on survival fraction in DMEM-grown “differentiated” GL-261 cells (Figure 7D). In stem cell-enriched culture, TRAM-34 treatment

showed a trend towards higher survival fractions, i.e., towards an increased radioresistance (Figure 7E).

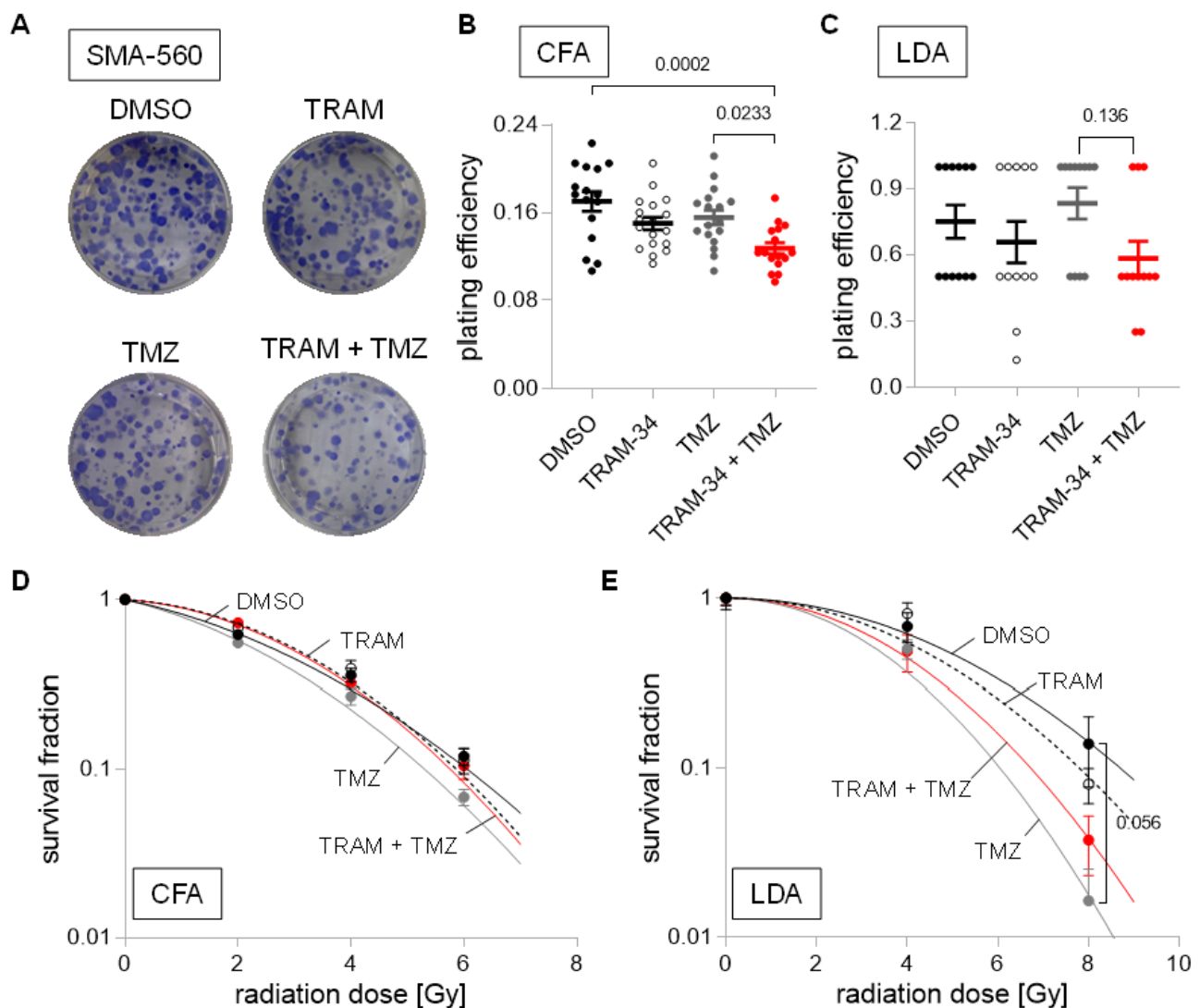


Figure 5. Cell culture condition-dependent effects of $K_{Ca}3.1$ blockade on sensitivity to irradiation and temozolomide in SMA-560 cells (A–C). Representative images of colony formation (A) and plating efficiencies (B) of DMEM-grown or (C) NSC-grown cells after irradiation with 0 Gy and co-treatment with vehicle (DMSO, closed black circles), TRAM-34 (5 μ M, open circles), temozolomide (TMZ, 30 μ M, closed grey circles), or TRAM-34 (5 μ M) together with temozolomide (TMZ, 30 μ M, closed red circles) (D,E) Survival fractions of irradiated (0–8 Gy) cells co-treated with vehicle (DMSO, closed black circles), TRAM-34 (5 μ M, open circles), temozolomide (TMZ, 30 μ M, closed grey circles), or TRAM-34 (5 μ M) together with temozolomide (TMZ, 30 μ M, closed red circles) as determined by colony formation assay for DMEM-grown (D) and limited dilution assay for NSC-grown SMA-560 cells (E). Data are individual values in (B,C) and mean \pm standard error in (B–E) of three experimental units with four to six observational units each. Survival fraction curves were fitted according to the linear quadratic model and given as follows: DMSO, solid black line; TRAM-34, dashed line; temozolomide, solid grey line; TRAM-34 and TMZ, solid red line. Numbers in (B,C,E) indicate error probabilities (p values) as calculated with one-way ANOVA and Tukey multiple comparison test.

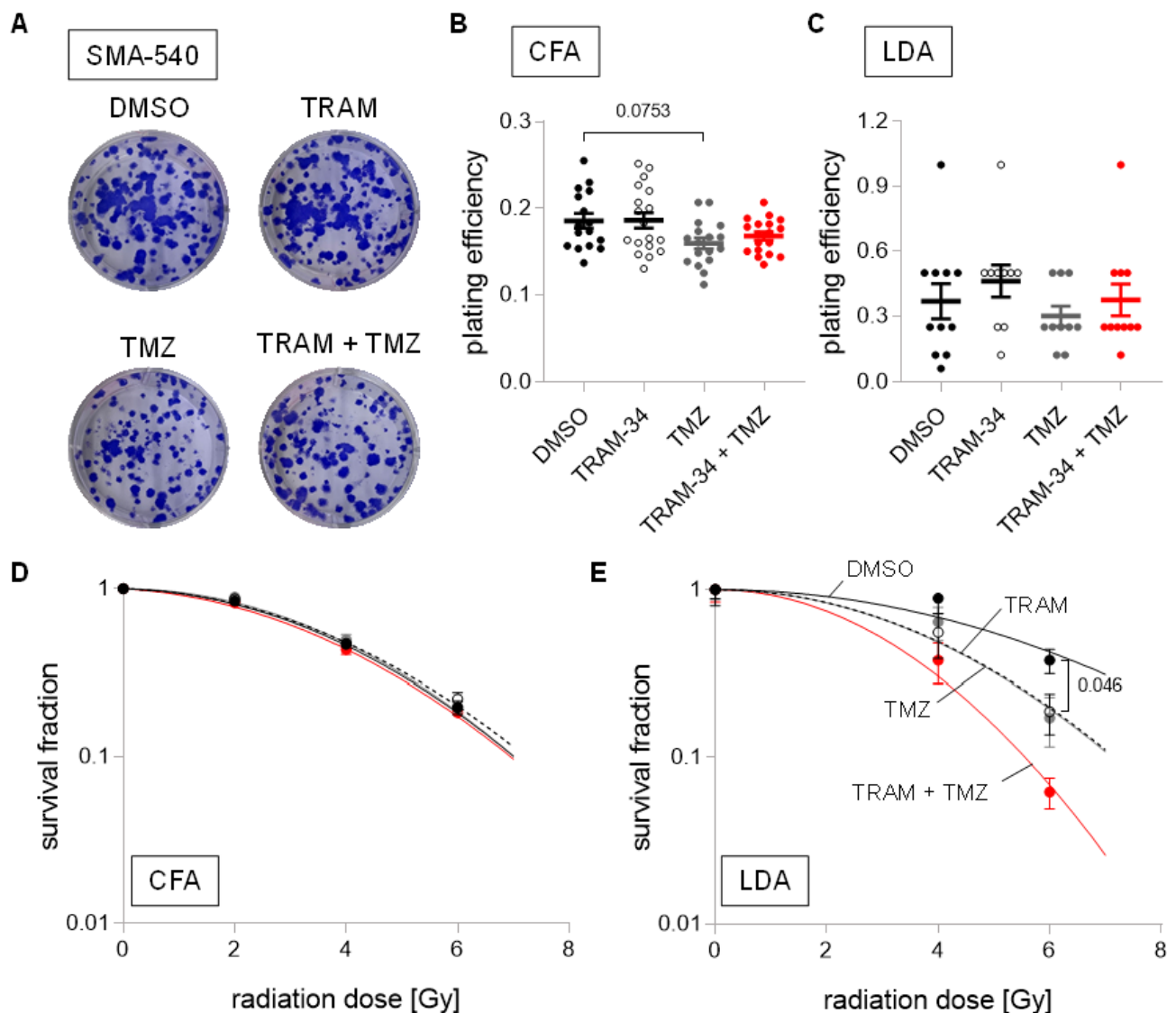


Figure 6. Cell culture condition-dependent effects of $K_{Ca}3.1$ blockade on sensitivity to irradiation and temozolomide in SMA-540 cells. (A–C). Representative images of colony formation (A) and plating efficiencies (B) of DMEM-grown or (C) NSC-grown cells after irradiation with 0 Gy and co-treatment with vehicle (DMSO, closed black circles), TRAM-34 (5 μ M, open circles), temozolomide (TMZ, 30 μ M, closed grey circles), or TRAM-34 (5 μ M) together with temozolomide (TMZ, 30 μ M, closed red circles). (D,E). Survival fractions of irradiated (0–6 Gy) cells co-treated with vehicle (DMSO, closed black circles), TRAM-34 (5 μ M, open circles), temozolomide (TMZ, 30 μ M, closed grey circles), or TRAM-34 (5 μ M) together with temozolomide (TMZ, 30 μ M, closed red circles) as determined by colony formation assay for DMEM-grown (D) and limited dilution assay for NSC-grown SMA-540 cells (E). Data are individual values in (B,C) and mean \pm standard error in (B–E) of three experimental units with four to six observational units each. Survival fraction curves were fitted according to the linear quadratic model and given as follows: DMSO, solid black line; TRAM-34, dashed line; temozolomide, solid grey line; TRAM-34 and TMZ, solid red line. Numbers in (B,E) indicate error probabilities (p values) as calculated with one-way ANOVA and Tukey multiple comparison test.

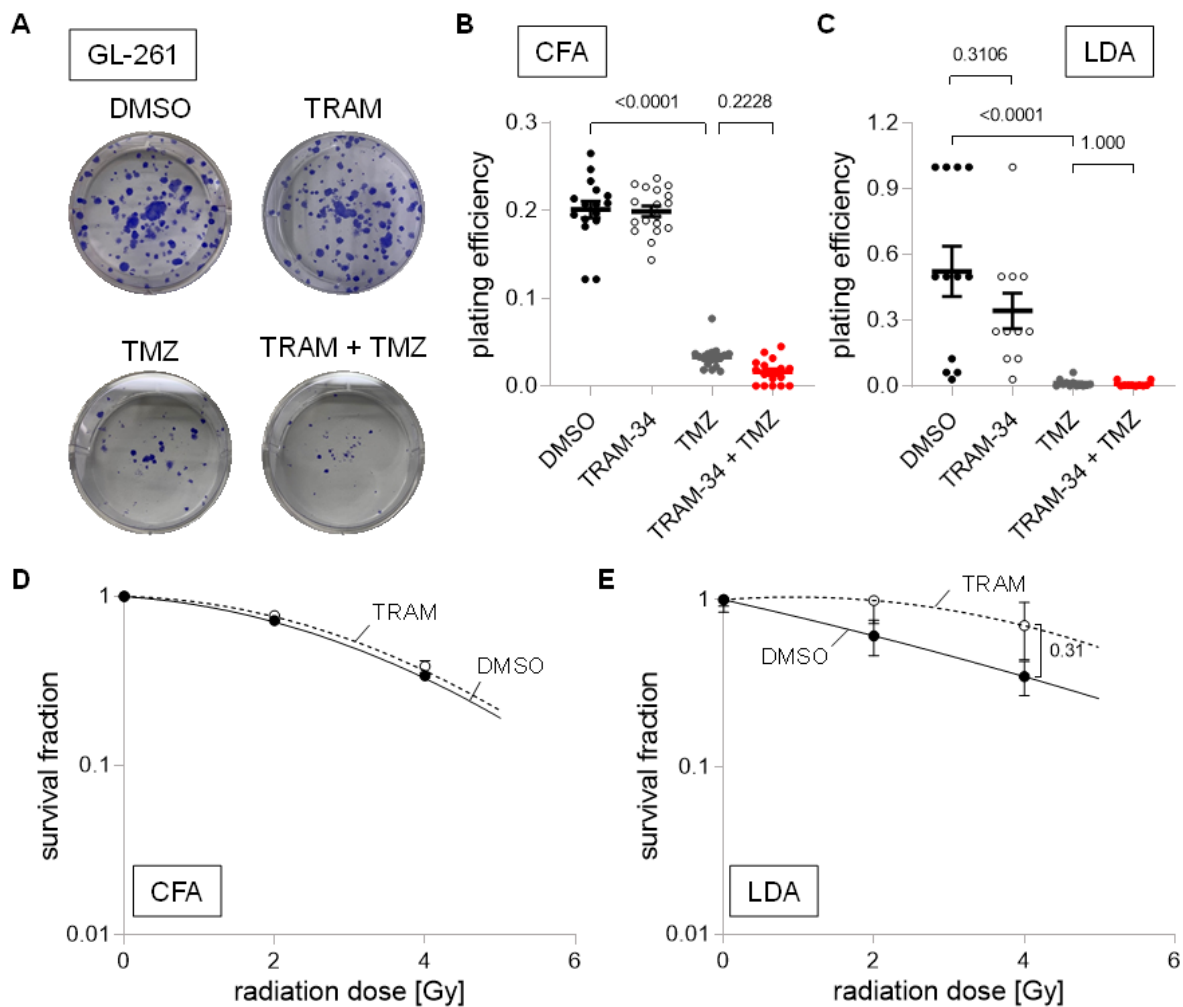


Figure 7. Cell culture condition-dependent effects of $K_{Ca}3.1$ blockade on sensitivity to irradiation and temozolomide in GL-261 cells. (A–C). Representative images of colony formation (A) and plating efficiencies (B) of DMEM-grown or (C) NSC-grown cells after irradiation with 0 Gy and co-treatment with vehicle (DMSO, closed black circles), TRAM-34 (5 μ M, open circles), temozolomide (TMZ, 30 μ M, closed grey circles), or TRAM-34 (5 μ M) together with temozolomide (TMZ, 30 μ M, closed red circles). (D,E). Survival fractions of irradiated (0–4 Gy) cells co-treated with vehicle (DMSO, closed black circles) or TRAM-34 (5 μ M, open circles) as determined by colony formation assay for DMEM-grown (D) and limited dilution assay for NSC-grown GL-261 cells (E). Data are individual values in (B,C) and mean \pm standard error in (B–E) of three experimental units with four to six observational units each. Survival fraction curves were fitted according to the linear quadratic model and given as follows: DMSO, solid black line; TRAM-34, dashed line. Numbers in (B,C,E) indicate error probabilities (*p* values) as calculated with one-way ANOVA and Tukey multiple comparison test.

Next, we did not identify changes in plating efficiency for human U-87MG cells cultured in DMEM medium for any treatment group (Figure 8A,B). Interestingly, NSC cultured U-87MG showed an 80% reduction in plating efficiency when incubated with TRAM-34, and near total reductions when TRAM-34 and TMZ were applied concomitantly (Figure 8C). We observed only small effects of any treatment on survival fraction after irradiation in DMEM cultured U-87MG cells, with only numerical reductions of the survival fraction at 3 Gy in the TMZ and TRAM-34 + TMZ treatment group. Due to the large effects of TRAM-34 and TRAM-34 + TMZ on U-87MG cells cultured in NSC medium alone, only TMZ's effect was analyzed regarding its effect on radiation sensitivity, showing ambiguous results depending on the irradiation dose (Figure 8D,E).

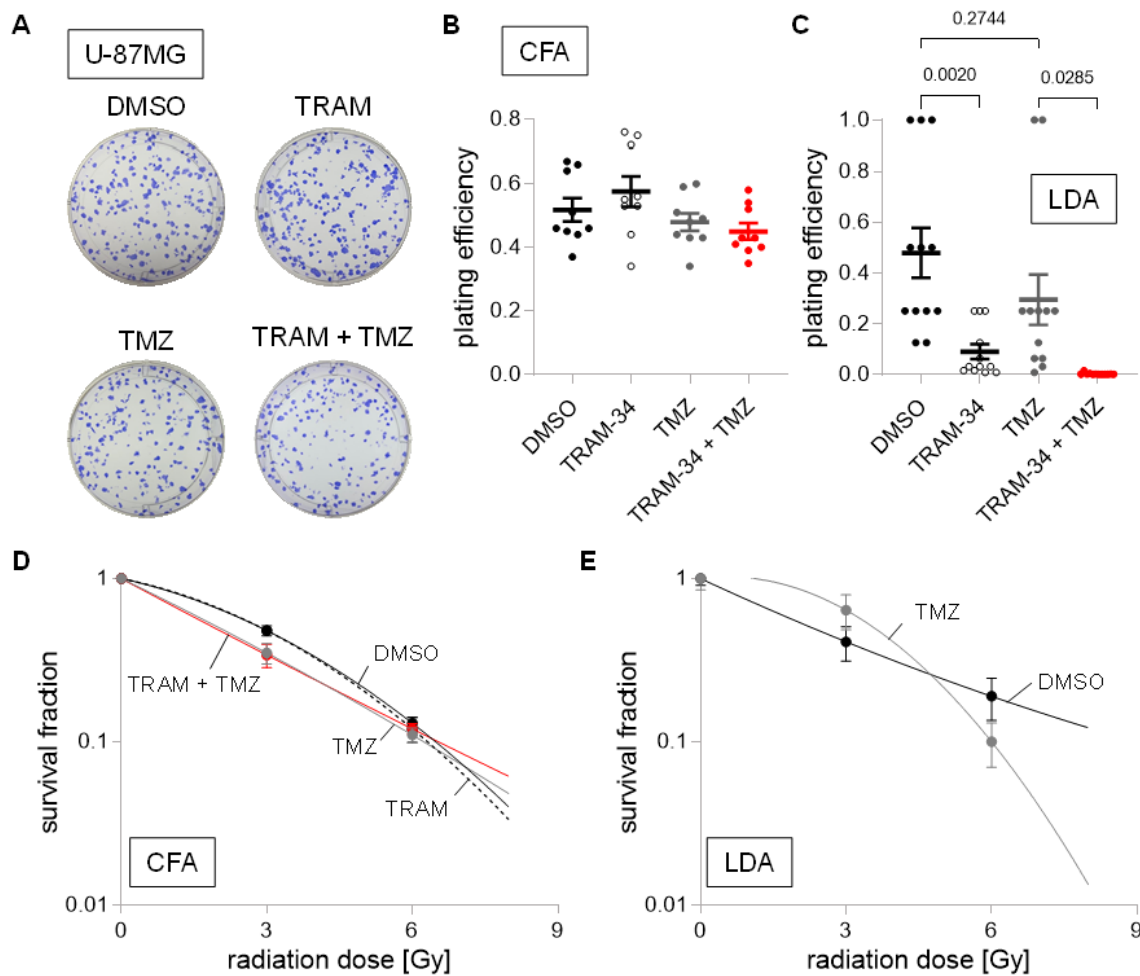


Figure 8. Cell culture condition-dependent effects of $K_{Ca}3.1$ blockade on sensitivity to irradiation and temozolomide in U-87MG cells. (A–C). Representative images of colony formation (A) and plating efficiencies (B) of DMEM-grown or (C) NSC-grown cells after irradiation with 0 Gy and co-treatment with vehicle (DMSO, closed black circles), TRAM-34 (5 μ M, open circles), temozolomide (TMZ, 30 μ M, closed grey circles), or TRAM-34 (5 μ M) together with temozolomide (TMZ, 30 μ M, closed red circles). (D,E). Survival fractions of irradiated (0–6 Gy) cells co-treated with vehicle (DMSO, closed black circles), TRAM-34 (5 μ M, open circles), temozolomide (TMZ, 30 μ M, closed grey circles), or TRAM-34 (5 μ M) together with temozolomide (TMZ, 30 μ M, closed red circles) as determined by colony formation assay for DMEM-grown (D) and limited dilution assay for NSC-grown U-87MG cells (E). Data are individual values in (B,C) and mean \pm standard error in (B–E) of three experimental units with three to four observational units each. Survival fraction curves were fitted according to the linear quadratic model and given as follows: DMSO, solid black line; TRAM-34, dashed line; temozolomide, solid grey line; TRAM-34 and TMZ, solid red line. Numbers in (C) indicate error probabilities (p values) as calculated with one-way ANOVA and Tukey multiple comparison test.

Last, we analyzed the human U-251MG cell line, which exhibited a large sensitivity towards TMZ with large reductions in plating efficiency in both culture conditions (Figure 9A–C). Moreover, TRAM-34 reduced plating efficiency in limited dilution assay by approximately 40%, even though statistical significance was not reached (Figure 9C; $p = 0.0649$). Due to the large effects of TMZ on its own, only TRAM-34 treatment was subsequently analyzed regarding its radio-sensitization effects. Overall, only small effects of TRAM-34 trending towards reduced survival fractions after irradiation were found (Figure 9D,E).

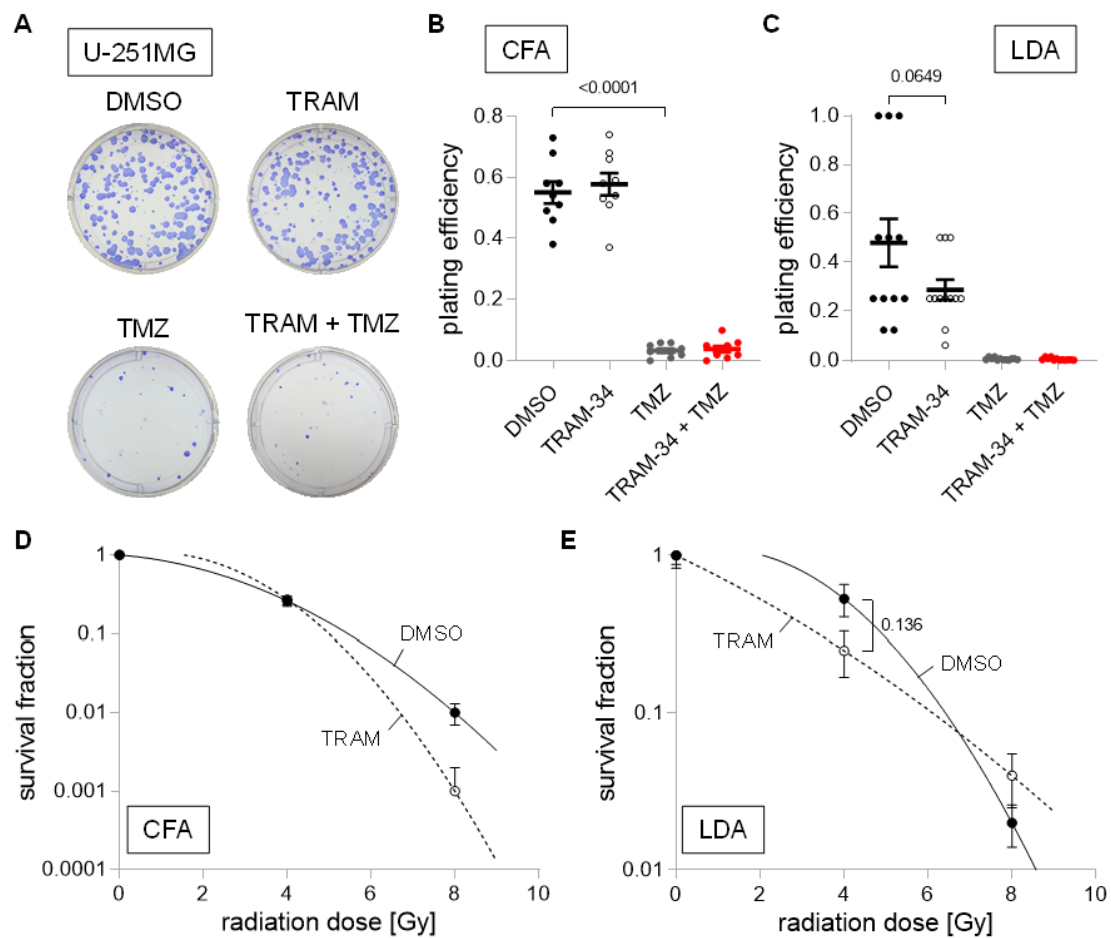


Figure 9. Cell culture condition-dependent effects of $K_{Ca}3.1$ blockade on sensitivity to irradiation and temozolomide in U-251MG cells. (A–C). Representative images of colony formation (A) and plating efficiencies (B) of DMEM-grown or (C) NSC-grown cells after irradiation with 0 Gy and co-treatment with vehicle (DMSO, closed black circles), TRAM-34 (5 μ M, open circles), temozolomide (TMZ, 30 μ M, closed grey circles), or TRAM-34 (5 μ M) together with temozolomide (TMZ, 30 μ M, closed red circles). (D,E). Survival fractions of irradiated (0–8 Gy) cells co-treated with vehicle (DMSO, closed black circles) or TRAM-34 (5 μ M, open circles) as determined by colony formation assay for DMEM-grown (D) and limited dilution assay for NSC-grown U-251MG cells (E). Data are individual values in (B,C) and mean \pm standard error in (B–E) of three experimental units with three to four observational units each. Survival fraction curves were fitted according to the linear quadratic model and given as follows: DMSO, solid black line; TRAM-34, dashed line. Numbers in (B,C,E) indicate error probabilities (p values) as calculated with one-way ANOVA and Tukey multiple comparison test.

4. Discussion

The present study showed that radio-sensitivity was influenced by culture conditions. SMA-560, SMA-540 and (to a smaller degree) U-251MG cells were more radio-resistant when cultured in stem cell-enriching NSC medium as compared to the “bulk” glioma DMEM/FBS cell cultures. Culture medium-induced changes of radiation sensitivity in GL-261 cells and U-87MG were only small (see Figure 2). Notably, U-87MG cells were the only cell line studied which did not show a clear induction of any of the four tested stem cell markers when grown in NSC medium. The increased radioresistance in stem cell-enriched cultures is in line with previous reports, showing increased radioresistance of cancer stem cells as compared to “differentiated bulk” tumor cells, which is most probably due to upregulation of repair mechanisms, increased oxidative defense and/or activation of pro-survival pathways in cancer stem cells (as reviewed in [20]).

The main finding of the present study is that tumoricidal, but also radio- and temozolomide-sensitizing effects of the $K_{Ca}3.1$ inhibitor TRAM-34 varied considerably between glioma cell lines and culture conditions. Specifically, TRAM-34 had radio-sensitizing effects in stem cell-enriched but not in “differentiated” SMA-540 cells (see Figure 6D,E). While TRAM-34 had no effect on clonogenic survival in DMEM-cultured U-87MG cells, plating efficiency was reduced by 80% when applied to NSC-cultured U-87MG cells (see Figure 8B,C). A similar trend was found in U-251MG; however, TRAM-34’s effect in NSC medium did not quite reach statistical significance (see Figure 9B,C; $p = 0.0649$). Furthermore, no effect of TRAM-34 was seen in GL-261 cells, arguably due to its low $K_{Ca}3.1$ expression compared to the other cell lines (see Figures 3 and 7). This contrasts a previous study [16], which reported both direct tumoricidal but also TMZ-sensitizing effects of TRAM-34 in GL-261 cells. Notably, D’Alessandro et al. [16] applied 5 μ M TRAM-34 in DMEM medium containing 1% FBS for TRAM-34 single and temozolomide co-treatment, while our experiments on “bulk-differentiated” GL-261 cells were conducted with 5 μ M TRAM-34 in DMEM medium containing 10% FBS (see Section 2).

In theory, differences in free TRAM-34 concentration may explain intra-cell line differences between both culture conditions, and the differences between this and D’Alessandro et al.’s paper: Given the reported high plasma protein binding rates (around 98% in rat plasma) of TRAM-34 [35], it is justified to assume higher free TRAM-34 concentrations in culture media with less or no FBS, such as NSC. Nevertheless, IC_{50} values for TRAM-34 are reportedly around 20 nM [36], which should ensure quantitative blockage of $K_{Ca}3.1$ even when used in cell culture medium containing 10% FBS. To explore this possibility further, we conducted CFA using DMEM + 1% FBS with U-87MG cells, which showed the largest reduction in plating efficiency with TRAM-34 treatment in NSC medium (see Figure 8B). While colony formation was slower, TRAM-34 treatment did not lead to reductions in plating efficiency and resembled findings as when grown in DMEM + 10% FBS, rendering this hypothesis unlikely (Supplemental Figure S4).

Alternatively, this high variability might result from cell line- and culture condition-dependent differences in $K_{Ca}3.1$ expression. While $K_{Ca}3.1$ mRNA abundance did not differ in SMA-560 (high $K_{Ca}3.1$ expression), GL-261 (low $K_{Ca}3.1$ expression) and U-87MG (low $K_{Ca}3.1$ expression) cells between both culture conditions, SMA-540 cells (high $K_{Ca}3.1$ expression; $p = 0.154$) and U-251MG (low $K_{Ca}3.1$ expression) showed an increase in $K_{Ca}3.1$ mRNA abundance with stem cell enrichment in NSC medium (see Figure 3), which was also seen functionally in SMA-540 cells with patch-clamp recording (see Figure 4). This might explain why a radio-sensitizing effect of TRAM-34 alone and an additive radio-sensitizing effect of TRAM-34 combined with temozolomide treatment was only apparent in glioma stem cell-enriched SMA-540 cells (see Figure 6D–E) which was the culture with the highest $K_{Ca}3.1$ mRNA abundance (see Figure 3B). In contrast to this line of argumentation, the large tumoricidal effect of TRAM-34 in NSC-cultured U-87MG cells was not observed in DMEM culture, even though the expression of $K_{Ca}3.1$ did not differ between both culture conditions and was generally low compared to SMA-540 cells (see Figures 3D and 8B,C).

Temozolomide did not reduce the clonogenic survival in SMA-560, SMA-540 and U-87MG cells or only did so to a small, statistically non-significant amount (see Figures 5B,C, 6B,C and 8B,C). Speculatively, this may be due to high expression of the temozolomide resistance gene O6-methylguanine-DNA-methyltransferase (MGMT), or (as is the case for U-87MG with a methylated and hence low MGMT expression status [37]) result from a reduced expression of mismatch repair proteins [38,39], or an enhanced expression of DHC2, which interferes with nuclear transportation of DNA repair proteins [40]. This is contrasted by large and culture condition-independent effects of TMZ in GL-261 and U-251MG cells (see Figures 7B,C and 9B,C).

In contrast to the present study, previous work of our group and others have consistently disclosed a radioprotective function of $K_{Ca}3.1$. In particular, TRAM-34 treatment has been shown to radio-sensitize human glioblastoma cell lines (T98G and U87MG, both cultured in RPMI medium supplemented with 10% FCS and using higher TRAM-34 con-

centrations of up to 10 $\mu\text{mol/L}$). Strikingly, knockdown of $K_{Ca}3.1$ by RNA interference in T98G cells mimicked the radio-sensitizing TRAM-34 effect and concomitantly abolished the sensitivity to TRAM-34 [17]. Vice versa, downregulation of the stem cell marker *musashi-1* in U251 human glioblastoma cells reportedly upregulates $K_{Ca}3.1$ and induces TRAM-34-sensitive radioresistance [41]. Likewise, genetic knockdown of $K_{Ca}3.1$ radio-sensitizes murine breast cancer cells with loss of TRAM-34-sensitive radioresistance [42].

Combined with the data of the present study, this might suggest that $K_{Ca}3.1$ targeting with TRAM-34 may sensitize glioma cells to radiation (or temozolomide) only under specific culture conditions and in selected glioma cell lines/cultures, speculatively preferentially in stem cell-enriching (serum-free) culture conditions. In our previous work on patient-derived primary glioblastoma stem cell cultures, $K_{Ca}3.1$ expression varied considerably between individual tumors and was associated with mesenchymal subpopulations of stem cells [3,43], which are especially radiation-resistant [44] and may, hence, represent the subpopulation of glioblastoma cells to test further anti- $K_{Ca}3.1$ therapies in.

Importantly, several groups identified also anti-migratory or anti-invasive effects of anti- $K_{Ca}3.1$ treatment [9,12–16], properties which were not part of our present assessment. Moreover, other authors found the immune constitution of animals to be a better predictor for response to radiation treatment than intrinsic radiosensitivity of cancer cells [45]. This might be especially interesting in light of the findings of Grimaldi et al. [46], demonstrating anti-immunosuppressive effects of TRAM-34 in glioma-infiltrating microglia/macrophages, which led to decreased tumor volumes in a glioma mouse model.

Limitations. There are several limitations, potentially challenging the generalizability of the present study. First, NSC medium was originally developed for culturing human stem cells. However, as shown in Figure 1, expression of stem cell associated genes was also increased in all three murine cell lines. Second, while we did show inter-assay concordance of CFAs and LDAs, incubation times were chosen based on proliferation rate of each cell line in each culture medium. This led to different incubation times of SMA-540 cells in CFA and LDA (7 days versus 14 days), which may complicate direct comparisons of radiosensitivity between DMEM and NSC cultures of SMA-540 cells. Last, determining drug concentrations is challenging. While there is evidence that TMZ may reach brain tissue concentrations of up to 30 μM in human patients [47,48], no human pharmacokinetic data are available for TRAM-34. Experiments in rats identified peak concentration levels of 2.5 $\mu\text{mol/l}$ in brain tissue after intraperitoneal injections [35], while other authors found concentrations of up to 1.3 $\mu\text{mol/L}$ in mice brain tissue [13].

5. Conclusions

We identified tumoricidal, TMZ- and radiation-sensitizing effects of pharmacological $K_{Ca}3.1$ targeting by TRAM-34 in our tested glioma cell lines. However, these effects were not only cell line-specific, but also dependent on the culture conditions used. Notably, TRAM-34 was especially effective against stem-cell enriched cell cultures, which are generally thought of as responsible for therapy resistance and tumor relapse. This underpins the importance of testing new drug targets in various cell lines and different culture conditions, to mimic intra- and inter-tumor heterogeneity in glioblastoma patients at least partially [49,50].

Supplementary Materials: The following supporting information can be downloaded at: <https://www.mdpi.com/article/10.3390/cancers14246199/s1>, Figure S1: Representative images of growth phenotypes in “bulk” cell-“differentiating” DMEM/10% FBS (top) and glioma stem cell-enriching NSC (bottom) medium; Figure S2: Survival fractions of irradiated (0–6 Gy) SMA-560 cells grown in DMEM + 10% FBS determined by limited dilution assay (LDA; B, open circles) or colony formation assay (CFA; B, closed circles) are not different; Figure S3: Irradiation does not affect mRNA abundance of (A) *ALDH1A3*, (B) *CXCR4*, (C) *Nestin*, (D) *SOX2* or (E) *KCNN4* in SMA-560 (left), SMA-540 (middle) or GL-261 (right) cells systematically irrespective of culture condition; Figure S4: TRAM-34 does not exhibit tumoricidal effects on U-87MG cells when incubated in DMEM + 1% FBS.

Author Contributions: Conceptualization, N.S., K.G., S.M.H. and P.R.; formal analysis, N.S. and S.M.H.; funding acquisition, S.M.H. and P.R.; investigation, N.S. and K.G.; methodology, N.S. and K.G.; resources, U.N.; supervision, U.N., S.M.H. and P.R.; visualization, N.S. and S.M.H.; writing—original draft, N.S. and S.M.H.; writing—review and editing, N.S., K.G., U.N., S.M.H. and P.R. All authors have read and agreed to the published version of the manuscript.

Funding: N.S., K.G., S.M.H. and P.R. were funded by a grant from the German Cancer Aid (70112872, 70113144).

Institutional Review Board Statement: Not applicable.

Informed Consent Statement: Not applicable.

Data Availability Statement: The datasets used or analyzed during the current study are available from the corresponding author on reasonable request.

Acknowledgments: The authors thank Heidrun Faltin (from the Department of Radiation Oncology, University Hospital, Tübingen, Germany) for excellent technical assistance.

Conflicts of Interest: All authors declare no competing interests.

Abbreviations

ANOVA	analysis of variance
CFA	colony formation assay
DMEM	Dulbecco's modified eagle medium
DMSO	dimethylsulfoxide
FBS	fetal Bovine Serum
LDA	limited dilution assay
NSC	neural stem cell inducing medium
qPCR	quantitative Polymerase Chain Reaction
RT	reverse transcriptase
TMZ	temozolomide

References

- Ostrom, Q.T.; Cioffi, G.; Waite, K.; Kruchko, C.; Barnholtz-Sloan, J.S. CBTRUS Statistical Report: Primary Brain and Other Central Nervous System Tumors Diagnosed in the United States in 2014–2018. *Neuro.-Oncol.* **2021**, *23*, iii1–iii105. [[CrossRef](#)]
- Stupp, R.; Taillibert, S.; Kanner, A.; Read, W.; Steinberg, D.M.; Lhermitte, B.; Toms, S.; Idbaih, A.; Ahluwalia, M.S.; Fink, K.; et al. Effect of Tumor-Treating Fields Plus Maintenance Temozolomide vs. Maintenance Temozolomide Alone on Survival in Patients With Glioblastoma: A Randomized Clinical Trial. *JAMA* **2017**, *318*, 2306–2316. [[CrossRef](#)]
- Klump, L.; Sezgin, E.C.; Skardelly, M.; Eckert, F.; Huber, S.M. KCa3.1 Channels and Glioblastoma: In Vitro Studies. *Curr. Neuropharmacol.* **2018**, *16*, 627–635. [[CrossRef](#)]
- Catacuzzeno, L.; Sforza, L.; Esposito, V.; Limatola, C.; Franciolini, F. Ion Channels in Glioma Malignancy. In *Transportome Malfunction in the Cancer Spectrum: Ion Transport in Tumor Biology*; Stock, C., Pardo, L.A., Eds.; Springer International Publishing: Cham, Germany, 2021; pp. 223–267.
- Brown, B.M.; Pressley, B.; Wulff, H. KCa3.1 Channel Modulators as Potential Therapeutic Compounds for Glioblastoma. *Curr. Neuropharmacol.* **2018**, *16*, 618–626. [[CrossRef](#)]
- Ferreira, R.; Lively, S.; Schlichter, L.C. IL-4 type 1 receptor signaling up-regulates KCNN4 expression, and increases the KCa3.1 current and its contribution to migration of alternative-activated microglia. *Front. Cell Neurosci.* **2014**, *8*, 183. [[CrossRef](#)]
- Wei, T.; Yi, M.; Gu, W.; Hou, L.; Lu, Q.; Yu, Z.; Chen, H. The Potassium Channel KCa3.1 Represents a Valid Pharmacological Target for Astroglial-Induced Neuronal Impairment in a Mouse Model of Alzheimer's Disease. *Front. Pharm.* **2016**, *7*, 528. [[CrossRef](#)]
- Faragó, N.; Kocsis, Á.K.; Braskó, C.; Lovas, S.; Rózsa, M.; Baka, J.; Kovács, B.; Mikite, K.; Szemenyei, V.; Molnár, G.; et al. Human neuronal changes in brain edema and increased intracranial pressure. *Acta Neuropathol. Commun.* **2016**, *4*, 78. [[CrossRef](#)]
- Ruggieri, P.; Mangino, G.; Fioretti, B.; Catacuzzeno, L.; Puca, R.; Ponti, D.; Miscusi, M.; Franciolini, F.; Ragona, G.; Calogero, A. The inhibition of KCa3.1 channels activity reduces cell motility in glioblastoma derived cancer stem cells. *PLoS ONE* **2012**, *7*, e47825. [[CrossRef](#)]
- Jäger, H.; Dreker, T.; Buck, A.; Giehl, K.; Gress, T.; Grissmer, S. Blockage of intermediate-conductance Ca²⁺-activated K⁺ channels inhibit human pancreatic cancer cell growth in vitro. *Mol. Pharm.* **2004**, *65*, 630–638. [[CrossRef](#)]

11. Lallet-Daher, H.; Roudbaraki, M.; Bavencoffe, A.; Mariot, P.; Gackière, F.; Bidaux, G.; Urbain, R.; Gosset, P.; Delcourt, P.; Fleurisse, L.; et al. Intermediate-conductance Ca²⁺-activated K⁺ channels (IKCa1) regulate human prostate cancer cell proliferation through a close control of calcium entry. *Oncogene* **2009**, *28*, 1792–1806. [[CrossRef](#)]
12. Cuddapah, V.A.; Turner, K.L.; Seifert, S.; Sontheimer, H. Bradykinin-induced chemotaxis of human gliomas requires the activation of KCa3.1 and CLC-3. *J. Neurosci.* **2013**, *33*, 1427–1440. [[CrossRef](#)]
13. D’Alessandro, G.; Catalano, M.; Sciacaluga, M.; Chece, G.; Cipriani, R.; Rosito, M.; Grimaldi, A.; Lauro, C.; Cantore, G.; Santoro, A.; et al. KCa3.1 channels are involved in the infiltrative behavior of glioblastoma in vivo. *Cell Death. Dis.* **2013**, *4*, e773. [[CrossRef](#)]
14. Turner, K.L.; Honasoge, A.; Robert, S.M.; McFerrin, M.M.; Sontheimer, H. A proinvasive role for the Ca(2+)-activated K(+) channel KCa3.1 in malignant glioma. *Glia* **2014**, *62*, 971–981. [[CrossRef](#)]
15. D’Alessandro, G.; Monaco, L.; Catacuzzeno, L.; Antonangeli, F.; Santoro, A.; Esposito, V.; Franciolini, F.; Wulff, H.; Limatola, C. Radiation Increases Functional KCa3.1 Expression and Invasiveness in Glioblastoma. *Cancers* **2019**, *11*, 279. [[CrossRef](#)]
16. D’Alessandro, G.; Grimaldi, A.; Chece, G.; Porzia, A.; Esposito, V.; Santoro, A.; Salvati, M.; Mainiero, F.; Ragozzino, D.; Di Angelantonio, S.; et al. KCa3.1 channel inhibition sensitizes malignant gliomas to temozolomide treatment. *Oncotarget* **2016**, *7*, 30781–30796. [[CrossRef](#)]
17. Stegen, B.; Butz, L.; Klumpp, L.; Zips, D.; Dittmann, K.; Ruth, P.; Huber, S.M. Ca²⁺-Activated IK K⁺ Channel Blockade Radiosensitizes Glioblastoma Cells. *Mol. Cancer Res.* **2015**, *13*, 1283–1295. [[CrossRef](#)]
18. Smith, J.C.; Sheltzer, J.M. Genome-wide identification and analysis of prognostic features in human cancers. *Cell Rep.* **2022**, *38*, 110569. [[CrossRef](#)]
19. Batlle, E.; Clevers, H. Cancer stem cells revisited. *Nat. Med.* **2017**, *23*, 1124–1134. [[CrossRef](#)]
20. Schulz, A.; Meyer, F.; Dubrovskaja, A.; Borgmann, K. Cancer Stem Cells and Radioresistance: DNA Repair and Beyond. *Cancers* **2019**, *11*, 862. [[CrossRef](#)]
21. Serano, R.D.; Pegram, C.N.; Bigner, D.D. Tumorigenic cell culture lines from a spontaneous VM/Dk murine astrocytoma (SMA). *Acta Neuropathol.* **1980**, *51*, 53–64. [[CrossRef](#)]
22. Pilkington, G.J.; Darling, J.L.; Lantos, P.L.; Thomas, D.G.T. Cell lines (VMDk) derived from a spontaneous murine astrocytoma: Morphological and immunocytochemical characterization. *J. Neurol. Sci.* **1983**, *62*, 115–139. [[CrossRef](#)]
23. Ausman, J.I.; Shapiro, W.R.; Rall, D.P. Studies on the Chemotherapy of Experimental Brain Tumors: Development of an Experimental Model. *Cancer Res.* **1970**, *30*, 2394–2400.
24. Pontén, J.; Macintyre, E.H. Long term culture of normal and neoplastic human glia. *Acta Pathol. Microbiol. Scand.* **1968**, *74*, 465–486. [[CrossRef](#)]
25. Allen, M.; Bjerke, M.; Edlund, H.; Nelander, S.; Westermark, B. Origin of the U87MG glioma cell line: Good news and bad news. *Sci. Transl. Med.* **2016**, *8*, 354re3. [[CrossRef](#)]
26. Torsvik, A.; Stieber, D.; Enger, P.; Golebiewska, A.; Molven, A.; Svendsen, A.; Westermark, B.; Niclou, S.P.; Olsen, T.K.; Enger, M.C.; et al. U-251 revisited: Genetic drift and phenotypic consequences of long-term cultures of glioblastoma cells. *Cancer Med.* **2014**, *3*, 812–824. [[CrossRef](#)]
27. Lazic, S.E.; Clarke-Williams, C.J.; Munafò, M.R. What exactly is ‘N’ in cell culture and animal experiments? *PLoS Biol.* **2018**, *16*, e2005282. [[CrossRef](#)]
28. McMahon, S.J. The linear quadratic model: Usage, interpretation and challenges. *Phys. Med. Amp. Biol.* **2018**, *64*, 01TR01. [[CrossRef](#)]
29. Huang, L.; Xu, S.; Hu, D.; Lu, W.; Xie, X.; Cheng, X. IQGAP1 is Involved in Enhanced Aggressive Behavior of Epithelial Ovarian Cancer Stem Cell-Like Cells During Differentiation. *Int. J. Gynecol. Cancer* **2015**, *25*, 559–565. [[CrossRef](#)]
30. Quiñones-Hinojosa, A.; Sanai, N.; Gonzalez-Perez, O.; Garcia-Verdugo, J.M. The human brain subventricular zone: Stem cells in this niche and its organization. *Neurosurg. Clin. N Am.* **2007**, *18*, 15–20, vii. [[CrossRef](#)]
31. Soehngen, E.; Schaefer, A.; Koeritzer, J.; Huelsmeyer, V.; Zimmer, C.; Ringel, F.; Gempt, J.; Schlegel, J. Hypoxia upregulates aldehyde dehydrogenase isoform 1 (ALDH1) expression and induces functional stem cell characteristics in human glioblastoma cells. *Brain. Tumor. Pathol.* **2014**, *31*, 247–256. [[CrossRef](#)]
32. Gatti, M.; Pattarozzi, A.; Bajetto, A.; Würth, R.; Daga, A.; Fiaschi, P.; Zona, G.; Florio, T.; Barbieri, F. Inhibition of CXCL12/CXCR4 autocrine/paracrine loop reduces viability of human glioblastoma stem-like cells affecting self-renewal activity. *Toxicology* **2013**, *314*, 209–220. [[CrossRef](#)] [[PubMed](#)]
33. Jin, X.; Jin, X.; Jung, J.-E.; Beck, S.; Kim, H. Cell surface Nestin is a biomarker for glioma stem cells. *Biochem. Biophys. Res. Commun.* **2013**, *433*, 496–501. [[CrossRef](#)] [[PubMed](#)]
34. Behnan, J.; Stangeland, B.; Hosainey, S.A.M.; Joel, M.; Olsen, T.K.; Micci, F.; Glover, J.C.; Isakson, P.; Brinchmann, J.E. Differential propagation of stroma and cancer stem cells dictates tumorigenesis and multipotency. *Oncogene* **2017**, *36*, 570–584. [[CrossRef](#)] [[PubMed](#)]
35. Chen, Y.J.; Raman, G.; Bodendiek, S.; O’Donnell, M.E.; Wulff, H. The KCa3.1 blocker TRAM-34 reduces infarction and neurological deficit in a rat model of ischemia/reperfusion stroke. *J. Cereb. Blood. Flow. Metab.* **2011**, *31*, 2363–2374. [[CrossRef](#)]
36. Wulff, H.; Miller, M.J.; Hansel, W.; Grissmer, S.; Cahalan, M.D.; Chandy, K.G. Design of a potent and selective inhibitor of the intermediate-conductance Ca²⁺-activated K⁺ channel, IKCa1: A potential immunosuppressant. *Proc. Natl. Acad. Sci. USA* **2000**, *97*, 8151–8156. [[CrossRef](#)]

37. Sesen, J.; Dahan, P.; Scotland, S.J.; Saland, E.; Dang, V.T.; Lemarié, A.; Tyler, B.M.; Brem, H.; Toulas, C.; Moyal, E.C.-J.; et al. Metformin inhibits growth of human glioblastoma cells and enhances therapeutic response. *PLoS ONE* **2015**, *10*, e0123721. [[CrossRef](#)]
38. McFaline-Figueroa, J.L.; Braun, C.J.; Stanciu, M.; Nagel, Z.D.; Mazzucato, P.; Sangaraju, D.; Cerniauskas, E.; Barford, K.; Vargas, A.; Chen, Y.; et al. Minor Changes in Expression of the Mismatch Repair Protein MSH2 Exert a Major Impact on Glioblastoma Response to Temozolomide. *Cancer Res.* **2015**, *75*, 3127–3138. [[CrossRef](#)]
39. Lin, K.; Gueble, S.E.; Sundaram, R.K.; Huseman, E.D.; Bindra, R.S.; Herzon, S.B. Mechanism-based design of agents that selectively target drug-resistant glioma. *Science* **2022**, *377*, 502–511. [[CrossRef](#)]
40. Yi, G.Z.; Huang, G.; Guo, M.; Zhang, X.; Wang, H.; Deng, S.; Li, Y.; Xiang, W.; Chen, Z.; Pan, J.; et al. Acquired temozolomide resistance in MGMT-deficient glioblastoma cells is associated with regulation of DNA repair by DHC2. *Brain* **2019**, *142*, 2352–2366. [[CrossRef](#)]
41. Stegen, B.; Klumpp, L.; Misovic, M.; Edalat, L.; Eckert, M.; Klumpp, D.; Ruth, P.; Huber, S.M. K⁺ channel signaling in irradiated tumor cells. *Eur. Biophys. J.* **2016**, *45*, 585–598. [[CrossRef](#)]
42. Mohr, C.J.; Gross, D.; Sezgin, E.C.; Steudel, F.A.; Ruth, P.; Huber, S.M.; Lukowski, R. K(Ca)₃.1 Channels Confer Radioresistance to Breast Cancer Cells. *Cancers* **2019**, *11*, 1285. [[CrossRef](#)]
43. Ganser, K.; Eckert, F.; Riedel, A.; Stransky, N.; Paulsen, F.; Noell, S.; Krueger, M.; Schittenhelm, J.; Beck-Wödl, S.; Zips, D.; et al. Patient-individual phenotypes of glioblastoma stem cells are conserved in culture and associate with radioresistance, brain infiltration and patient prognosis. *Int. J. Cancer* **2022**, *150*, 1722–1733. [[CrossRef](#)] [[PubMed](#)]
44. Mao, P.; Joshi, K.; Li, J.; Kim, S.-H.; Li, P.; Santana-Santos, L.; Luthra, S.; Chandran, U.R.; Benos, P.V.; Smith, L.; et al. Mesenchymal glioma stem cells are maintained by activated glycolytic metabolism involving aldehyde dehydrogenase 1A3. *Proc. Natl. Acad. Sci. USA* **2013**, *110*, 8644–8649. [[CrossRef](#)] [[PubMed](#)]
45. Weichselbaum, R.R.; Liang, H.; Deng, L.; Fu, Y.-X. Radiotherapy and immunotherapy: A beneficial liaison? *Nat. Rev. Clin. Oncol.* **2017**, *14*, 365–379. [[CrossRef](#)] [[PubMed](#)]
46. Grimaldi, A.; D'Alessandro, G.; Golia, M.T.; Grössinger, E.M.; Di Angelantonio, S.; Ragozzino, D.; Santoro, A.; Esposito, V.; Wulff, H.; Catalano, M.; et al. KCa₃.1 inhibition switches the phenotype of glioma-infiltrating microglia/macrophages. *Cell Death Dis.* **2016**, *7*, e2174. [[CrossRef](#)]
47. Becker, A.P.; Sells, B.E.; Haque, S.J.; Chakravarti, A. Tumor Heterogeneity in Glioblastomas: From Light Microscopy to Molecular Pathology. *Cancers.* **2021**, *13*, 761. [[CrossRef](#)]
48. Patel, A.P.; Tirosh, I.; Trombetta, J.J.; Shalek, A.K.; Gillespie, S.M.; Wakimoto, H.; Cahill, D.P.; Nahed, B.V.; Curry, W.T.; Martuza, R.L.; et al. Single-cell RNA-seq highlights intratumoral heterogeneity in primary glioblastoma. *Science* **2014**, *344*, 1396–1401. [[CrossRef](#)]
49. Brada, M.; Judson, I.; Beale, P.; Moore, S.; Reidenberg, P.; Statkevich, P.; Dugan, M.; Batra, V.; Cutler, D. Phase I dose-escalation and pharmacokinetic study of temozolomide (SCH 52365) for refractory or relapsing malignancies. *Br. J. Cancer* **1999**, *81*, 1022–1030. [[CrossRef](#)]
50. Rosso, L.; Brock, C.S.; Gallo, J.M.; Saleem, A.; Price, P.M.; Turkheimer, F.E.; Aboagye, E.O. A New Model for Prediction of Drug Distribution in Tumor and Normal Tissues: Pharmacokinetics of Temozolomide in Glioma Patients. *Cancer Res.* **2008**, *69*, 120–127. [[CrossRef](#)]

Perspective

Can Any Drug Be Repurposed for Cancer Treatment? A Systematic Assessment of the Scientific Literature

Nicolai Stransky ^{1,2,*} , Peter Ruth ¹, Matthias Schwab ^{3,4,5,6} and Markus W. Löffler ^{4,5,6,7,8,*} 

- ¹ Department of Pharmacology, Toxicology and Clinical Pharmacy, Institute of Pharmacy, University of Tübingen, Auf der Morgenstelle 8, 72076 Tübingen, Germany; peter.ruth@uni-tuebingen.de
 - ² Department of Radiation Oncology, University Hospital Tübingen, Hoppe-Seyler-Str. 3, 72076 Tübingen, Germany
 - ³ Dr. Margarete Fischer-Bosch Institute of Clinical Pharmacology, Auerbachstr. 112, 70376 Stuttgart, Germany; Matthias.Schwab@ikp-stuttgart.de
 - ⁴ Department of Clinical Pharmacology, University Hospital Tübingen, Auf der Morgenstelle 8, 72076 Tübingen, Germany
 - ⁵ Cluster of Excellence iFIT (EXC2180) 'Image-Guided and Functionally Instructed Tumor Therapies', Faculty of Medicine, University of Tübingen, 72076 Tübingen, Germany
 - ⁶ German Cancer Consortium (DKTK), Partner Site Tübingen, 72076 Tübingen, Germany
 - ⁷ Department of General, Visceral and Transplant Surgery, University Hospital Tübingen, Hoppe-Seyler-Str. 3, 72076 Tübingen, Germany
 - ⁸ Department of Immunology, Interfaculty Institute for Cell Biology, University of Tübingen, Auf der Morgenstelle 15, 72076 Tübingen, Germany
- * Correspondence: nicolai.stransky@med.uni-tuebingen.de (N.S.); markus.loeffler@med.uni-tuebingen.de (M.W.L.)



Citation: Stransky, N.; Ruth, P.; Schwab, M.; Löffler, M.W. Can Any Drug Be Repurposed for Cancer Treatment? A Systematic Assessment of the Scientific Literature. *Cancers* **2021**, *13*, 6236. <https://doi.org/10.3390/cancers13246236>

Academic Editor: Carlos M. Telleria

Received: 25 October 2021

Accepted: 8 December 2021

Published: 13 December 2021

Publisher's Note: MDPI stays neutral with regard to jurisdictional claims in published maps and institutional affiliations.



Copyright: © 2021 by the authors. Licensee MDPI, Basel, Switzerland. This article is an open access article distributed under the terms and conditions of the Creative Commons Attribution (CC BY) license (<https://creativecommons.org/licenses/by/4.0/>).

Simple Summary: Drug repurposing strategies utilize drugs, already approved by regulatory authorities, to test their efficacy against different diseases. While this approach is increasingly used, according to the literature, there are few systematic assessments of these efforts so far. In this work, we tried to answer the question: How many approved drugs show anti-cancer effects according to the literature? We found that the majority (69%) of the approved drugs we analyzed did show anti-cancer effects in preclinical studies. The assessment of the methodological quality of the reports, namely, the reporting quality and usage of bias-reducing methods, showed that the methodological quality of the articles was by and large moderate, while many items of the quality assessment were lacking in most reports (for example, blinding, preregistration, power calculations, and detailed information on lab animals). We hypothesize that the current reward systems favor positive results over high methodological quality, probably leading to many false-positive results.

Abstract: Drug repurposing is a complementary pathway for introducing new drugs against cancer. Broad systematic assessments of ongoing repurposing efforts in oncology are lacking, but may be helpful to critically appraise current and future efforts. Hence, we conducted a systematic PubMed search encompassing 100 frequently prescribed and 100 randomly selected drugs, and assessed the published preclinical anti-cancer effects. Furthermore, we evaluated all the identified original articles for methodological quality. We found reports indicating anti-cancer effects for 138/200 drugs, especially among frequently prescribed drugs (81/100). Most were reports suggesting single-agent activity of the drugs (61%). Basic information, such as the cell line used or control treatments utilized, were reported consistently, while more detailed information (e.g., excluded data) was mostly missing. The majority (56%) of in vivo studies reported randomizing animals, while only few articles stated that the experiments were conducted in a blinded fashion. In conclusion, we found promising reports of anti-cancer effects for the majority of the assessed drugs, but speculate that many of them are false-positive findings. Reward systems should be adjusted to encourage the widespread usage of high reporting quality and bias-reducing methodologies, aiming to decrease the rate of false-positive results, and thereby increasing the trust in the findings.

Keywords: repurposing; repositioning; cancer; systematic assessment; meta research

1. Introduction

Drug development faces numerous challenges. In oncology, most drugs entering clinical trials will eventually fail to receive regulatory approval (i.e., 14 out of 15 fail) [1]. Across all the drugs approved for solid cancers between 2002 and 2014 by the Federal Drug Administration (FDA), the median overall survival benefit was merely 2.1 months [2]. Despite a steadily widening scope in cancer research, encompassing, e.g., immunotherapy, elucidation of new cancer cell dependencies, and targeting the tumor microenvironment [3], the prognosis for many cancer entities remains poor; this is reflected by the dismal 5-year overall survival rates, e.g., ~5% in glioblastoma [4], ~10% in pancreatic cancer [5], and ~21% in lung cancer [5].

Drug repurposing, also known as drug repositioning, has gained traction as a potential complementary pathway for introducing new treatments in oncology [6] (see Figure 1), utilizing already approved drugs for non-cancer indications against specific cancer entities.

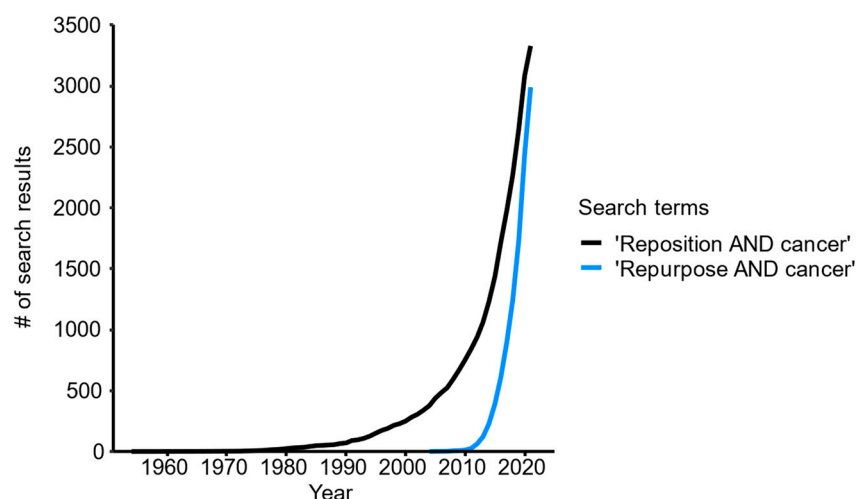


Figure 1. Total number (#) of publications identified in PubMed (<https://pubmed.ncbi.nlm.nih.gov>, accessed on 13 July 2021) with search terms “reposition AND cancer” or “repurpose AND cancer”.

The strategy holds several potential benefits, which are as follows: Since the drug has already been clinically developed, early development may be shortened. Further, due to an already established use in patients, the safety profile can be well appraised, probably reducing the number of failures in early stage development, due to safety signals [7,8], even though the adverse event profiles may differ in a different patient population or with a different dosing scheme. This may result in a shorter development period, translating to lower costs. A decrease in respective costs, from USD 2–3 billion to USD 300 million, and a shortened development time, from 13–15 years to 6 years, have been estimated for this scenario [9], particularly related to preclinical studies and phase 1 and 2 clinical trials. Drug repurposing may also facilitate precision medicine; for example, the overexpression of COX-2 in human breast cancer tissue [10,11] may be amenable for treatment with celecoxib, a selective COX-2 inhibitor introduced as an analgesic. Further, since targeting multiple pathways with repurposed drugs might prove effective, the tolerability of combined drug regimens may be derived from other patient groups. Real-world observations of beneficial associations, using electronic health records and clinical trial data, are currently driving the intensified repurposing efforts, potentially elucidating new cancer cell dependencies and targets [7]. Another approach is based on the extraction of genes from genome-wide association studies (GWAS) related to traits and/or diseases, to identify novel targets, which may be druggable or can be addressed with biologicals [12].

However, there are also several limitations of the drug repurposing concept, demonstrated by failures in the late-stage development of repositioned drugs [8]. Some authors assume that most repurposed drugs lack single-agent activity and merely increase the efficacy of already existing therapies [13]. While such multi-pronged approaches seem intuitive, critics caution against widespread testing of agents lacking single-agent activity in early stage development, since the pre-test probability for substantial benefits is low. Therefore, abandoning agents without single-agent-activity in early clinical development is recommended [14]. Another problem arising in the context of repurposed drugs is the lower potential revenue, due to shortened or expired patent protection [15]. This contrasts the benefits of confined development expenses, since proving efficacy still requires large and costly clinical trials, usually exceeding the funding available to academic institutions. Furthermore, observational data supporting specific drugs for repurposing suffer from several structural weaknesses, including immortal-time bias [16], selection bias, or the vibration of effects [17]. Hence, many hypotheses will likely fail to confer stable benefits for patients, diluting the benefit of reduced development costs. Finally, it is dangerous to promote drugs approved for other indications, due to easy access and off-label prescribing, which may result in patients demanding access to drugs with insufficient evidence [18], as has previously occurred with methadone [19].

While reviews summarizing the findings from repurposing efforts in oncology are available for specific drugs [6], a systematic assessment of how many approved drugs are actually implicated with anti-cancer effects is lacking, according to our own research.

Here, we report the results of a systematic search in PubMed, identifying preclinical reports of anti-cancer effects for the majority of the assessed drugs. These findings may help readers to contextualize and critically appraise current and future repurposing efforts.

2. Methods

We systematically searched PubMed (<https://pubmed.ncbi.nlm.nih.gov>, accessed between 1 September 2020 and 31 December 2020) for reports of anti-cancer drug effects of 200 approved pharmaceuticals and assessed the results, reporting quality and bias-reducing methods in identified articles (see Figure 2). Through this attempt we aim to provide an overview of the landscape of drug repurposing efforts in oncology.

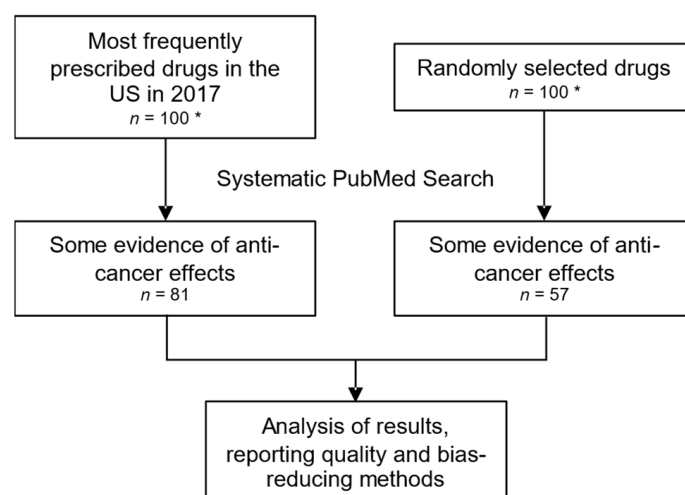


Figure 2. Flowchart of drug selection and subsequent analyses. * All drugs that could be classified as a non-small molecule, mineral, vitamin or endogenous hormone, and all drugs that were already approved for any cancer entity, were excluded.

2.1. Compilation of Drugs

In order to obtain a more representative sample of drugs, both a set of frequently prescribed drugs as well as a set of randomly selected drugs were compiled. Most frequently prescribed drugs in the year 2017 in the US were extracted from <https://clincalc.com>

[om/DrugStats/Top300Drugs.aspx](https://www.accessdata.fda.gov/scripts/cder/daf/) (accessed on 1 September 2020). Randomly selected drugs were randomly picked from all FDA-approved drugs (<https://www.accessdata.fda.gov/scripts/cder/daf/>, accessed on 1 September 2020). Drugs were excluded if they could be classified as a non-small molecule, mineral, vitamin or endogenous hormone, or if the drug was already approved for any cancer entity (in this regard we excluded methotrexate, prednisone and levothyroxine among the most frequently prescribed drugs). Enantiomers were included as their racemic mixture (e.g., citalopram was selected instead of escitalopram). If a drug for the randomly selected drug list was also present among the most frequently prescribed drugs, we replaced it with another random drug to avoid overlap. In this way we selected 100 drugs per group.

2.2. Search Strategy and Number of Drugs Implicated with Anti-Cancer Effects

The following three search strategies were utilized in PubMed: The first search strategy ((name of drug) AND ((repurpose AND cancer) OR (reposition AND cancer))) aimed at identifying drugs already being discussed to have repurposing potential in the scientific literature; for example, the first search strategy for acitretin was acitretin AND ((repurpose AND cancer) OR (reposition AND cancer)).

The second search strategy ((name of drug) AND cancer) was intended to identify a broader range of articles. After analyzing all 200 drugs, we utilized a third search strategy ((name of drug) AND cancer proliferation) for all remaining drugs without any hits in the previous searches. The first 20 articles identified by each search strategy were screened for information regarding preclinical anti-cancer effects and all results and methodologies were summarized after discussion and agreement by two reviewers. In general, only information from the article with the most relevant findings, defined by our categorization efforts described below, was extracted and used for the subsequent assessment of methodological quality.

2.3. Categorizing Findings of the Studies

Articles were categorized in the following order, which we believe strongly supports future translational potential of respective drugs: Highest priority was given to reviews summarizing the preclinical effectiveness of a drug against cancer. Furthermore, we assigned the same level of evidence to drugs already being tested in clinical trials, since we assumed institutional review board approval for clinical studies should have included a summary of preclinical evidence. Next highest priority was given to drugs with established single-agent activity in (i) in vivo models and (ii) in vitro models. Results describing anti-cancer effects when combined with other drugs were assigned a lower priority and again subdivided into (i) in vivo studies and (ii) in vitro studies. Ultimately, biological plausibility, such as inhibition of a driver mutation, was ranked with lowest priority.

2.4. Assessment of the Methodological Quality

All identified original articles were assessed for items indicating high methodological quality, i.e., high reporting standards and the use of methods to reduce bias. In general, we assessed the methods section and searched the whole report for specific terms indicating methodological aspects or reporting quality (see all criteria and a full list of search terms for each item in Tables S1 and S2). For in vitro studies we assessed whether the authors reported the respective cell line, the drug dosage, duration of exposure and solvent of the drug used, whether authors specified exclusion criteria and whether experiments were preregistered and conducted in a blinded fashion. In vivo studies were analyzed regarding information about the species and baseline characteristics of the animals (age, sex and weight), dosing of the drug, route of administration, whether or not the control conditions were specified, adverse events and specification of exclusion criteria. Furthermore, the reports were searched for information about preregistration of the experiments, randomization of animals, blinding of experiments and power calculations.

3. Results

Overall, our systematic search identified articles for 138/200 drugs (69%) that implied some activity against cancer. While, amongst the 100 most frequently prescribed drugs, reports of anti-cancer effects were found for 81 pharmaceuticals, we could identify reports showing anti-cancer effects for 57 drugs in the randomly selected group (see Table 1). The first two search strategies identified the majority of reports indicating anti-cancer effects (125/138), whereas strategy 3, which was applied in the remainder of the drugs, identified reports of anti-cancer activity for only 13 drugs, mainly used as supportive treatments in cancer patients.

Table 1. Results of the systematic search.

Systematic Search	Frequently Prescribed Drugs	Randomly Selected Drugs
Drugs reported to have anti-cancer effects		
Identified by all search strategies	81	57
Identified by search strategy 1	42	29
Identified by search strategy 2	30	24
Identified by search strategy 3	9	4
Categorization of findings		
Review	19	16
Single-agent activity	in vivo	13
	in vitro	21
Combination therapy	in vivo	1
	in vitro	3
Biological plausibility	6	3

Our search and categorization efforts revealed that the vast majority of articles identified were reviews (35/138 drugs, 25%; see Figure 3), or described preclinical single-agent activity (84/138 drugs, 61%). When comparing the identified articles of the most frequently prescribed drugs with randomly selected drugs, the differences between the relative proportions of each category were small, suggesting that the general composition of the articles was comparable between the two selected sets of drugs.

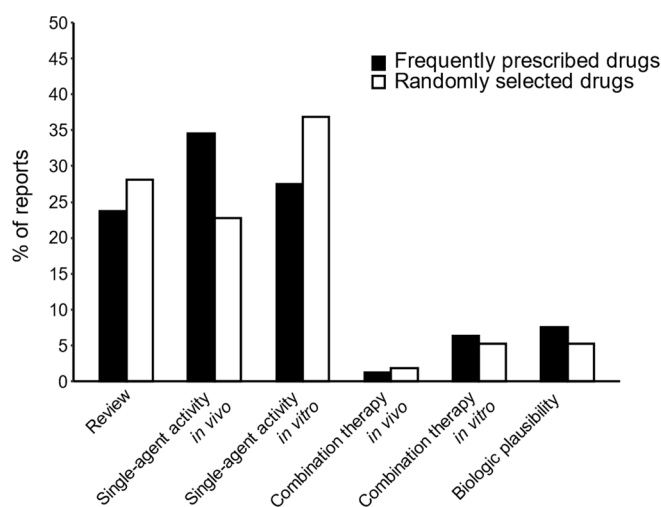


Figure 3. Categorization of identified articles subdivided into frequently prescribed drugs and randomly selected drugs.

We also compared our search results with the ReDO database (<https://www.anticancerfund.org/en/redo-db>, accessed on 5 November 2020), a database listing drugs with potential anti-cancer effects that are already approved for other indications. While our

search strategy identified all but one drug also contained in the database, we could identify an additional 59 drugs reported to have anti-cancer effects (26 drugs among the most frequently prescribed drugs and 33 among the randomly selected drugs).

To address the methodological quality, we assessed all 103 articles with original data identified by our search strategies, except for 9 reports, which were unavailable, and 3 articles, which did not present novel data. In total, we identified 50 articles that provided in vitro or in silico data, and 41 in vivo studies. The assessments of reporting quality and bias-reducing methods are shown in Figure 4.

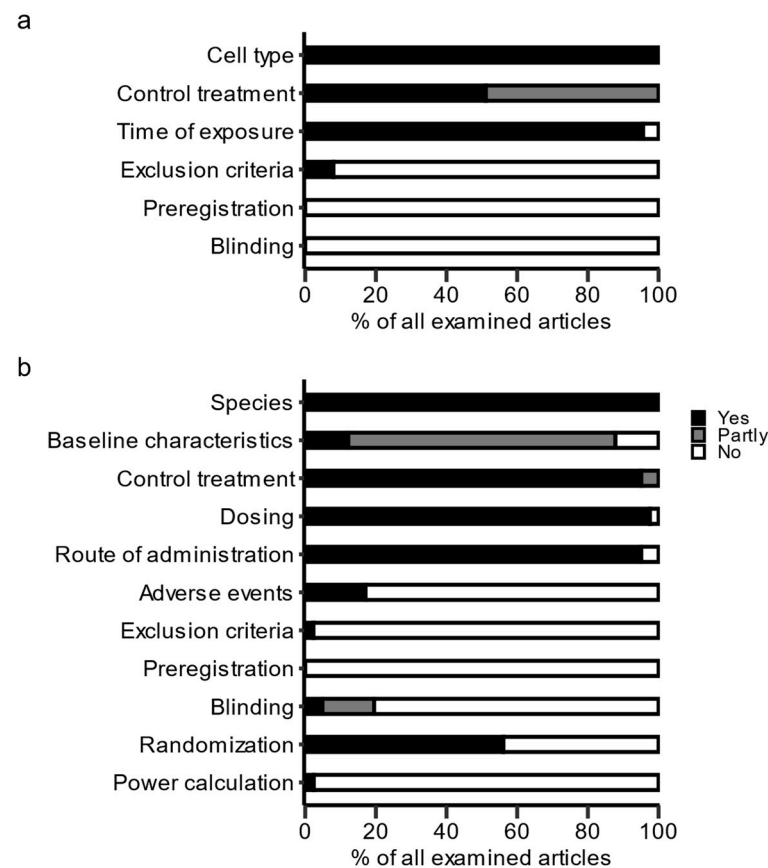


Figure 4. Methodological quality of original articles: (a) in vitro studies ($n = 50$) and (b) in vivo studies ($n = 41$). Depicted are percentages of articles reporting or applying the respective item.

All the assessed in vitro studies reported the cell line used for the experiments. Furthermore, all the publications reported using a control; however, 49% of the studies did not explicitly mention the diluent used to dissolve the drugs. The duration of drug exposure was reported in most of the publications (96%). The authors of in vivo studies reported the species of the animals in every article, and 76% provided some baseline characteristics. However, only 11% of the assessed articles reported precise baseline characteristics of the animals, including the age, weight and sex of the animals. In addition, adverse events were only mentioned in 17% of the assessed articles. Disclosure of exclusion criteria or mentioning excluded data were the exceptions, and were only reported in 8% of the in vitro studies and 2% of the in vivo studies.

Bias-reducing methods mostly consisted of the randomization of animals for in vivo studies; 56% of the publications reported randomizing the animals to different treatment arms. None of the in vitro studies reported blinding of experiments, whereas 5% of the in vivo studies consistently used blinding and 15% blinded some of their experiments. Only one article (2%) reported a power calculation to determine the required sample size of the planned animal experiments, and none of the 91 analyzed articles stated that the study had been preregistered.

All the relevant raw data are provided in the Supplementary Materials of this article (Table S3).

4. Discussion

This study originated from the simple assumption that there are probably published reports of anti-cancer effects for most of the frequently prescribed drugs. We reasoned that, if found to be true, this might cast some critical light on drug repurposing efforts in general, since it is not conceivable that nearly all drugs actually do work against cancer. Instead, this finding might support some of the widespread criticism of biomedical research, which argues that many published results are probably false-positives [20].

Our findings show that the scientific literature actually contains findings of anti-cancer effects for the majority of the assessed drugs. As expected, anti-cancer effects were reported more often for frequently prescribed drugs than for randomly selected drugs, speculatively due to easier access, lower purchasing costs, or well-known pharmacokinetics and pharmacodynamics.

After assessing all 200 drugs with our first two search strategies, we recognized the following pattern: our search strategies were too simple to also account for drugs that are used as supportive treatments in cancer patients, and we primarily identified articles dealing with their original use; for example, our search strategies yielded several articles regarding gabapentin's analgesic effects in cancer patients. Hence, we additionally searched the remaining drugs that did not produce any hits in the previous searches with a third search strategy, ((name of drug) AND cancer proliferation), identifying another 13 drugs with putative anti-cancer effects. This supports the notion that more nuanced search strategies might have identified even more drugs. To further add to this point, we used three additional search strategies after finalizing the manuscript and identified another six drugs with anti-cancer activity according to the literature (see the results in the Supplementary Materials).

While single-agent activity may be useful for prioritizing drugs in the clinical setting, our results indicate that most of the drugs implicated with anti-cancer properties show single-agent activity (84/138 drugs, 61%). Hence, suggesting trialists to focus on drugs with single-agent activity in preclinical studies may be futile for the prioritization of promising drug candidates.

We classified the methodological quality of the analyzed articles as moderate. Basic information about the conducted experiments, such as animal species, cell lines, or control treatments used, was consistently reported, whereas more detailed information, e.g., about the exclusion of data, precise baseline characteristics of the animals, or adverse events, was missing in the majority of the assessed articles. Such information may be relevant to replicate the findings and to gain more trust in the results. We found higher ratios of randomization in the *in vivo* studies (56%) as compared to the findings of other authors, who found randomization rates of 4% [21] up to 33% [22]. In contrast, the blinding of experiments remained the exception. Previous findings suggest that nonblinded experiments may lead to more significant findings and higher effect sizes compared to blinded experiments [23]. Only one study reported using a power calculation according to our research, while other authors identified mostly low-powered studies in preclinical research [24], which may lead to even more false-positive findings [25]. Finally, none of the articles mentioned a preregistration of experiments, which is an effective method to reduce selective reporting of results and statistical flexibility [26]. Two recent studies reported that only about two thirds of all animal experiments are eventually published or presented at conferences, even after long follow-up periods [27,28], potentially skewing the literature even more towards significant results.

Given these findings, we question that the majority of approved drugs can actually be repurposed against cancer, and, therefore, we speculate that a relevant proportion of these findings may likely constitute false-positives [29,30]. In contrast to the many positive findings in preclinical research, there are very few examples of successfully repurposed

drugs in oncology. The most prominent example is thalidomide, which was first clinically tested in multiple myeloma patients more than 20 years ago [31,32]. Another example is the selective estrogen receptor modulator raloxifene, which was approved by the FDA in 2007, to reduce the risk of invasive breast cancer in postmenopausal women at high risk [33], once again long before most systematic repurposing efforts were even started (see Figure 1).

This current situation may be fueled by reward systems emphasizing traditional promotion criteria [34], favoring selective reporting of ‘significant’ findings and the utilization of permissive research practices. It has been suggested that this bias might be remedied by several methods [35], many of which are already common practice in clinical research, including preregistration of experiments, more detailed reporting of experiments, reporting of negative studies, blinding of experiments, randomization of animals, powering animal studies adequately, and independent replication efforts. Reward systems should be adjusted to account for several of these non-traditional items to foster higher methodological standards in preclinical science, potentially reducing the number of false-positive findings reported, and, hence, making drug repurposing efforts more reliable and efficient.

This work has several limitations. Randomly selected drugs were influenced by redundancy, e.g., by different drug formulations or trade names present in the FDA drug list, potentially favoring more common drugs over rather exotic ones; for example, the list contained different formulations or trade names of phenytoin, which appeared at least five times, while diatrizoate was only present twice. Secondly, our search strategy was simple and cannot claim comprehensiveness, conceivably biasing our findings towards lower percentages of potentially repurposable drugs against cancer. Thirdly, it was beyond the scope of this work to critically appraise the quality of each study in detail, and we only reported the results as published by the respective authors. Lastly, in determining the methodological quality of the original articles, some articles may have been misclassified, e.g., when the items were reported in unusual ways and, thus, not adequately identified by our assessment.

5. Conclusions

Our results support the notion that the scientific literature contains reports of anti-cancer effects for a large portion of approved drugs, particularly those frequently prescribed. The possibility that all of these drugs actually work against some kind of cancer cannot be excluded; however, this is a rather unlikely scenario. While overly optimistic analyses of not-yet approved drugs are dangerous in themselves, this is aggravated for approved drugs. Public media may hype repurposable drugs based on unreliable findings in preclinical studies, leading to patients demanding off-label prescriptions. Researchers evaluating the repurposing potential of approved drugs should thus apply particularly high standards and methodological rigor to avoid bias that might impact the trust in physicians, and in science itself. Changes in reward systems may be considered as a potential solution, since they could lead to changes in this regard.

Supplementary Materials: The following are available online at <https://www.mdpi.com/article/10.3390/cancers13246236/s1>: Table S1: Reporting quality; Table S2: Methods to reduce bias; Table S3: Raw data.

Author Contributions: Conceptualization, N.S. and M.W.L.; Data curation, N.S. and M.W.L.; Formal analysis, N.S. and M.W.L.; Funding acquisition, P.R. and M.S.; Investigation, N.S.; Methodology, N.S., P.R. and M.W.L.; Resources, N.S.; Supervision, P.R., M.S. and M.W.L.; Validation, N.S.; Visualization, N.S. and M.W.L.; Writing—original draft, N.S. and M.W.L.; Writing—review & editing, P.R. and M.S. All authors have read and agreed to the published version of the manuscript.

Funding: We acknowledge support by Open Access Publishing Fund of University of Tübingen. The work was supported by the Robert Bosch Stiftung (Stuttgart, Germany), and the Deutsche Forschungsgemeinschaft (DFG, German Research Foundation) under Germany’s Excellence Strategy—EXC

2180–390900677). The funders had no role in the design of the study, in the collection, analyses, or interpretation of data, in the writing of the manuscript, or in the decision to publish the results.

Conflicts of Interest: M.W.L. is a co-inventor of several patents owned by Immatics Biotechnologies, and has acted as a consultant and/or advisory board member for Boehringer Ingelheim. The other authors declare no conflict of interest.

References

1. Hay, M.; Thomas, D.W.; Craighead, J.L.; Economides, C.; Rosenthal, J. Clinical development success rates for investigational drugs. *Nat. Biotechnol.* **2014**, *32*, 40–51. [CrossRef] [PubMed]
2. Fojo, T.; Mailankody, S.; Lo, A. Unintended consequences of expensive cancer therapeutics—The pursuit of marginal indications and a Me-Too mentality that stifles innovation and creativity. *JAMA Otolaryngol. Neck Surg.* **2014**, *140*, 1225–1236. [CrossRef]
3. Bernards, R.; Jaffee, E.; Joyce, J.A.; Lowe, S.W.; Mardis, E.R.; Morrison, S.J.; Polyak, K.; Sears, C.L.; Vousden, K.H.; Zhang, Z. A Roadmap for the Next Decade in Cancer Research. Available online: <https://www.nature.com/articles/s43018-019-0015-9> (accessed on 30 March 2020).
4. Ostrom, Q.T.; Gittleman, H.; Fulop, J.; Liu, M.; Blanda, R.; Kromer, C.; Wolinsky, Y.; Kruchko, C.; Barnholtz-Sloan, J.S. CBTRUS statistical report: Primary brain and central nervous system tumors diagnosed in the United States in 2008–2012. *Neuro-Oncol.* **2015**, *17*, iv1–iv62. [CrossRef] [PubMed]
5. Siegel, R.L.; Miller, K.D.; Fuchs, H.E.; Jemal, A. Cancer statistics, 2021. *CA Cancer J. Clin.* **2021**, *71*, 7–33. [CrossRef]
6. Pantziarka, P.; Bouche, G.; Meheus, L.; Sukhatme, V.; Sukhatme, V.P. The Repurposing Drugs in Oncology (ReDO) Project. Available online: <http://ecancer.org/en/journal/article/442-the-repurposing-drugs-in-oncology-redo-project> (accessed on 12 June 2020).
7. Lesko, L.J. Efficacy from strange sources. *Clin. Pharmacol. Ther.* **2017**, *103*, 253–261. [CrossRef]
8. Pushpakom, S.; Iorio, F.; Eyers, P.A.; Escott, K.J.; Hopper, S.; Wells, A.; Doig, A.; Guilliams, T.; Latimer, J.; McNamee, C.; et al. Drug repurposing: Progress, challenges and recommendations. *Nat. Rev. Drug Discov.* **2019**, *18*, 41–58. [CrossRef]
9. Nosengo, N. Can you teach old drugs new tricks? *Nature* **2016**, *534*, 314–316. [CrossRef] [PubMed]
10. Hwang, D.; Byrne, J.; Scollard, D.; Levine, E. Expression of Cyclooxygenase-1 and Cyclooxygenase-2 in human breast cancer. *J. Natl. Cancer Inst.* **1998**, *90*, 455–460. [CrossRef]
11. Goradel, N.H.; Najafi, M.; Salehi, E.; Farhood, B.; Mortezaee, K. Cyclooxygenase-2 in cancer: A review. *J. Cell. Physiol.* **2019**, *234*, 5683–5699. [CrossRef]
12. Sanseau, P.; Agarwal, P.; Barnes, M.; Pastinen, T.; Richards, J.B.; Cardon, L.R.; Mooser, V. Use of genome-wide association studies for drug repositioning. *Nat. Biotechnol.* **2012**, *30*, 317–320. [CrossRef]
13. Pantziarka, P. Drug Repurposing and Oncology—Pitfalls and Potentials. *Oncol. Cent.* 2017. Available online: <https://www.onco-logy-central.com/drug-repurposing-oncology-pitfalls-potentials/> (accessed on 25 October 2021).
14. Gyawali, B.; Prasad, V. Drugs that lack single-agent activity: Are they worth pursuing in combination? *Nat. Rev. Clin. Oncol.* **2017**, *14*, 193–194. [CrossRef] [PubMed]
15. Breckenridge, A.; Jacob, R. Overcoming the legal and regulatory barriers to drug repurposing. *Nat. Rev. Drug Discov.* **2019**, *18*, 1–2. [CrossRef] [PubMed]
16. Lévesque, E.L.; Hanley, A.J.; Kezouh, A.; Suissa, S. Problem of immortal time bias in cohort studies: Example using statins for preventing progression of diabetes. *BMJ* **2010**, *340*, b5087. [CrossRef] [PubMed]
17. Patel, C.J.; Burford, B.; Ioannidis, J.P. Assessment of vibration of effects due to model specification can demonstrate the instability of observational associations. *J. Clin. Epidemiol.* **2015**, *68*, 1046–1058. [CrossRef] [PubMed]
18. Theile, D.; Mikus, G. Methadone against cancer: Lost in translation. *Int. J. Cancer* **2018**, *143*, 1840–1848. [CrossRef] [PubMed]
19. Ergebnisse der Online-Umfrage. Methadon in der Krebstherapie. Available online: <https://www.dgho.de/aktuelles/news/new-sarchiv/2017/ergebnisse-umfrage-methadon> (accessed on 13 June 2020).
20. Ioannidis, J.P.A. Why most published research findings are false. *PLoS Med.* **2005**, *2*, e124. [CrossRef]
21. Wieschowski, S.; Chin, W.W.L.; Federico, C.; Sievers, S.; Kimmelman, J.; Strech, D. Preclinical efficacy studies in investigator brochures: Do they enable risk–benefit assessment? *PLoS Biol.* **2018**, *16*, e2004879. [CrossRef]
22. MacLeod, M.R.; McLean, A.L.; Kyriakopoulou, A.; Serghiou, S.; de Wilde, A.; Sherratt, N.; Hirst, T.; Hemblade, R.; Babor, Z.; Nunes-Fonseca, C.; et al. Risk of bias in reports of in vivo research: A focus for improvement. *PLoS Biol.* **2015**, *13*, e1002273. [CrossRef] [PubMed]
23. Holman, L.; Head, M.L.; Lanfear, R.; Jennions, M.D. Evidence of experimental bias in the life sciences: Why we need blind data recording. *PLoS Biol.* **2015**, *13*, e1002190. [CrossRef]
24. Schmidt-Pogoda, A.; Bonberg, N.; Koecke, M.H.M.; Strecker, J.; Wellmann, J.; Bruckmann, N.; Beuker, C.; Schäbitz, W.; Meuth, S.G.; Wiendl, H.; et al. Why most acute stroke studies are positive in animals but not in patients: A systematic comparison of preclinical, early phase, and Phase 3 clinical trials of neuroprotective agents. *Ann. Neurol.* **2020**, *87*, 40–51. [CrossRef] [PubMed]
25. Button, K.S.; Ioannidis, J.P.A.; Mokrysz, C.; Nosek, B.A.; Flint, J.; Robinson, E.S.J.; Munafò, M.R. Power failure: Why small sample size undermines the reliability of neuroscience. *Nat. Rev. Neurosci.* **2013**, *14*, 365–376. [CrossRef]
26. Dirnagl, U. Preregistration of exploratory research: Learning from the golden age of discovery. *PLoS Biol.* **2020**, *18*, e3000690. [CrossRef] [PubMed]

27. Van Der Naald, M.; Wenker, S.; Doevendans, A.P.; Wever, E.K.; Chamuleau, S.A.J. Publication rate in preclinical research: A plea for preregistration. *BMJ Open Sci.* **2020**, *4*, e100051. [[CrossRef](#)]
28. Wieschowski, S.; Biernot, S.; Deutsch, S.; Glage, S.; Bleich, A.; Tolba, R.; Strech, D. Publication rates in animal research. Extent and characteristics of published and non-published animal studies followed up at two German university medical centres. *PLoS ONE* **2019**, *14*, e0223758. [[CrossRef](#)]
29. Tsilidis, K.K.; Panagiotou, O.; Sena, E.S.; Aretouli, E.; Evangelou, E.; Howells, D.; Salman, R.A.-S.; Macleod, M.R.; Ioannidis, J.P.A. Evaluation of excess significance bias in animal studies of neurological diseases. *PLoS Biol.* **2013**, *11*, e1001609. [[CrossRef](#)]
30. Bastian, H. Biomedical Research: Believe It or Not? *Absol. Maybe* 2013. Available online: <https://absolutelymaybe.plos.org/2013/12/16/biomedical-research-believe-it-or-not/> (accessed on 25 October 2021).
31. Palumbo, A.; Facon, T.; Sonneveld, P.; Bladé, J.; Offidani, M.; Gay, F.; Moreau, P.; Waage, A.; Spencer, A.; Ludwig, H.; et al. Thalidomide for treatment of multiple myeloma: 10 years later. *Blood* **2008**, *111*, 3968–3977. [[CrossRef](#)] [[PubMed](#)]
32. Ashburn, T.T.; Thor, K.B. Drug repositioning: Identifying and developing new uses for existing drugs. *Nat. Rev. Drug Discov.* **2004**, *3*, 673–683. [[CrossRef](#)] [[PubMed](#)]
33. FDA Approves Raloxifene for Breast Cancer Prevention. Available online: <https://prevention.cancer.gov/news-and-events/news/fda-approves-raloxifene> (accessed on 25 November 2021).
34. Rice, D.B.; Raffoul, H.; Ioannidis, A.J.P.; Moher, D. Academic criteria for promotion and tenure in biomedical sciences faculties: Cross sectional analysis of international sample of universities. *BMJ* **2020**, *369*, m2081. [[CrossRef](#)]
35. Begley, C.G.; Ioannidis, J.P. Reproducibility in science. *Circ. Res.* **2015**, *116*, 116–126. [[CrossRef](#)]